DOKUZ EYLÜL UNIVERSITY
GRADUATE SCHOOL OF NATURAL AND APPLIED SCIENCES

MODELING AND OPTIMIZATION OF THE DRONE BASE STATIONS LOCATION-ALLOCATION PROBLEM

by
Özge ŞATIR AKPUNAR

July, 2025
İZMİR

MODELING AND OPTIMIZATION OF THE DRONE BASE STATIONS LOCATION-ALLOCATION PROBLEM

A Thesis Submitted to the
Graduate School of Natural and Applied Sciences of Dokuz Eylül University
In Partial Fulfillment of the Requirements for the Degree of Doctor of Philosophy in Department of Industrial Engineering, Industrial Engineering Program

by
Özge ŞATIR AKPUNAR

July, 2025
İZMİR

Ph.D. THESIS EXAMINATION RESULT FORM

We have read the thesis entitled **"MODELING AND OPTIMIZATION OF THE DRONE BASE STATIONS LOCATION-ALLOCATION PROBLEM"** completed by **ÖZGE ŞATIR AKPUNAR** under supervision of **PROF.DR. ŞENER AKPINAR** and we certify that in our opinion it is fully adequate, in scope and in quality, as a thesis for the degree of Doctor of Philosophy.

Prof.Dr. Şener AKPINAR

Supervisor

Prof. Dr. Umay Zeynep UZUNOĞLU KOÇER

Thesis Committee Member

Prof. Dr. Bilge BİLGEN

Thesis Committee Member

Prof. Dr. Pınar MIZRAK ÖZFIRAT

Examining Committee Member

Assoc. Prof. Dr. Leyla DEMİR

Examining Committee Member

Prof. Dr. Abdullah SEÇGİN

Director

Graduate School of Natural and Applied Sciences

ACKNOWLEDGMENT

Completing this thesis has been a highly formative and intellectually challenging journey. I would like to express my sincere gratitude to all individuals and institutions whose support, guidance, and encouragement made this work possible. Firstly, I would like to express my deepest gratitude to my advisor, Prof. Dr. Şener AKPINAR, for his steadfast support, insightful guidance, and continuous encouragement throughout this journey. His trust in my independence as a researcher, combined with his readiness to offer direction whenever needed, has been invaluable. His academic perspective, professionalism, and empathy have not only shaped this dissertation but also inspired my future path in research. I am also grateful to the esteemed members of my thesis committee, Prof. Dr. Bilge BİLGEN and Prof. Dr. Umay Zeynep UZUNOĞLU KOÇER, for their valuable feedback and contributions to the development of this work.

I would like to extend my sincere gratitude to the Scientific and Technological Research Council of Türkiye (TÜBİTAK) for its financial and academic support throughout my doctoral studies. I gratefully acknowledge the support provided under the TÜBİTAK 2211/A National PhD Scholarship Programme (Grant No: 1649B032100637) and the TÜBİTAK 2214/A-International Research Fellowship Programme for PhD Students (Grant No: 1059B142201444), which enabled the continuity of my research and supported my international academic engagement.

I am truly grateful to my parent Perihan and İbrahim ŞATIR, and my sister Müge HATİP for their endless love, trust, and quiet encouragement. Their constant presence and belief in me gave me strength and comfort throughout this entire journey.

My deepest and most heartfelt gratitude goes to my beloved spouse, Anıl AKPUNAR. His unwavering support, patience, and strength have been my greatest comfort in the most challenging times. He has stood beside me not only as a partner in life, but also as my greatest source of calm, clarity, and motivation.

Özge ŞATIR AKPUNAR

MODELING AND OPTIMIZATION OF THE DRONE BASE STATIONS LOCATION-ALLOCATION PROBLEM

ABSTRACT

This study addresses the problem of designing equitable drone-based communication systems for emergency response operations. The focus is on the optimal deployment and routing of multiple drone base stations (DBSs) to ensure both spatial and temporal fairness in coverage under operational constraints such as limited battery capacity and mobility. The research contributes a structured solution framework that combines exact mathematical formulations, and metaheuristic approaches to tackle the complexity and scalability limitations inherent in such problems. Initially, two mixed-integer linear programming (MILP) models are developed based on the Maximal Covering Location Problem (MCLP), incorporating fairness through time-balancing constraints with spatial and temporal coverage objectives. These models are tested on synthetic problem instances to evaluate performance under varying parameters and to investigate trade-offs between equity and energy efficiency. Subsequently, an alternative formulation based on the Covering Tour Problem (CTP) is also proposed, in which fairness is embedded directly into the objective function. This led to the development of new MILP models integrating three fairness metrics—Total Pairwise Differences, Maximin, and Distribution-based fairness—and a unified evaluation framework. Finally, a metaheuristic algorithm is designed using the Greedy Randomized Adaptive Search Procedure (GRASP), further enhanced with Variable Neighborhood Search (VNS) and Simulated Annealing (SA) mechanisms. This approach effectively constructs feasible solutions incrementally, making it suitable for dynamic and large-scale settings where the solution structure cannot be defined in advance.

All proposed models and algorithms are implemented and subjected to comprehensive computational testing. A set of benchmark instances, including both small- and medium-scale cases, are utilized to evaluate the performance, applicability, and limitations of the approaches. The resulting outcomes were systematically

analysed and discussed to assess the quality and practicality of the solutions generated. Overall, the thesis contributes both theoretical insights and algorithmic strategies for equitable and adaptive DBS deployment, with strong implications for future research in operations research, humanitarian logistics, and real-time disaster communication planning.

Keywords: Drone base stations, Disaster response, Spatial-temporal fairness, Coverage optimization, Mixed integer linear programming, GRASP

DRONE BAZ İSTASYONLARININ YERLEŞİM-TAHSİS PROBLEMİNİN MODELLENMESİ VE OPTİMİZASYONU

ÖZ

Bu çalışma, acil durum müdahale operasyonları için adil insansız hava aracı tabanlı iletişim sistemlerinin tasarımı problemini ele almaktadır. Sınırlı batarya kapasitesi ve hareket kabiliyeti gibi operasyonel kısıtlar altında, birden fazla insansız hava aracı baz istasyonunun (DBS) en uygun şekilde konumlandırılması ve yönlendirilmesi yoluyla kapsamada hem mekânsal hem de zamansal adaletin sağlanmasına odaklanmaktadır. Araştırma, bu tür problemlere özgü karmaşıklık ve ölçeklenebilirlik sınırlamalarını ele almak üzere, kesin matematiksel modeller ile sezgisel algoritmaları birleştiren yapılandırılmış bir çözüm çerçevesi sunmaktadır. İlk olarak, Maksimum Kapsama Yeri Problemi'ne (MCLP) dayalı iki tamsayılı doğrusal programlama (MILP) modeli geliştirilmiş; bu modellerde adalet, zaman dengesi kısıtları aracılığıyla, hem mekânsal hem de zamansal kapsama hedefleriyle birlikte ele alınmıştır. Bu modeller, farklı parametreler altında performansı değerlendirmek ve adalet ile enerji verimliliği arasındaki dengeyi incelemek amacıyla sentetik örneklem setleri üzerinde test edilmiştir. Alternatif olarak, adaletin doğrudan amaç fonksiyonuna entegre edildiği Kapsama Turu Problemi'ne (CTP) dayalı yeni bir formülasyon önerilmiş; bunun sonucunda, Toplam Çiftler Arası Fark, Maximin ve Dağılım-temelli adalet ölçütlerini içeren yeni MILP modelleri geliştirilmiş ve bu modeller için birleşik bir değerlendirme çerçevesi oluşturulmuştur. Ayrıca, Çeşitlendirme ve yoğunlaştırma süreçlerini desteklemek amacıyla Değişken Komşuluk Araması (VNS) ve Tavlama Benzetimi (SA) mekanizmalarıyla geliştirilen Açgözlü Rastgeleleştirilmiş Uyarlanabilir Arama Yöntemi (GRASP) tabanlı hibrit bir sezgisel algoritma tasarlanmıştır. Bu yaklaşım, çözüm yapısının önceden belirlenemediği dinamik ve büyük ölçekli problemler için uygun olan, çözümleri artımlı olarak oluşturan etkili bir yöntem sunmaktadır.

Önerilen tüm modeller ve algoritmalar uygulanmış ve kapsamlı hesaplamalı testlere tabi tutulmuştur. Küçük ve orta ölçekli örneklemleri içeren karşılaştırma setleri kullanılarak, yaklaşımların performansı, uygulanabilirliği ve sınırlılıkları değerlendirilmiştir. Elde edilen sonuçlar sistematik şekilde analiz edilmiş ve üretilen çözümlerin kalitesi ile pratik kullanıma uygunluğu tartışılmıştır. Genel olarak, bu tez adil ve uyarlanabilir DBS yerleştirmesi için kuramsal içgörüler ve algoritmik stratejiler sunmakta olup, yöneylem araştırması, insani lojistik ve gerçek zamanlı afet iletişim planlaması alanlarında gelecekteki araştırmalar için güçlü çıkarımlar sağlamaktadır.

Anahtar kelimeler: Drone baz istasyonları, Afet müdahalesi, Mekânsal-zamansal adalet, Kapsama optimizasyonu, Tamsayılı doğrusal programlama, GRASP

CONTENTS

Page

LIST OF FIGURES

Page

LIST OF TABLES

Page

CHAPTER ONE
INTRODUCTION

1.1 Motivation and the Importance of the Problem

An unmanned aerial vehicle (UAV), commonly referred to as a drone, is a type of aircraft that operates without a human pilot onboard, either through remote control or autonomous flight systems. Drones can potentially be used in various industries due to their flexibility, rapid deployment, low maintenance costs, high mobility, and relatively small operating costs. They have been utilized in many application areas such as monitoring, agriculture, network communication, search and rescue operations, security and surveillance, delivery of goods and civil infrastructure inspection (Shakhatreh, et al., 2019). Drone technology is rapidly growing, and drone use provides varying market opportunities for new and attractive applications. As a result, projections indicate a swift expansion in the commercial drone industry. Drones have already performed regular commercial operations or package deliveries. For example, companies such as Amazon, UPS, Google, and several European courier services have been conducting trials involving drone-based delivery systems (Mack, 2018). Wireless connectivity through UAVs represents another promising direction for future communication infrastructures, as drones functioning as drone base stations (DBSs) can assist in restoring network services in post-disaster or emergency scenarios where terrestrial infrastructure is unavailable. From this point of view, this thesis investigates the use of drones as DBSs for communication in disaster situations. Accordingly, drones will be referred to as DBSs for the remainder of the thesis.

Natural or human-made disasters are unpredictable and lead to significant infrastructure damages as well as lives and economical losses. Although disasters are unavoidable, their adverse effects could be alleviated thanks to an effective and enhanced disaster management system. Disaster management refers to a strategic framework and set of practices implemented to safeguard critical infrastructure against major damages resulting from natural or human-made disasters (Oktari, Munadi, Idroes, & Sofyan, 2020). Such a management system is required for reducing disaster physical impacts, number of deaths and economical damages as well as responding on a timely manner. Disaster management cycle consists of three-stages: preparedness - involving precautions such as forecasting and early warning systems before breakout of disaster, response – acquiring information of destruction and providing situational awareness during disaster, recovery – including infrastructure reconstruction during post-disaster. Although many effective technological solutions are developed to reduce the effects of disasters, drones have recently shown their ability to tackle the most challenging issues of an urgent event (Khan, Gupta, & Gupta, 2022; Song, Park, & Park, 2022).

DBSs can be integrated into the stages of disaster management that involves collaboration with early warning systems to plan disaster intervention tasks at the preparedness stage; providing real-time imaging and hazard assessment to guide responders to make an appropriate rescue plan during disaster; aiding relief dispatch, victim localization, rescue optimization and providing communication at the recovery stage. Network communication services are essential for a successful disaster management and drones can play a valuable role in providing uninterrupted emergency communication systems. Major disasters, such as earthquakes and storms, usually result in damage to telecommunication infrastructures and power supply networks which are vital services in the early hours of rescue. In the aftermath of a disaster, the foremost priority is ensuring the protection and preservation of human life. Short response time is the key to save lives in disasters. Such breakdown of primary infrastructures limits authority control for acquiring situational awareness about human casualties, primary infrastructure damages, disruption of supply chain services and coordinated rescue operation efforts. In these situations, individuals require guidance, timely information, and situational updates, and frequently need to communicate distress signals or share their whereabouts with emergency response units. Therefore, it is vital that an efficient temporary uninterrupted communication network is deployed as fast as possible to coordinate emergency response teams and find isolated victims. Such a temporary network will provide people with great help in emergency situations. In this case, DBSs can be deployed where in case of failure or complete damage of terrestrial infrastructure as a result of a disaster. The main advantage of DBS assisted communication is that it is the most favourable method to provide wireless coverage and connectivity to the end-users who have no infrastructure coverage (Shahzadi, Ali, Khan, & Naeem, 2021). DBS is the most cost-effective and fastest method to recover the connectivity for disaster management. In addition, they can easily change positions and move continuously covering a particular area. Therefore, DBSs are becoming a vital part of communication networks during post-disaster due to their high mobility, reliable connectivity, fast deployment, and low-cost factor. Hence, the usage of DBSs can be an applicable solution to provide rapid public safety communication. For example, DBSs were used to provide emergency 4G coverage to Puerto Rico in the aftermath of Hurricane Maria in 2017 (Parvaresh, Kulhandjian, Kulhandjian, D'Amours, & Kantarci, 2022).

This thesis focuses on the DBS deployment problem in the communication systems to provide uninterrupted communication services therefore to prop disaster recovery operations. The employment of DBSs for that purpose reveals the DBS deployment and trajectory problem (DBSDTP), which must be studied from the optimization point of view. The DBSDTP involves identifying both the quantity and optimal placement of DBSs to be positioned within the target area and determining the optimal trajectories for DBSs' locations and charging stations to guarantee network connectivity as uninterrupted and accurate as possible. By considering energy limitations and the fairness in service time distribution together with the deployment and routing decisions, the DBSDTP turns into an equitable and efficient resource allocation problem, particularly in emergency response. In essence, this thesis aspires to formulate and solve the DBSDTP from the optimization point of view to support and guide the post-disaster management from the communicational perspective as accurately as possible.

1.2 Framework of the Dissertation

This thesis introduces the DBSDTP as an optimization problem, with a particular emphasis on the notion of fairness, which plays a critical role in disaster scenarios. Two distinct optimization models are developed, each incorporating a different interpretation of fairness. Both models share a common set of constraints, including limitations related to battery capacity, DBS mobility (expressed through routing constraints), and structural constraints derived from the underlying system network configuration.

The first model builds upon the well-established Maximal Covering Location Problem (MCLP) from the literature, which is extended by integrating assumptions and constraints specific to the problem context. In this formulation, fairness is enforced via hard constraints, while the objective function aims to maximize both spatial and temporal coverage.

The second model, in contrast, addresses fairness through the objective function rather than via strict constraints. By relaxing certain hard constraints and simplifying structural components, this version of the problem is reformulated as a covering tour problem (CTP). The dual modelling perspectives allow for a rich analysis of a relatively underexplored area in the existing literature.

To solve the proposed problem formulations, Mixed Integer Linear Programming (MILP) is employed. The models are tested on synthetically generated instances, demonstrating effectiveness for small- and medium-scale scenarios. For large-scale instances, a metaheuristic approach based on the Greedy Randomized Adaptive Search Procedure (GRASP) is proposed to obtain high-quality solutions within reasonable computational times.

The main objectives of this thesis are to define the optimization problem of using DBSs for emergency communication, to formally specify the problem environment (including assumptions and constraints), to present a comprehensive literature review, and to develop mathematical formulations of the problem variants. Furthermore, the thesis aims to demonstrate the applicability of MILP for smaller problem instances and to design a GRASP-based metaheuristic suitable for deployment in large-scale disaster scenarios.

1.3 Contributions

This thesis offers several key contributions to the literature on disaster response optimization through the development of two complementary mathematical models for DBS deployment:

- A novel coverage model is proposed that utilizes multiple DBSs to establish an effective communication network for search and rescue operations. The model incorporates problem-specific constraints to ensure the continuity of service and spatial fairness across affected regions. These constraints reflect realistic operational limitations, including battery capacity, DBS mobility, and structural constraints of the communication system.
- In the second model, the study moves beyond spatial equity by introducing a new fairness measure that explicitly accounts for temporal coverage, an aspect often overlooked in previous work. Building on and extending the classic CTP, this model integrates service time optimization and scheduling constraints that allow for multiple coverage for the same location, thereby offering a more dynamic and temporally balanced response strategy. Unlike the first model where fairness is enforced via hard constraints, this version embeds equity considerations directly within the objective function, enabling a flexible and adaptive approach to service distribution.
- A GRASP-based metaheuristic algorithm is designed to handle large-scale problem instances effectively, delivering high-quality solutions in practical computation times, particularly in cases where MILP approaches become computationally infeasible.

Together, these contributions advance the state of research in equitable and effective deployment of DBS communication systems for disaster environments by addressing both spatial and temporal dimensions of fairness, and by offering scalable solution approaches suitable for real-world applications.

1.4 Outline of the Thesis

This thesis is structured into six chapters, beginning with the introduction presented in Chapter One. The subsequent chapters are organized as outlined below.

Chapter Two provides a comprehensive literature review on the field of DBS communication applications from an operational research perspective and relates the problem addressed in this thesis by highlighting its novelty. The challenges of using DBSs in network communication are presented with detailed explanations. More precisely, the optimization problems developed for DBS applications are categorized and analysed in detail.

Chapter Three presents the problem characteristics and constraints with an innovative coverage model designed to deploy multiple DBSs to build a reliable communication network for emergency situations. The model embeds tailored constraints that promote uninterrupted service delivery and spatial equity among impacted areas. These constraints are grounded in practical considerations, such as battery limitations, mobility requirements, and the structural characteristics of the communication infrastructure. Additionally, a set of problem instances is generated and included in this chapter to evaluate the model's performance under various scenarios and operational conditions.

Chapter Four focuses on a new model in which fairness is incorporated directly into the objective function. Building upon and extending the classical CTP, the formulation integrates service time optimization and scheduling constraints that enable multiple visits to individual locations, resulting in a more responsive and temporally balanced deployment strategy. Unlike the first model, which enforces fairness through hard constraints, this approach embeds equity into the objective itself, offering greater flexibility and adaptability in service distribution. To assess its performance, the model is tested on the generated problem instances, ensuring a consistent basis for evaluating solution quality under diverse operational conditions.

Chapter three and four provide a comprehensive evaluation of the proposed models by analysing their performances. Recognizing that the mathematical formulations are well-suited for small- and medium-scale problems but become computationally impractical for larger instances, therefore a GRASP-based metaheuristic algorithm is introduced early on as a complementary solution approach in Chapter Five. The chapter presents a detailed analysis using performance indicators such as computation time, coverage levels, and fairness metrics to assess the models' effectiveness. The results highlight and demonstrate that embedding fairness into the objective function enhances service responsiveness without compromising overall solution quality.

Chapter Six presents the main contributions and conclusions of the work presented in this thesis, concluding remarks, and suggestions for future research.

CHAPTER TWO

AN OVERVIEW ON THE COMMUNICATION NETWORKS SUPPORTED WITH THE DRONE BASE STATIONS IN EMERGENCY SITUATIONS

2.1 Chapter Introduction

This chapter presents DBS applications specifically for communication and emergency situations and is organized as follows: Section 2.2 briefly explains the use of DBS for communication applications, including its specifications. Section 2.3 presents the challenges of using DBS in network communication by categorizing each challenge with detailed explanations. Section 2.4 provides a comprehensive literature review focusing on operational research methodologies and relates the problem addressed in this thesis by highlighting its novelty. Finally, Section 2.5 summarizes the context of this chapter.

2.2 DBS Supported Communication Networks

Communication networks supported by DBSs possess distinct features such as sustained high-altitude hovering, extended coverage duration without the need for recharging, and agile mobility across three-dimensional space. Effective utilization of DBSs in specific wireless networking applications requires careful consideration of various factors, including their operational capabilities and flight altitudes. This section categorizes drones according to their characteristics and applications of DBS supported communication networks. The operational domains of drones differ considerably based on features like size, flight duration, and load capacity. Accordingly, they are categorized using various classification frameworks depending on specific parameters. Many researchers classified drones into different categories based on their weights (Zakora & Molodchick, 2014) ranges and operational purposes (Hassanalian & Abdelkefi, 2017). Generally, they can be categorized by their features including weights, wing spans, wing loadings, ranges, maximum altitudes, speeds, endurances, and production costs. These features must be considered in the modelling. This section briefly summarizes the types of drones and their restrictions for the operations.

2.2.1 Types of Drones

Drones can be categorized into fixed-wing drones and rotary-wing drones. Among the various drone categories, fixed-wing models are regarded as the most sophisticated. They use wings and require relatively higher speeds for flight. They have long endurance and can stay in the air for up to 16 hours. Fixed wings can float into the air without moving in any direction. Fixed-wing drones are primarily employed in applications such as aerial surveying and the inspection of infrastructure like pipelines and power transmission lines. Fixed-wing drones are additionally utilized in delivery operations, where extended flight duration and payload capacity are essential. For instance, the medical logistics company Zipline employs its custom-designed fixed-wing drones to transport blood and other critical medical supplies to remote regions (Dukowitz, 2019). Their high cost and the necessity for specialized operator training present notable limitations to their widespread adoption (Tahir, Böling, Haghbayan, Toivonen, & Plosila, 2019). However, this type is not suitable for hovering and flying slowly. On the other hand, rotary-wing drones possess dynamic mobility, enabling vertical take-off and landing as well as the ability to hover steadily at a fixed point, which allows for sustained cellular coverage in targeted areas. Their high degree of maneuverability makes them particularly well-suited for supporting cellular networks, either by precisely positioning base stations (BSs) at strategic locations or by following predefined flight paths while transporting BSs (Fotouhi, et al., 2019). They are designed based on the number of rotors (usually up to eight). Multirotor ones are cheaper and easier to build. Quadcopters are the most known among them. These types of drones are frequently utilized for fundamental tasks including aerial photography and video-based surveillance. Additionally, quadcopters are well-suited for observational missions, particularly in the assessment of areas affected by natural disasters. However, rotary-wings have time and speed limitations. These drones are capable of covering distances up to 7 kilometers, maintaining an average flight duration of 25 to 30 minutes, and reaching a typical maximum speed of 60 km/h without performance issues (Ruiz Estrada & Ndoma, 2017). They consume significant power compared to fixed wings.

With the development of technology, to bridge the gap between fixed-wing and rotary-wing models, hybrid drones combining features of both types have recently been introduced to the market. Hybrid fixed/rotary wing is called Parrot Swing which can take off vertically, quickly reach its destination by gliding through the air, and then switch to hovering using four rotors.

2.2.2 Altitude

Altitude refers to the maximum height of a drone can reach. In DBS-supported communication systems, the maximum operational altitude is a key factor, as altitude adjustments are necessary to optimize ground coverage and meet varying quality of service (QoS) demands (Al-Hourani, Kandeepan, & Lardner, 2014). Overall, aerial communication platforms can be divided into two types: high altitude platform (HAP) and low altitude platform (LAP). HAPs provide wider coverage and can stay in the air for a long duration, while LAPs have high mobility and allow fast deployment. LAPs are more cost-effective however can be used for short period. On the other hand, HAPs rarely considered in the literature on DBS-aided communication since their deployment is more complex and expensive.

2.2.3 Weight, Size, and Payload

Drones can be classified into nano, micro, and small according to their weight and size. Compared to micro and nano drones, small UAVs are generally heavier, larger, and capable of achieving higher speeds. On the other hand, payload is a measurement for maximum weight capability that can carry. Their weight range spans from a few tens of grams to several hundred kilograms. Larger ones can carry larger payloads or the more equipment, so they require higher battery capacity. These payloads could be video cameras or sensors being used for surveillance and commercial purposes. For providing network communication services via DBSs, a minimum payload threshold of a few kilograms is generally expected.

2.2.4 Endurance and Energy

The duration a drone can remain airborne without the need for recharging or refueling is commonly termed its flight endurance or operational flight time (Fotouhi, et al., 2019). Most drones have limited flight range because of their restricted energy capacity. Therefore, they require to exchange or recharge their batteries during flight operations. This aspect can be modelled as maximal operation time (Wang, et al., 2018; Tokekar, Vander Hook, Mulla, & Isler, 2016), maximal flying distance (Savuran & Karakaya , 2016; Guerriero, Surace, Loscri, & Natalizio, 2014) or the limited number of drones during one flight (Ergezer & Leblebicioğlu, 2014). Energy consumption of a drone may depend on the type, flying altitude, payload and weather conditions. As the weight increases, its energy consumption increases. Nevertheless, the constrained flight endurance of drones remains a significant barrier to their widespread integration into communication networks, as energy is needed not only for propulsion but also to operate onboard components such as base stations. Utilizing solar energy as a power source presents a promising solution to mitigate this limitation (Shaheed, et al., 2015).

2.2.5 Controlling Methods

While certain drones require continuous manual operation by a human pilot, fully autonomous systems possess the capability to independently execute complex missions even under uncertain or dynamic environmental conditions (Dalamagkidis, 2014). Autonomous control can be divided into two types. Semi-autonomous in which drones are controlled by human only start-stop while other functions are independent. Fully autonomous includes only initiated by human. However, swarm control where drones are used in the swarm for cooperative mission, e.g., multi-DBS-assisted wireless networks. A drone is also capable of dynamically determining its trajectory in real time by processing environmental data—such as terrain features, obstacles, and the positions of nearby drones—collected through its onboard sensors.

In the DBS wireless communication literature, the multirotor DBSs, especially quadcopters, are considered for using due to their advantages such as the ability to take off and land vertically, as well as hovering (Zeng, Xu, & Zhang, 2019). They are rotorcraft types which is lifted and propelled up to eight rotors as well as they can hover at a fixed location. Since they can carry relatively heavy objects, it can be mounted camera, wireless communication platforms and base stations on them. The quadrotor DBS is a relatively simple, affordable, and easy to fly system, and thus it has been widely used to implement in mobile wireless networks, and communications (Valavanis & Vachtsevanos, 2014). In Scotland, the Finnish technology company Nokia, in collaboration with the UK-based mobile operator EE, has deployed compact quadcopter DBSs equipped with portable mobile base stations for aerial testing (Russon, 2018).

2.3 Network Connectivity Challenges

DBSs are emerging as a key component in the evolution of next-generation wireless communication systems, including 5G and beyond. DBSs can be deployed as flying base station where in case of failure or complete damage of terrestrial infrastructure due to some disaster situations. DBS is the most cost-effective and fastest method to recover the connectivity for disaster management. Therefore, DBSs are becoming a vital part of communication networks due to their high mobility, fast deployment and low-cost factors. Although DBSs offer numerous benefits in wireless communication systems, several critical challenges must be overcome to enable their effective deployment and utilization. Figure 2.1 summarizes the benefits, applications and challenges in DBS-aided communication networks. Some restrictions due to the aspects of DBSs must be considered in planning of operations. Challenges are addressed in the literature as below:

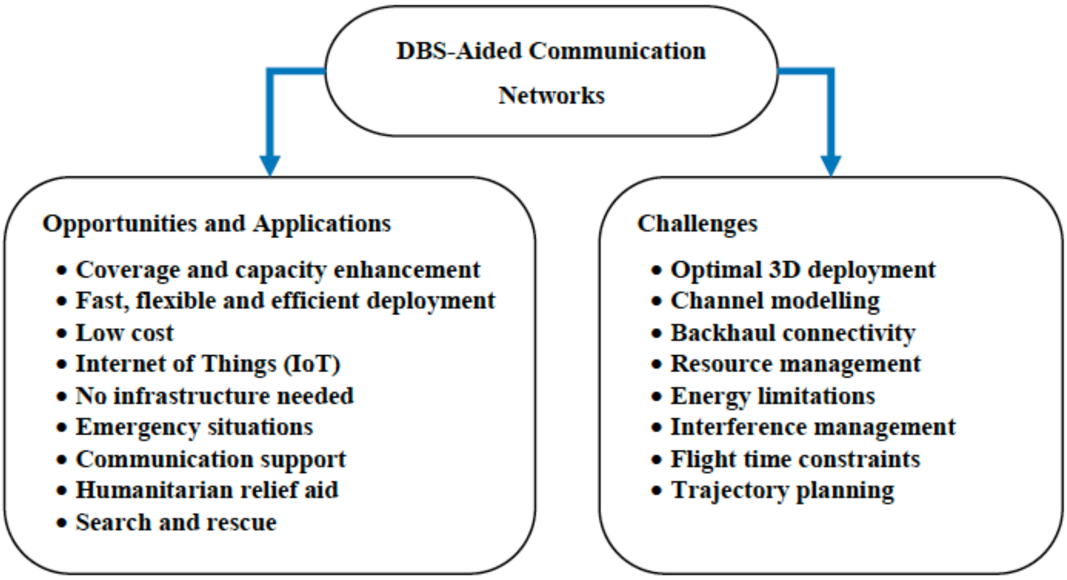

Figure 2.1 Opportunities, applications and challenges for DBS-aided communication networks (Mozaffari, Saad, Bennis, Nam, & Debbah, 2019)

2.3.1 DBS Placement

DBS placement is one of the biggest challenges since it has a direct impact on communication quality, coverage, throughput and connectivity. They can be deployed in different modes including 2D, 3D, single or multiple. In a 3D plane where the altitude is a key design consideration while in 2D placement, the altitude of a DBS is considered as a constant. 3D placement decides the optimal altitude where DBSs should have been deployed to cover as many users as possible while 2D placement aims to maximize the coverage area.

Due to resource constraints and their significance in managing network performance, numerous studies have aimed at optimizing both the 3D positioning of DBSs and the allocation of network resources to maximize throughput. While deploying DBSs, their flight times and energy constraints must also be considered, as they directly impact the network performance. Effective DBS deployment requires consideration of various elements such as user distribution, radio channel properties, terrain features, and operational constraints like energy availability, battery life, and allowable flight duration. In the case of multi-DBS deployment, the interference among them should be considered (Kalantari, Yanikomeroglu, & Yongacoglu, 2016; Košmerl & Vilhar, 2014).

2.3.2 Energy Management

DBSs' battery is a limited resource. On-board energy is utilized for various purposes such as communication, movement, flight control, and processing of collected data. Energy consumption also depends upon physical parameters like environmental conditions, navigation path, DBSs' physical characteristics and mission details etc. In the case of heavy weather conditions or the weight is also increasing, which results in high energy consumption. As a result, the limited flight duration often falls short of enabling sustained and long-term wireless coverage. Energy constraint directly defines DBS operation lifetime. Therefore, energy efficiency is extremely important to be considered to prolong the lifetime (Zeng & Zhang, 2017). Main components of DBS energy consumption are composed of communication and propulsion energy. Communication-related energy is expended on tasks such as signal transmission, computation, and signal processing, whereas propulsion energy is associated with the mechanical power required for maneuvering and maintaining the drone's position in the air (Mozaffari, Saad, Bennis, Nam, & Debbah, 2019). In general, propulsion energy is higher than communication energy.

In the literature, effective management of on-board energy is a vital research area to improve the operational lifetime. Many researchers investigate advanced battery technologies like batteries and fuel cells (Lee, Park, Kim, & Kwon, 2014) and utilization of green energy solutions, such as solar-based energy harvesting and wireless power transfer (Wu, et al., 2018) or via electromagnetic field generated by power lines (Simic, Bil, & Vojisavljevic, 2015). Antenna array configuration aimed at enabling wireless energy transmission constitutes another key focus in current research efforts (Shahzadi, Ali, Khan, & Naeem, 2021). Moreover, Boukoberine, Zhou, & Benbouzid, (2019) have studied a hybrid energy system incorporating multiple sources—such as batteries, fuel, solar panels, and supercapacitors—to ensure continuous power supply. On the other hand, a few studies review the wireless charging techniques for DBSs (Lu, Bagheri, James, & Phung, 2018).

2.3.3 Backhaul Connectivity

Ensuring reliable backhaul connectivity is essential in communication network architecture. Terrestrial networks typically employ wired solutions to connect base stations with the core network components. Since wired connections can be expensive, wireless backhauling can be considered. Backhauling refers to the process of aggregating data from access points and transmitting it to the core network. Wireless backhaul is required for the fast processing of data. As no infrastructure is required, backhauling via drones can be more efficient and cost effective (Masroor, Naeem, & Ejaz, 2021).

In DBS-assisted wireless communication systems, ensuring wireless backhaul connectivity—compared to terrestrial communication—presents a notable challenge. The backhaul process must address several critical issues, including optimal placement, capacity limitations, data security, and payload constraints, especially since it may be required to store information temporarily or for extended periods. The positioning of DBSs plays a vital role, as varying their altitude and coverage area can significantly enhance the efficiency of backhaul operations.

2.3.4 Interference Management

In case of multiple DBS deployment, DBSs must be deployed in such a way of avoiding interference among them. Interference avoidance must be considered to maximize network efficiency in terms of throughput and coverage. Intuitively, When the number of DBSs deployed increases, interference can be avoided by decreasing their operational altitude, which in turn reduces each station’s coverage area and prevents overlaps in their communication areas (Mozaffari M., Saad, Bennis, Nam, & Debbah, 2019). Developing effective scheduling strategies is essential to minimize interference not only among DBSs but also between aerial and terrestrial base stations in DBS-assisted cellular networks.

2.3.5 Resource Management

Resources in DBS network can be addressed as shared resources between DBSs and existing terrestrial base stations as well as related to DBS features like energy and time, interference from air to ground or air to air. Efficient resource management should be considered to design an optimized network.

An important resource while considering network coverage is on network bandwidth, where it may be expected that many users are trying to connect to each other (Guo, Devine, & Wang, 2014). Given the rapidly growing demand for bandwidth, allocation strategies must account for bandwidth scarcity as a critical constraint in network communication systems. In the literature, many researchers have presented the optimized bandwidth allocation problem in heterogeneous DBSs' networks (i.e. drone is acting as a relay node) (Pan, Yi, Yin, Yu, & Li, 2019; Yan, Peng, & Cao, 2019). Heterogeneous network represents a network including DBSs for supporting ground terrestrial nodes along with data transmission links which are used for connecting all the ground users (Shahzadi, Ali, Khan, & Naeem, 2021).

Studies in the literature indicate that dynamic time slot allocation outperforms fixed time-slot schemes in terms of network throughput (Cheon, Cho, & Kim, 2017). Their study examines two distinct scenarios: in the first, a single DBS simultaneously handles wireless charging and data reception, while in the second, these functions are distributed between two separate DBSs. Ye, Kang, Joung, & Liang, (2019) proposed an optimized scheme for allocating hovering and flight durations in a communication network wirelessly powered by DBS nodes. Guo, Yin, & Hao, (2019) investigated a wireless communication network where the DBS functions as a communication relay for ground terminals but requires periodic recharging to maintain uninterrupted service. Their study focuses on maximizing the minimum average data rate of ground users by optimizing the time allocation between the DBS's charging and service periods. Park, Lee, Eom, & Lee, (2019) addressed a time allocation problem within a DBS-assisted IoT network, wherein ground devices first receive wireless energy from DBSs and then forward their data signals to the same DBS units.

.

DBS-assisted communication networks have specified the power to transmit in a particular range. DBSs operate at varying altitudes to effectively transmit signals to designated users. However, transmitting at maximum power significantly increases battery consumption, thereby reducing their operational airtime unless recharged. To ensure energy efficiency and prolong flight duration, DBSs must deliver interference-free signals using minimal transmission power. Consequently, energy management emerges as a critical factor in their deployment (Zhan, Zeng, & Zhang, 2018). On the other hand, joint power and trajectory optimization problems were proposed to maximize the throughput or minimize the outage probability of the network (Chen, 2020).

DBS placement and user association are completely related problems. Many researchers have considered joint 3D placement and user association problem simultaneously (Huang, et al., 2019). On the other hand, as DBSs are battery operated, energy limitation is a major constraint for efficient DBS utilization. The wireless charging concepts have become a crucial part of DBS assisted communication networks. Therefore, joint energy management, placement and user association problems have been addressed recently and simultaneously (Yin, Li, & Yu, 2019).

2.3.6 Mobility and Trajectory Planning

Optimal path planning represents a critical challenge in DBS-assisted communication systems. In this context, trajectory design plays a central role, as it defines the sequence of discrete waypoints and ensures smooth transitions between them. Well-planned trajectories contribute to controlled mobility, reduce interference, and enhance overall coverage performance. The trajectory can have any mode of path horizontal, vertical, and circular, depending on the type of scenario. An optimal DBS path must consider several other parameters such as flight time, energy constraint, collision avoidance, user requirement etc. Furthermore, the continuous trajectory optimization problem for DBSs is analytically intractable due to the involvement of infinitely many variables, namely the drones' time-varying locations (Zeng, Zhang, & Lim, 2016).

2.3.7 *Channel Modelling*

Channel properties play a crucial role in determining communication quality, and in DBS-enabled networks, these characteristics differ significantly from those observed in terrestrial cellular systems due to their unique aerial architecture. In DBS communication channel modelling depends on its location, altitude, type and channel characteristics etc. Channel resource management becomes a critical challenge in scenarios involving multiple DBSs connected to ground users, particularly when signal propagation is obstructed by large buildings or other environmental obstacles. This loss is referred to as Path Loss (PL). In traditional communication networks it is computed according to the Euclidean distance between transmitter and receiver. However, altitude of a DBS must be considered while computing PL in the network. All communication paths between DBSs and users assumed Line of sight (LoS) and Non- Line of sight (NLoS) paths, making the channel model different each time (Masroor, Naeem, & Ejaz, 2021). LoS propagation describes a scenario in which data exchange between two nodes can occur only when there is a direct, obstacle-free path. Satellite links and microwave communications are standard examples of technologies that rely on this principle. LoS propagation is feasible only when the receiver lies within the circular area around the transmitter, where the radius corresponds to the tangential range of the transmitted signal (Line-of-sight propagation, n.d.). It is directly related to height. For example, as the altitude of DBS increases, chances of LoS path also increases. On the other hand, NLoS refers to the scenario in which radio signals are impeded by intervening objects, such as tall structures, trees, uneven terrain, or electrical infrastructure, thereby degrading the communication link between transmitter and receiver (Non-line-of-sight propagation, n.d.).

Based on the most cited model in the literature to compute PL, it can be referred to (Al-Hourani, Kandeepan, & Lardner, 2014). PL between user i and DBS j (PL_{ij}) can be expressed as follows.

$$PL_{ij} = 20\log_{10}\left(\frac{4\pi f_c E_{ij}}{c}\right) + \frac{\varphi_{LoS}-\varphi_{NLoS}}{1+\alpha e^{-\beta(\theta_{ij}-\alpha)}} + \varphi_{NLoS} \tag{2.1}$$

where E_{ij} is Euclidean distance and θ_{ij} is the elevation angle between user and DBS, and $f_c, c, \alpha, \beta, \varphi_{LoS}$ and φ_{NLoS} are certain fixed parameters defined by the characteristics of the operating environment (e.g., urban or suburban settings).

2.4 Literature Review on DBS-Assisted Communication Network Applications

DBS technology has being grown rapidly, and DBSs have being utilized in various application areas such as civil infrastructure inspection (Guerrero & Bestaoui, 2013; Outay, Mengash, & Adnan, 2020), agriculture for crop management (Campo, Ledezma, & Corrales, 2020; Tiotsop, Servetti, & Masala, 2020; Bah, Hafiane, & Canals, 2023), delivery of goods (Sacramento, Pisinger, & Ropke, 2019; Dukkanci, Kara, & Bektaş, 2021; Macias, Angeloudis, & Ochieng, 2020), search and rescue operations (Martinez-Alpiste, Golcarenarenji, Wang, & Alcaraz-Calero, 2021; Kyriakakis, Marinaki, Matsatsinis, & Marinakis, 2022; Zhang, Li, Wang, Li, & Li, 2022; Yanmaz, 2023) management of the recent COVID-19 outbreak (Vazquez-Carmona, Vasquez-Gomez, Herrera-Lozada, & Antonio-Cruz, 2022; Banik, Hossain, Govindan, Nur, & Babski-Reeves, 2023) and communication network capacity enhancement (Cicek, Gultekin, & Tavli, 2019; Nemer, Sheltami, & Mahmoud, 2020; Hayajneh, Bani-Hani, Shakhatreh, Anan, & Sawalmeh, 2021). Recently, DBSs have also been explored to help in emergency conditions by delivering humanitarian relief (Chowdhury, Emelogu, Marufuzzaman, Nurre, & Bian, 2017; Chauhan, Unnikrishnan, & Figliozzi, 2019; Jeong, Yu, Min, & Lee, 2020; Gentili, Mirchandani, Agnetis, & Ghelichi, 2022; Ghelichi, Gentili, & Mirchandani, 2022; Dukkanci, Koberstein, & Kara, 2023) and post-disaster assessment (Oruc & Kara, 2018; Coutinho, Fliege, & Battarra, 2019; Chowdhury, Shahvari, Marufuzzaman, Li, & Bian, 2021; Zhang, Jia, Zhu, Adulyasak, & Ma, 2023) Moreover, the utilization of DBSs for emergency communication systems in post-disaster scenarios have been addressed by (Tuna, Nefzi, & Conte, 2014). DBSs can be used as base stations to provide uninterrupted communication network coverage as part of the disaster management if the existing terrestrial network was damaged or is not fully operational (Mozaffari, Saad, Bennis, & Debbah, 2017). The purpose of using DBSs for communication can differ depending on the type of emergency held in the area. In a flood disaster, network coverage DBSs are used to assess the number of escaped people and vehicular traffic routes used resulting determining evacuation plan (Malandrino, Chiasserini, Casetti, Chiaraviglio, & Senacheribbe, 2019). In a wildfire situation, communication DBSs are used for acquiring real-time environmental data and transmitting it to the central control unit (Worden, Murray, Karwan, & Ortiz-Peña, 2020). In a disaster situation such as earthquake or hurricane where damage to roads and network infrastructure, DBSs can provide network coverage for first responders to connect with headquarters and disaster-affected people to inform about their location and request help (Masroor, Naeem, & Ejaz, 2021). Although many research endeavours have been conducted on DBS-aided communications, very few works have focused on how to use them as recovery mechanism in disasters (Qadir, Ullah, Munawar, & Al-Turjman, 2021; Khan, Gupta, & Gupta, 2022).

This thesis focuses on DBS deployment and trajectory optimization to establish communication network for effective disaster management. For this purpose, a set of popular search engines including Google Scholar, Web of Science and Scopus were analysed to retrieve articles relevant to the subject of interest. The keywords or search strings used within this analysis include phrases like “drone base station deployment”, “drone routing”, “drone trajectory planning”, “drone communication networks in disaster management”, “drone emergency communication”, and “drone public safety communication”. These keywords were also searched using “UAV” word, abbreviation for “unmanned aerial vehicle”, only replacing with “drone” in each string. Furthermore, the retrieved articles have been published in range of years 2010-2025 and the type of each article is a review or a research article. Accordingly, the current literature has scarcely investigated the DBSDTP on the aspect of communication network recovery after a disaster. This literature review has been conducted focusing on some challenges which need to be addressed to achieve efficient utilization of DBSs for communication recovery after a disaster. Studies are analysed according to optimization applications such as coverage, trajectory, energy efficiency and battery optimization.

2.4.1 *Coverage Optimization*

Area coverage is an application area of DBSs for generally examination of disaster and accident sites. DBSs can be used for assessing and monitoring risk as well as assisting until the damaged communication networks are repaired or helping deliver relief supplies to devastated areas. Advancements in technology have led to the enhancement of high-altitude platforms deployed in the stratosphere, enabling them to function as gateways and facilitate communication links for computing devices—for example, Facebook's Aquila drone (Otto, Agatz, Campbell, Golden, & Pesch, 2018). However, such platforms have high-cost and it is difficult to install them. Alternatively, low-altitude platforms like rotorcrafts and fixed-wing drones offer advantages in terms of quick deployment and reduced operational costs, making them ideal for temporary use cases, including large gatherings, sporting events, or post-disaster scenarios where ground communication systems are impaired (Zeng, Zhang, & Lim, 2016). Another optimization problem is the locations of recharging facilities on a network, also called DBS-recharging problem. However, DBSs have restricted flight range due to their limited battery. The potential locations of the recharging stations must be determined to maximize the travel range. These assumptions derive a coverage location model which optimizes the location of recharging stations to help increase coverage range of drones (Hong, Kuby, & Murray, 2018). On the other hand, the coverage location problems for DBSs are more closely related to the disaster response. Many facility location models are developed to maximize coverage in the context of delivering the humanitarian relief using DBSs in post-disaster circumstances (Chowdhury, Emeloglu, Marufuzzaman, Nurre, & Bian, 2017). The use of DBSs has emerged as a promising direction in the field of telecommunications (Gupta, Jain, & Vaszkun, 2016). Planning location-allocation of DBS also involve area coverage decisions. However, unlike traditional coverage problems, these decisions incorporate elements of probability theory and nonlinear formulations arising from communication-related constraints. For instance, to establish connectivity with a DBS, a mobile user should be located within its communication range.

Coverage problems with DBSs are closely related to general coverage location problems. Like in set covering problem (SCP), DBSs must find paths to cover *all* points of a given area at the lowest cost, called as *full coverage*. Typical objective functions are formulated to minimize cost metrics associated with distance (Torres, Pelta, Verdegay, & Torres, 2016), completion time (in case of several DBSs or setup times between DBS flights) (Avellar, Pereira, Pimenta, & Iscold, 2015; Nejdati, Izbirak, Vizvari, & Arkat, 2016), or minimizing energy expenditure, which varies depending on the drone's operating altitude and its acceleration vector (Li, Wang, & Sun, 2016). Several applications consider one DBS covering some area (Xu et al., 2014; Li et al., 2011) while the others take several DBSs considering limited energy capacity (Chauhan, Unnikrishnan, & Figliozzi, 2019; Nejdati, Izbirak, Vizvari, & Arkat, 2016; Avellar, Pereira, Pimenta, & Iscold, 2015). On the other hand, similarly in maximal covering location problem (MCLP), DBSs aim to maximize coverage given a limited budget such as limited energy or time, called as *partial coverage*. Such problems may be related to maximize information collection in many applications. For example, in use cases like precision agriculture, the informational importance of different subregions within the coverage area can vary, with some areas offering more critical insights than others. Therefore, objective function is to maximize the value of collected information which also called benefit or reward. For instance, during soil analysis, the soil area could be classified according to nitrogen levels with the aerial images (Tokekar, Vander Hook, Mulla, & Isler, 2016). Related to this information, a DBS may detect the flight area with associated rewards and take aerial images according to rewards. For general covering location problems, SCP and MCLP, readers refer to Farahani, Asgari, Heidari, Hosseininia, & Goh, (2012). DBSs can take stationary or mobile position during coverage problem. In some applications, such as emergency response monitoring may necessitate the deployment of multiple heterogeneous DBSs to fixed observation points, where they are required to hover for extended durations (Otto, Agatz, Campbell, Golden, & Pesch, 2018). Proposed optimization frameworks often ensure that every designated target is covered by at least one DBS, while simultaneously seeking to reduce the number of DBSs utilized and the overall energy expenditure (Zorbas, Pugliese, Razafindralambo, & Guerriero, 2016).

Placement of DBSs is one of the most challenging issues as it has a direct impact on communication quality and connectivity reliability. This challenge may include the placement of a single DBS or multiple DBSs over the stationary or mobile locations. Stationary placement involves positioning a set of DBSs at fixed locations over an area, while mobile placement involves changing their position over time. Some studies have focused on optimizing a single stationary DBS as a relay node to increase network capacity in a heterogeneous network including terrestrial base stations (Meer, Ozger, & Cavdar, 2023) or as a communication helper unit to replace non-functional terrestrial base stations (Cui, Hu, & Chen, 2021). However, in a larger disaster area with a large number of victims that need to be served, multiple DBSs are required to provide efficient coverage. Multiple DBS coverage has been considered in both the heterogeneous networks (Sharafeddine & Islambouli, 2019; Barick & Singhal, 2022) and DBS-only networks (Li, Lu, Zhang, Tian, & Pang, 2019; Akram, Awais, Naqvi, Ahmed, & Naeem, 2020; Park, Nielsen , & Moon, 2020; Bai, Li, Fang, Zhang, & Tao, 2020; Masroor, Naeem, & Ejaz, 2021). On the other hand, since victims in disasters are randomly distributed over a very large area, DBSs can fly over the area due to their mobility and flexibility. Although studies have shown that DBS placement is a compelling problem and have developed many approaches to solving it, the movement of the DBSs over the area has not been considered.

2.4.2 Trajectory Optimization

Optimal route planning for DBS placement is another important challenge in drone communication systems. It can help to moderate the movement of a limited number of DBSs and provide better coverage of the area. A single DBS route was designed to collect data (Amrallah, Mohamed, Tran, & Sakaguchi, 2023) and provide communication to victims from a central DBS flying in discrete time slots (Zhao, et al., 2019; Javed, et al., 2023) in a heterogeneous network. In a study addressing the DBS-only network, multiple DBSs were placed and clustered to account for DBS movement (Arafat & Moh, 2019). By developing a clustering approach, an anchor DBS was selected as the cluster head in each cluster, and other cluster members were positioned according to the position of the cluster head. Hence, their positions were randomly initialized, and then they all searched for better solutions by changing their current positions using particle swarm optimization- based algorithms. In this study, the movement of DBSs was designed to find accurate and efficient positions with a location-aware mechanism. Unlike previous works, this paper assumes that each DBS has a route to visit the disaster areas. This is because the need to effectively manage the limited number of DBSs and provide continuous coverage of the disaster area requires the movement of DBSs.

2.4.3 Energy Efficiency and Battery Optimization

The limited lifetime of a DBS is one of the main factors limiting its widespread use in communication networks. This challenge has not been well addressed in the relevant literature. Some works have considered a network of multiple DBSs hovering over a given location by considering the battery capacity only for the flight times of the DBSs (Deruyck, Wyckmans, Joseph, & Martens, 2018). Another work (Zhao, et al., 2022) considered an adaptive movement of DBSs to maintain connectivity with mobile users in a disaster area where some ground base stations have failed. However, the battery level and flight time tracking were not considered. Due to their limited flight time, the DBSs were unable to provide continuous coverage on the disaster area, and their batteries had to be either replaced or recharged while in flight. Some works (Malandrino, Chiasserini, Casetti, Chiaraviglio, & Senacheribbe, 2019; Jin, Luo, Shi, & Wang, 2024) considered the return to the recharging station. In the study by Malandrino, Chiasserini, Casetti, Chiaraviglio, & Senacheribbe, (2019), they restricted several DBS activities (covering, traveling, and recharging) to predefined time steps of 10 min each. They also assumed equal battery consumption rates for both movement and coverage activities, representing the DBS's battery capacity as the maximum allowable number of time steps before requiring a recharge. Jin, Luo, Shi, & Wang, (2024) developed an integrated placement model for DBSs and a Capsule Airport function as a recharging and retrieval hub for DBSs, aiming to enhance their limited coverage and operational endurance in emergency communication scenarios during disasters. Ramos-Ramos, González-Vegas, Berrocal, & Galán-Jiménez, (2024) aimed to reduce the total energy consumption of the DBS group while maintaining user service quality in rural areas. They provided an energy consumption model for information transmission and execution of the DBS itself. Bozkaya, Özçevik, Akkoç, Erol, & Canberk, (2022) also proposed energy efficient model for dynamic DBS placement considering handover management. Since DBSs are battery-constrained, handover is frequently required. They proposed a handover scheme while predicting the energy efficient DBS trajectories. Various handover procedures have been proposed to preserve uninterrupted user-DBS communication during instances when the serving DBS must be substituted due to battery depletion and subsequent recharging needs (Hu, Yang, Wang, & Chen, 2019; Banagar, Chetlur, & Dhillon, 2020). In our study, when a DBS returns to the charging station to recharge its battery, a handover process is performed between two neighbour cluster heads to ensure continuous communication.

Another important factor affecting the efficiency and fairness of such systems is hover time of DBSs providing communication for each disaster-affected area. Hover time refers to the length of time a DBS can remain stable without moving. A longer hover time allows the DBS to cover a definite area for a longer time. Since the maximum flight time of a DBS is limited by its battery capacity, it would be beneficial to determine the hover time of DBSs from an optimization perspective. Muntaha, Hassan, Jung, & Hossain, (2020) investigated the effect of the hover time in a heterogeneous network with varying numbers of DBSs to improve the coverage of a terrestrial base station. Stationary DBSs and users were considered during the communication period. Unlike Muntaha, Hassan, Jung, & Hossain, (2020) our work faces a different problem, where the mobility of DBSs over the disaster area is considered in a DBS-only system. Furthermore, this thesis investigates the balanced hover time for mobile DBSs in each cycle to ensure coverage reliability and fairness in each disaster area by introducing linear programming models. A general review and summary of the literature dealing with the DBS deployment in disasters are summarized in Table 2.1.

Table 2.1 Summary of related literature

Reference	Problem	Objective function	Mobility	Number of DBSs	Energy	Solution approach
Deruyck, Wyckmans, Joseph, & Martens, (2018)	Location	Finding optimal locations of DBSs with given number of DBSs	Static	Multiple	Considering battery capacity	Simulation
Li, Lu, Zhang, Tian, & Pang, (2019)	Location	Throughput and coverage maximization	Static	Multiple	-	Artificial Bee Colony Algorithm
Zhao, et al., (2019)	Scheduling/ Trajectory	Throughput and coverage maximization	Mobile	Single	-	Simulation
Arafat & Moh, (2019)	Location/ Routing	Finding optimal locations of DBSs with given number of DBSs	Mobile	Multiple	-	Swarm Intelligence Based Localization/Clustering Algorithm
Sharafeddine & Islambouli, (2019)	Location	Maximize network throughput and minimize number of DBSs deployed	Static	Multiple	-	Greedy Approach - Unsupervised Learning Approach
Malandrino, Chiasserini, Casetti, Chiaraviglio, & Senacheribbe, (2019))	Task scheduling	Throughput maximization	Mobile	Multiple	Recharging	Simulation
Akram, Awais, Naqvi, Ahmed, & Naeem, (2020)	Location	Maximization the number of users and minimization the number of DBSs	Static	Multiple	-	Branch and Bound algorithm with Relaxation Induced Neighborhood Search
Park, Nielsen , & Moon, (2020)	Set covering	Minimization the number of DBSs	Static	Multiple	-	Branch and Price Algorithm
Muntaha, Hassan, Jung, & Hossain, (2020)	Allocation	Maximizing system energy efficiency	Static	Multiple	-	Langrangian Method
Bai, Li, Fang, Zhang, & Tao, (2020)	Location	Maximization transmission rates	Static	Multiple	-	Dynamic Swarm Model
Cui, Hu, & Chen, (2021)	Location	Maximization transmission rates	Static	Single	-	Heuristics Algorithm
Hayajneh, Bani-Hani, Shakhatreh, Anan, & Sawalmeh, (2021)	Location	Coverage maximization	Static	Multiple	-	Statistical analysis
Masroor, Naeem, & Ejaz, (2021)	Location	Minimization the number of DBSs, maximization the number of user	Static	Multiple	-	Branch and Bound Algorithm

Table 2.2 Summary of related literature (cont.)

Bozkaya, Özçevik, Akkoç, Erol, & Canberk, (2022)	Location	Minimizing the energy consumption	Mobile	Multiple	Recharging	Reinforcement Learning- Simulation
Zhao, et al., (2022)	Location/ Trajectory	Maximization transmission rates, minimization the number of DBSs	Mobile	Multiple	Considering battery capacity	Genetic Algorithm - Simulation
Barick & Singhal, (2022)	Location/ Allocation	Maximization transmission rates	Static-Mobile	Multiple	-	Allocation Algorithm - Simulation
Amrallah, Mohamed, Tran, & Sakaguchi, (2023)	Trajectory	Throughput maximization	Mobile	Single	Considering battery capacity	Dual Energy Aware Multi-armed Bandit Algorithm
Javed, et al., (2023)	Trajectory	Minimizing distance	Mobile	Single	-	Clustering Algorithm
Jin, Luo, Shi, & Wang, (2024)	Location	Maximizing the number of users	Static	Multiple	-	K-means Algorithm-Variable Neighborhood Search Algorithm
Ramos-Ramos, González-Vegas, Berrocal, & Galán-Jiménez , (2024)	Location	Minimizing the energy consumption	Static	Multiple	Considering battery capacity	Simulation
Current Study	Allocation/ Routing	Coverage maximization, minimization the number of DBSs, hovering/service time maximization	Mobile	Multiple	Recharging	Mathematical Model - GRASP Algorithm

To the best of our knowledge, as shown in our analysis presented in Table 2.1, none of the previous works has conducted a similar analysis with this work which integrates DBS deployment and trajectory mechanism while balancing flight and hovering time under battery constraints to provide continuous communication in an emergency. More in depth, an optimization model intending to deploy DBSs in positions that are visited over time and schedule DBSs' activities including flight, hovering, and charging in terms of time and energy capabilities is developed. Furthermore, the developed optimization model aspires to provide continuous coverage fairly by focusing on a large number of victims through a realistic scenario.

2.5 Chapter Conclusion

This chapter provided a comprehensive examination of DBS applications, particularly in the context of communication and emergency response. It explored the technical capabilities of DBSs, as well as the operational challenges associated with their use in network-based communication systems. The chapter also reviewed the existing body of literature from an operational research perspective, offering a detailed classification and analysis of optimization problems relevant to DBS deployment. Through this review, the chapter highlighted the research gaps and clearly positioned the problem addressed in this thesis as a novel contribution to the field. Overall, the chapter established the foundational context and motivation for the development of the mathematical models presented in the following sections.

CHAPTER THREE
MIXED INTEGER LINEAR PROGRAMMING FORMULATION OF THE DBS-SUPPORTED COMMUNICATION NETWORKS UNDER POST-DISASTERS CONDITIONS

3.1 Chapter Introduction

This chapter presents an optimization problem designed for establishing a reliable communication system using DBSs in disaster-affected areas. The problem focuses on ensuring spatial and temporal coverage while accounting for operational constraints such as limited battery life and the need for recharging. Two mathematical models based on MILP are introduced, each with distinct objectives: one aiming to maximize spatial coverage, and the other to enhance temporal coverage. The models determine optimal DBS hovering locations and the sequence in which these locations and recharging station should be visited. Fairness is incorporated into the problem through hard constraints—such as time-balancing of hover durations.

Computational experiments are conducted using a generated dataset to evaluate model performance, assess the impact of fairness constraints, and explore behaviour under different parameter settings. This chapter also analyse the trade-offs between spatial and temporal coverage, and the complexity introduced by fairness constraints.

3.2 Problem Description

The literature survey conducted thoroughly in the previous section puts forward the alternative usage of DBSs for temporary communication in disaster areas where terrestrial base stations were lost. In this section, the structure for the considered problem will be described. As mentioned above, pre-disaster preparations are as important as post-disaster recovery efforts in disaster management. Pre-disaster preparations include evacuation plan, determining emergency assembly point and humanitarian shelter etc. These preparations must be well planned to support post-disaster recovery activities as effectively as possible. After a disaster occurred, emergency assembly points can be used as first response and humanitarian aid logistics centres. Existing practices in emergency management provide for pre-planning and determining emergency assembly points in the disaster affected area. By excluding the location planning of these points from the scope of this study, it is assumed that DBSs are initially placed at central sites representing the charging stations located in emergency assembly points in pre-disaster stage. When a disaster is detected, they are first positioned in their initial locations in the air to cover then they are moved between the assigned locations over time. The first aspect interested in is how long a DBS should hover to cover a location. Hence, it is aimed to provide as much as possible to stay at the location to ensure maximum service. Under such a structure, a wireless communication system enabled by a rotary-wing DBSs that have ability to hover in a stationary position to provide network connectivity and reliable communication in an emergency is proposed. Correspondingly, the emerged problem is to find the optimal hovering locations and service/hover time at each location, as well as the visiting order among these locations considering the limited battery and time. It is also assumed that the proposed DBS network architecture is self-sustainable, in a sense, each DBS is equipped with a battery and moves toward a central site to be recharged at the end of each cycle. The novelty of this study's approach is the design of such a network with multiple-DBS deployment and trajectory optimization while accounting DBS's battery lifetime.

Before introducing the formulation of the considered problem as an optimization problem, the key components of the system model, as well as an illustrative example, are presented in the following subsections.

3.2.1 System Network Model

In most of the coverage models, it is important to determine how to divide the target area continuously. Given the constrained flight time of DBSs, designing an efficient coverage approach is essential. The way in which the target area is segmented plays a pivotal role in determining solution efficiency. The hexagonal tiling method is recognized as an optimal partitioning strategy, as it ensures the shortest cumulative distance from all locations within a cell to its geometric center (Wang & Wu, 2019). When the hexagonal structure is implemented, DBS can communicate with six neighbouring grids. Hence, it provides coverage of large area than square cells and it also reduces the exploration time as there are six degrees of directions. It can cover a higher proportion of the given area with same number of DBSs compared to square model and with increasing probability of coverage. Consequently, when hexagonal tessellation is used for path planning, the area covered by a DBS per charge is greater than that achieved through square tessellation (Datta, Tallamraju, & Karlapalem). Furthermore, recent studies proposed by Kadioglu, Urtis, & Papanikolopoulos, (2019) and Bibin Christopher & Jasper, (2020), showed that hexagonal partition is markedly superior to square partition and presented the advantages of hexagonal shape.

Within the context of this study, it is considered multiple-DBS coverage network that is divided into certain hexagonal cells. Each cell represents an affected area including victims, and each cell is grouped into clusters as shown in Figure 3.1, so that DBSs hover only above cluster centres to ensure communication. Considering return to the charging station, it is created a path that passes through the centres of the tiling hexagons. In each case, cluster head and its adjacent neighbours are enclosed in a circle that represents the coverage area of DBS as shown in Figure 3.2. The area that is within the coverage area of a DBS is a disc of radius Γ. Each DBS covers a circular area and serves the users in it.

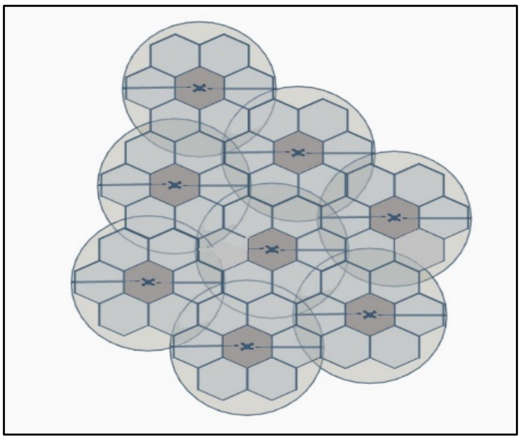

Figure 3.1 Hexagonal cells with cluster

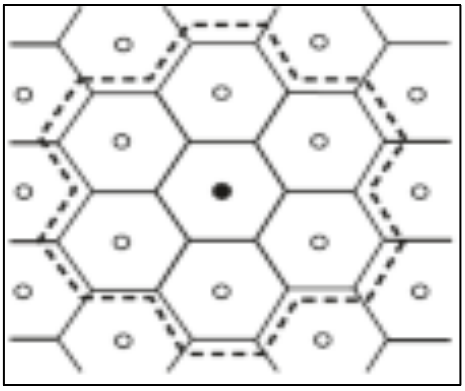

Figure 3.2 Centre of the tiling hexagons (Wang & Wu, 2019)

The coverage radius, influenced by the altitude of the DBS, is defined by the extent of the area that the DBS is capable of servicing. The relation between the altitude and coverage radius is presented as a linear equation in the related literature (Mozaffari M. , Saad, Bennis, & Debbah, 2016). The authors derived an equation considering service threshold in terms of maximum allowable pathloss. They translated this threshold into a coverage disk of radius which means all areas (victims) within the coverage disk have a pathloss that is less than or equal to allowable pathloss value. They presented a coverage probability for a region using the altitude h and the coverage radius Γ in Figure 3.3 and calculated by the following equation (Eq. 3.1).

$$\Gamma \leq h.\tan(\theta) \tag{3.1}$$

Where θ is the elevation angle which denotes the coverage range of the DBS's directional antenna. Al-Hourani, Kandeepan, & Lardner, (2014) stated that the optimal elevation angle (θ) is contingent upon the characteristics of the deployment environment (suburban — 20.34◦, urban — 42.44◦, dense urban — 54.62◦, high-rise urban — 75.52◦). It can be concluded that changing the DBS's altitude impacts the coverage radius. In the literature, the optimal altitude for maximum coverage have been studied (Al-Hourani, Kandeepan, & Lardner, 2014; Alzenad, El-Keyi, Lagum, & Yanikomeroglu, 2017; Esubonteng & Rojas-Cessa, 2022). This study assumes that DBSs are flying at the fixed optimal height.

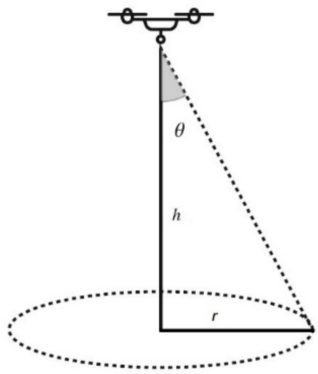

Figure 3.3 Coverage radius of DBS

Another reason to use hexagon tessellation that it offers efficient coverage of the region by minimizing overlapped areas between adjacent areas and ensuring no gaps between them. Hereby, a deployment approach is introduced that ensures maximal coverage efficiency, subject to the constraint that the coverage regions of DBSs remain non-overlapping.

3.2.2 Energy Consumption Model and Charging Techniques

The on-board energy of a DBS is consumed by various operational functions, including signal transmission, control mechanisms, mobility, data processing, horizontal navigation, and hovering. However, this energy is a limited resource which needs to be efficiently used to prolong the DBS operation lifetime and enhance the communication performance (Zeng, Xu, & Zhang, 2019). The various DBS energy consumption models have been proposed resulting of different scopes and assumptions of the models, different design features of the DBSs and different operation types. Therefore, there is no standards for DBS energy consumption. Since the drone technology is evolving rapidly, it is an open research area for improvement of DBS energy consumption and development of standards. Our consideration limits to developed power and energy models for battery-powered DBSs in wireless communication networks.

Main components of DBS energy consumption are composed of communication and propulsion energy. The communication related energy is used for various communication functions such as signal transmission, computations, and signal processing. The propulsion energy pertains to the mechanical energy consumption for movement and hovering of DBSs (Mozaffari M., Saad, Bennis, Nam, & Debbah, 2019). Compared to the propulsion energy used for physical movements, the energy consumption caused by wireless transmission during communication is neglected. Besides, the energy consumption caused by acceleration/deceleration is ignored since the DBS manoeuvring duration takes a small portion of the total time. Specifically, the energy consumed for movement can be categorized into two components: the energy required for flying between different locations, and the energy expended while hovering over designated areas to facilitate network coverage.

There are large differences for models in the literature in modelling DBS energy consumption due to the different types of DBSs, different operating conditions, and different model structures. Application field can affect energy consumption since it differs according to the types being used. Fixed Wings are more suitable for delivery operations since they can float at higher speeds while rotary-wings can move dynamically perform the vertical take-off, landing, and hover over a fixed location. Hence, these features make the rotary-wing DBSs be suitable for providing continuous cellular coverage for certain areas. Accordingly, the energy consumption model for rotary-wing DBSs is considered. Zhang, Campbell, Sweeney II, & Hupman, (2021) provided an assessment in detail for the energy consumption models for delivery operations. DBS energy consumption models in the literature generally assumed a constant rate of energy consumption per time or distance unit. Although certain studies have represented energy consumption as a nonlinear function of payload and travel distance (Cheng, Adulyasak, & Rousseau, 2020), the majority of the literature models energy consumption linearly with respect to travel distance or the duration of travel and hovering (Ha, Deville, Pham, & Hà, 2018; Huang, Savkin, & Huang, 2021). In fact, some energy consumption models were derived from the results of the field tests (Dorling, Heinrichs, Messier, & Magierowski, 2016; Liu, Sengupta, & Kurzhanskiy, 2017). Zhang, Campbell, Sweeney II, & Hupman, (2021) formulated several equations to calculate the energy consumption rate (*Epm*) by using information provided by the drone manufacturer. For the sake of simplicity, they suggested a formula based on

BatteryEnergy (in *Joules*) and *FlightDistance* (in *meter*). So, *Epm (J/m)* for flight can be calculated as follows:

$$Epm = \frac{BatteryEnergy}{FlightDistance} \tag{3.2}$$

BatteryEnergy can be provided by the drone manufacturer as capacity and voltage ($\mathcal{V}$), where the constant 3.6 is an expression in Watt-hours (1 *Wh* = 3600 *J*).

$$BatteryEnergy\ (in\ J) = Capacity(in\ mAh) \times Voltage\ (in\ \mathcal{V}) \times 3.6 \tag{3.3}$$

Although there are some realistic approaches that reflect real-world DBS operations since considering some fundamental consumption parameters such as mass, lift-to-drag ratio, and battery's power efficiency as in the study of D'Andrea, (2014), for the sake of simplicity, this study employs Equations (3.2) and (3.3) with the parameters provided by the manufacturer. However, the *FlightDistance* (in *m*) or *FlightTime* (in *min*) only reflects the steady flight time, in the continuous coverage problem, each DBS hovers over an assigned locations for maximum possible service time. Hovering at a specific position to serve the regions consume a considerable energy. Therefore, it must be considered while quantifying the energy consumption by each DBS. Dorling, Heinrichs, Messier, & Magierowski, (2016) formulated an equation expressing the power consumption of a multirotor DBS during hovering as a function of its weight. The equation considers the power consumed by an n-rotor copter that each rotor shares the total mass $m_p + m_d$ of the copter equally. So, the power consumed by all n rotors in Watts is calculated as below, where ρ = 1.204 kg/m^3 is the density of the air and ζ = 0.2 m^2 is the rotor swept area. The value of g is equal to 9.8 m/s^2.

$$P_h = (m_p + m_d)^{3/2}\sqrt{\frac{g^3}{2\rho\zeta n}} \tag{3.4}$$

The weakness of the given consumption models for both flight and hovering are that they ignore the impact of the weather conditions and changes in temperature. Energy consumption affected by the weather conditions require additional measurements. To determine optimal and feasible flight schedules for DBSs in practical applications, it is essential for researchers to consider uncertainties related to temperature variations and fluctuations in battery capacity (Kim, Lim, & Cho, 2018). However, for the sake of generality, this study ignores the effects of the weather and the temperature.

Limited battery capacity is one of the crucial challenges in DBS applications. Various techniques are available in the literature on the DBS charging. Most recent implemented technique is to charge the battery via external energy source, i.e., solar power (Galán-Jiménez, Moguel, García-Alonso, & Berrocal, 2021). Battery swapping is the most common way of charging a DBS, where a depleted battery is replaced with a fully charged one (Asadi & Pinkley, 2021). However, these techniques need the human intervention and stable air conditions as well, affects the autonomous DBS operations. On the other side, wired techniques limit the movement and require long times during charging operation (Lu, Bagheri, James, & Phung, 2018). These techniques also need the DBSs to return to the charging station more frequently. However, wireless techniques provide freedom for movement.

Wireless charging techniques can eliminate such drawbacks. Many innovative wireless charging techniques have been proposed. Among them, Wireless Power Transmission (WPT) is favored as an optimal charging method due to its potential as a promising technology for simultaneously charging multiple DBS units and enabling autonomous management of multiple devices (Chittoor, Chokkalingam, & Mihet-Popa, 2021). This process involves the transmission of electromagnetic energy directly from the source to the receiver without the use of any intermediate components (Lu, Bagheri, James, & Phung, 2018). In the literature, practical implementations of this technique have been published (Yan, Chen, & Yang, 2020; Ahmadian, Lim, Torabbeigi, & Kim, 2022). Attempts to develop WPT charging have been demonstrated by companies such as Global Energy Transmission has launched its wireless charging technology, where the DBS is charged for six minutes (Chittoor, Chokkalingam, & Mihet-Popa, 2021). Additionally, the DBS can sustain charging without the need to land, maintaining flight during the entire charging duration. There is no requirement of any human interaction. The DBS has on-board receiving, so when the DBS gets inside the area of the magnetic field generated within the critical to land area, it starts to charge.

Since the disaster management require low response times, DBSs deployment should be well managed such that they can be recharged before running out of battery. To maintain a seamless coverage of the field, the straight method proposes $\mathcal{N}$ DBSs cover for areas and $\mathcal{N}$ number of additional DBSs that are available at the charging station. According to this approach, the first group is serving while the second group is charging or ready for flying. However, DBSs that wait at the charging station are idle DBSs to be replaced. This situation can lead to excess cost and complexity during management. On the other hand, wireless charging for DBSs means shorter charging times, flexible charging alignment, reliable connections, and durability for weather conditions. By using the benefits of wireless charging technology, DBSs could be charged quickly and continue to cover where they are deployed. Indeed, thanks to wireless charging of DBSs, it is possible to utilize more DBSs to provide network connectivity, instead of keeping them waiting at the charging station as idle or being charged for longer times. Accordingly, this thesis considers the wireless charging of the DBSs, while planning the DBSs utilization to provide accurate network connectivity in the post-disaster conditions.

3.2.3 An Illustrative Example

Figure 3.4 depicts a disaster area, which was partitioned into hexagonal areas and includes one charging station, as a small DBSDTP with 27 areas. Northwest corner represents the charging station while grey-coloured hexagons represent the disaster-affected areas to each may one DBS be assigned.

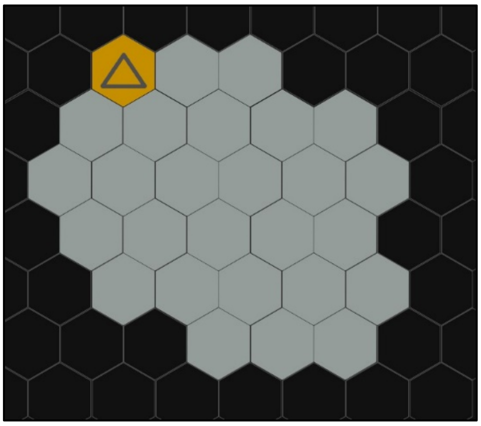

Figure 3.4 Illustrative example for a small DBSDTP

It is assumed that victims are evenly distributed across the region, implying that each area has an equal probability of being selected as a DBS deployment site. Given the failure of existing wireless network infrastructures, all victims within the area must be reconnected via the emergency communication network. The areas can only be able to connect to a DBS if they are in the coverage range, meaning that the area could be the DBS location allocating at cluster head of areas or one of the adjacent neighbours of it. A DBS visits a cluster head and covers a circle with it and its six adjacent hexagonal neighbours. A cluster head can be visited more than once; however, it can be covered by one DBS during hovering process. Furthermore, a DBS must follow a route while visiting the cluster heads. A route is feasible if it starts and ends at the charging station and must not exceed a cycle time based on endurance of the DBS. The limit of endurance is tracked by the energy consumption model. Energy consumption includes battery consumed during hovering and flying. Since the DBS manufacturers provide maximum flight time for only considering DBS flight and the energy consumptions for flight and hover are different, this study restricts the total flight and hover time by controlling the battery level at each area. DBSs fly at the same altitude and can decrease their altitude for charging; however, this situation is ignored.

DBSDTP will be formulated and optimized according to two different objectives as mentioned before. In case of limited number of DBSs are available to use for post-disaster management, the first and second variants of the DBSDTP aim to provide maximal spatial coverage and to maximize total hovering time (temporal coverage), respectively. It must be underlined here that all the DBSDTP variants are composed of two interdependent problems independently of the objective function required to be optimized: (1) determining the number and locations of DBSs to be deployed over the area of interest, and (2) determining the optimal trajectories for DBSs' locations and charging station to provide network connectivity as uninterrupted as possible.

To ensure continuous communication, handoff process is performed between two neighbour cluster heads. During the handoff process an additional DBS moves through the first area while the hovering DBSs move through the next area in the route. The last DBS returns to the charging station. The hovering and flight times must be tracked and balanced to ensure fair coverage in each area as well as provide synchronous DBS movement. Flight and hovering times must also be tracked to ensure DBSs battery is fully utilized for coverage. Since the limit of endurance is tracked according to the energy consumption, the main reason to track the time is to control the usage of additional DBSs together with the balanced service time. It is clear that $\mathcal{N}$ DBSs are needed to service $\mathcal{N}$ disaster-affected area at any given time. To provide continuous and maximal coverage with minimum number of DBSs and therefore maximize the usage rate of DBSs as resources, it is required to allocate minimal number of additional DBSs for each route. This requirement could be derived from a relation that could have been established by means of the hovering time at the first visiting area, the arrival time of DBS from the last visiting area to the charging station and the charging time.

Figure 3.5 illustrates the DBS deployments and trajectories determined through two variants of the DBSDTP for the illustrative example. The number of DBSs is limited to six for the first and second variants of the DBSDTP, while the coverage lower bound is set as 80% for the second variant. Figure 3.5 provides the trajectories of deployed DBSs, travelling time (d_{ij}) between the locations and hovering time (w_{ir}) at each location as well as covered areas considering spatial coverage maximization (Figure 3.5(a)) and temporal coverage maximization (Figure 3.5(b)). The dotted lines in Figure 3.5 depicts the routes of DBSs. Covered areas are indicated by circles in which the DBSs are centred in its six adjacent hexagonal neighbours.

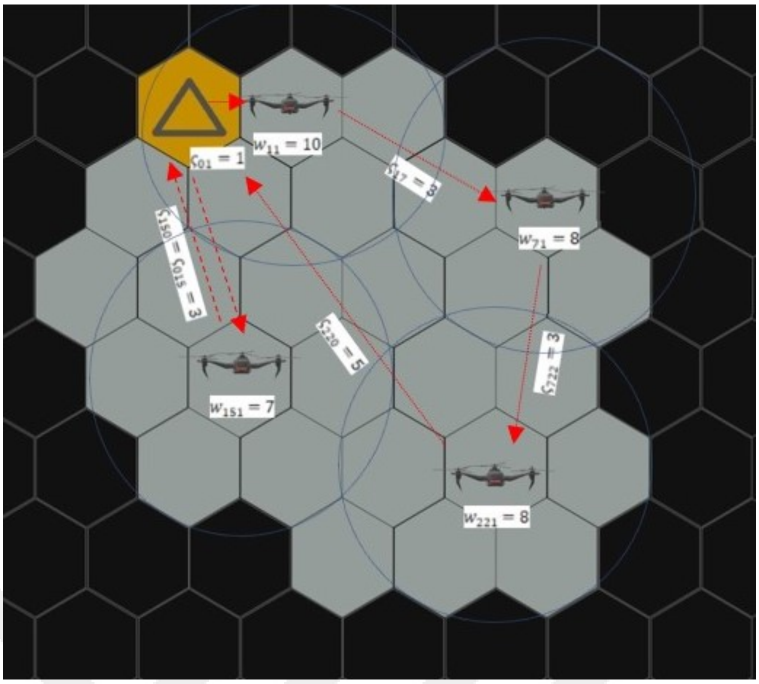

(a) Spatial coverage maximization

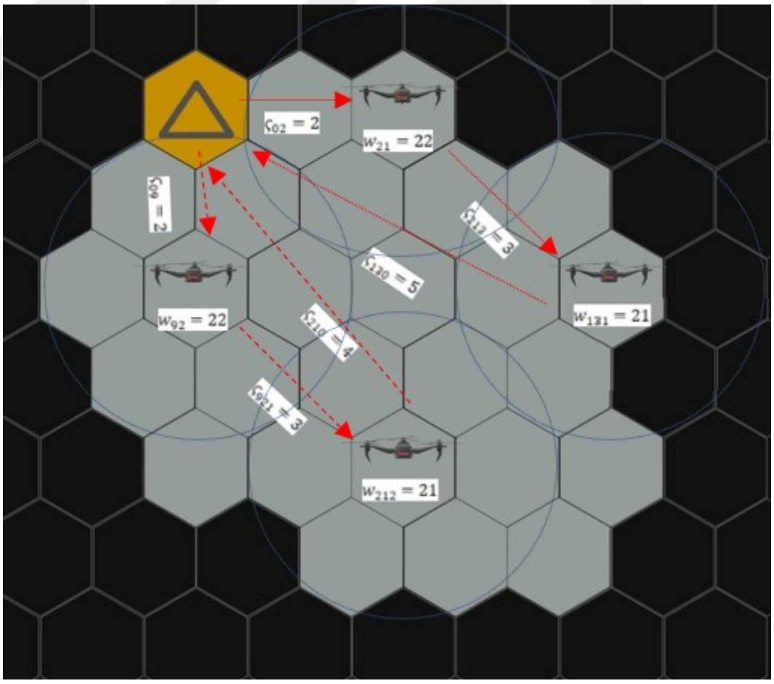

(b) Temporal coverage maximization

Figure 3.5 DBS deployments and trajectories

As can be clearly seen from Figure 3.5, each variant of the DBSDTP provided coverage over 22 disaster-affected areas out of 26. Such that, all variants ensured 85% coverage over the disaster area. Furthermore, both the spatial and temporal coverage maximization problems (see Figures 3.5(a) and 3.5(b)) established two routes with four DBSs and the remaining two DBSs are utilized as additional DBSs one per route. When the hovering time considered, the spatial coverage maximization problem ensured total hovering times as 33-time units while the temporal coverage maximization problem ensured total hovering time as 86-time units for the illustrative example. According to the objective functions, two solutions output different deployments and trajectories. The spatial coverage maximization problem relaxes the hover time since there is no hovering time maximization goal in the considered objective function. Therefore, DBSs could return to the charging station even they have adequate battery for service. The temporal coverage maximization problem aims to serve the disaster-affected areas as long as possible. Hence, the battery usage of the DBSs is maximal for this variant of the DBSDTP. In essence, all variants of aim at identifying the optimal locations of DBSs and determining the optimal trajectories for DBSs locations and charging station. Hereby, network connectivity could be provided as smooth and uninterrupted as possible in conjunction with the balanced hover and travel times of the employed DBSs. Problem formulizations of all variants of the DBSDTP will be developed as MILP models in the next subsection.

3.3 Maximal Spatial-Temporal Coverage Location Problem Formulation

This subsection introduces the MILP models. Let us consider a directed graph $G = (V, A)$, where $V = \{1, 2, \ldots, n\}$ of nodes is partitioned into a set of disaster-affected areas N with the maximum number of available DBSs (K). Set of arcs $A = \{(\mathrm{i}, \mathrm{j}): i, j \in V \text{ and } \{i, j\} \cap N \neq \emptyset\}$ is characterized by two attributes, namely the travel time and the energy consumption. Each arc $(i, j) \in A$ has a travel time $d_{ij} > 0$ with a time limit denoting by L (seconds). Π_{init} denotes the initial time at the start of operations. The energy consumption rates per unit time for flight and hovering are captured by α and β, respectively. These parameters ensure that the model accurately reflects the energy dynamics of the DBSs, allowing feasible route planning and coverage optimization. Each DBS travels through its route r at a constant speed and hovers with limited battery capacity. A feasible DBS route starts and ends at the recharging station. The battery level of a DBS decreases as it leaves the recharging station. Therefore, the battery of a DBS reaches full charge level Q when the DBS visits the recharging station. Furthermore, TC denotes the charging time at recharging station, which accounts for scheduling decisions for efficient energy replenishment. The disaster area is divided into hexagonal cells. Each cell represents an affected area with victims and is organized into clusters. DBSs are positioned to hover over the cluster centres and follow return paths to recharging stations to traverse the centres of these cells. To capture neighbourhood relationships between disaster areas, a_{ij} is introduced as a binary parameter, taking the value 1 if area i is a neighbor of another area j and 0 otherwise. To guarantee a minimum level of service, the parameter ϑ specifies the minimum desired percentage of coverage of the disaster-affected areas. Finally, M is a very large number. The following is a brief definition of sets and indices, parameters and decision variables, followed by the mathematical formulations.

Sets and indices

N: Set of disaster-affected areas indexed by *i, j, k,* and *u*

R : Set of potential routes, ($|R| = |N|$), indexed by *r*

V : Set of nodes including disaster-affected areas and battery recharging station, i.e., $V = N \cup 0$

Parameters

L: Maximum allowable cycle time for each route

K : Maximum number of DBSs available

ϑ : Minimum desired percentage of coverage

TC : Charging time at the recharging station

α : Unit energy consumption rate for flight

β : Unit energy consumption rate for hovering

Q: Battery capacity of a DBS

d_{ij}: Travelling time required by a DBS through arc $(i,j)\epsilon\ V|i \neq j$

$a_{ij} \in \{0,1\}$: Equals 1 if an area $i \in N$ is a neighbour of another area $j \in N$, and 0 otherwise

M : A very large number

Π_{init} : Initial time

Decision variables

$x_j \in \{0,1\}$: Equals 1 if a DBS is located over area $j \in N$, and 0 otherwise

$z_{ij} \in \{0,1\}$: Equals 1 if an area $i \in N$ is covered by a DBS located over an area $j \in N$, and 0 otherwise

$y_{ijr} \in \{0,1\}$: Equals 1 if arc $(i,j) \in \mathrm{V}|i \neq j$ is traversed by a DBS along with the route $r\ \epsilon\ R$, and 0 otherwise

$g_{jr} \in \{0,1\}$: Equals 1 if an area $i \in \mathrm{V}$ is travelled along with the route $r \in \mathrm{R}$, and 0 otherwise

$s_r \in \{0,1\}$: Equals 1 if a route $r \in \mathrm{R}$ is active, and 0 otherwise

$b_{ir} \in [0, Q]$: Battery level of a DBS at an area $i \in \mathrm{V}$ in route $r\ \epsilon\ R$

$\tau_{ir} \in [0, L]$: Arrival time of a DBS at an area $i \in \mathrm{V}$ in route $r\ \epsilon\ R$

$w_{jr} \in [0, L]$: Hovering time provided by a DBS at an area $j \in \mathrm{V}$ along with the route $r\ \epsilon\ R$

In the following, MILPs developed according to two different objectives are presented. The first model (see Sect. 3.3.1) formulates the spatial coverage maximization problem based on the MCLP which is one of the well-known facility location problems (Farahani, Asgari, Heidari, Hosseininia, & Goh, 2012). Then, in conjunction with the maximal coverage formulation, the second model (see Sect. 3.3.2) formulates the hover time (temporal coverage) maximization problem.

3.3.1 Formulation of the Spatial Coverage Maximization Problem (MILP-1)

This subsection first introduces the basic mathematical programming model for the spatial coverage maximization problem. As mentioned above, the formulation of this problem variant is developed based on the MCLP. Model constraints can be grouped into five sets: assignment, routing, battery capacity, time tracking and balancing, and integrality constraints. All these constraints are explained in detail in the following subsections.

3.3.1.1 Objective Function

$$\max \sum_{j \in N} \sum_{i \in N} z_{ij} \tag{3.5}$$

The objective function (3.5) maximizes the number of disaster areas covered.

3.3.1.2 Assignment Constraints

Assignment constraints are proposed to establish the relationship between DBS allocated locations and covered areas.

$$z_{ij} \leq x_j \qquad \forall\, i,j \in N \tag{3.6}$$

$$\sum_{j \in N} z_{ij} \leq 1 \qquad \forall\, i \in N \tag{3.7}$$

$$z_{jj} = x_j \qquad \forall\, j \in N \tag{3.8}$$

$$\sum_{j \in N} x_j + \sum_{r \in R} s_r \leq K \tag{3.9}$$

$$x_i \leq 1 - (a_{ij} x_j) \qquad \forall i,j \in N, (i \neq j) \tag{3.10}$$

$$z_{ij} \geq 1 - |V| * \left(1 - a_{ij} x_j\right) \qquad \forall i,j \in N \tag{3.11}$$

$$z_{ij} \leq |V| * \left(a_{ij} x_j\right) \qquad \forall i,j \in N \tag{3.12}$$

Constraints set (3.6) links a disaster-affected area to a DBS allocated disaster-affected area; the deployment of a DBS precedes the assignment to a disaster-affected area. Constraints set (3.7) ensures that each disaster-affected area is covered by at most one DBS located disaster-affected area. Constraints set (3.8) indicates that each disaster-affected area must be covered by itself if a DBS was already assigned to that area. Constraints set (3.9) limits the total number of DBSs in the system. Constraints set (3.10) forbids to allocate a DBS any adjacent neighbour of a disaster-affected area if a DBS was already allocated to that area. Constraints set (3.11) obliges a DBS located area to cover its all-adjacent neighbours. In contrast to constraints set (3.11), constraints set (3.12) forbids a DBS allocated area to cover its adjacent neighbours if a DBS was already not allocated to that area.

3.3.1.3 Routing Constraints

To provide accurate network connectivity across the disaster area and utilize the available DBSs as effectively as possible, it is necessary to move the DBSs along a route. In line with these objectives, the following routing constraints have been established to optimize the routes between charging station and DBS-allocated locations.

$$\sum_{i \in V} \sum_{r \in R} y_{ijr} = x_j \qquad \forall\, j \in \mathrm{N}, (i \neq j) \qquad (3.13)$$

$$\sum_{i \in V} \sum_{r \in R} y_{ijr} \leq 1 \qquad \forall\, j \in \mathrm{N}, (i \neq j) \qquad (3.14)$$

$$\sum_{i \in V} y_{ijr} - \sum_{i \in V} y_{jir} = 0 \qquad \forall r \in \mathrm{R}, \forall\, j \in \mathrm{V}, (i \neq j) \qquad (3.15)$$

$$\sum_{r \in \mathrm{R}} g_{jr} \leq x_j \qquad \forall j \in \mathrm{N} \qquad (3.16)$$

$$\sum_{j \in 0} g_{jr} \leq 1 \qquad \forall r \in \mathrm{R} \qquad (3.17)$$

$$s_r + (|V| * (1 - g_{jr})) \geq 1 \qquad \forall j \in \mathrm{N}, \forall r \in \mathrm{R} \qquad (3.18)$$

$$s_r - (|V| * \sum_{j \in N} g_{jr}) \leq 0 \qquad \forall r \in \mathrm{R} \qquad (3.19)$$

$$s_r \geq s_{r+1} \qquad \forall r \in R \backslash \{R\} \qquad (3.20)$$

Constraints set (3.13) permits an area to constitute an arc in a route if and only if a DBS was already assigned to that area, while constraints set (3.14) ensures that each arc is being assigned to one route at most. Constraints set (3.15) represents the flow balance constraints. Constraints set (3.16) links a DBS location and its belonging route. Constraints set (3.17) permits each route to contain at most one charging station. Constraints sets (3.18) and (3.19) ensure that a route is active if and only if it contains a DBS located area while constraints set (3.20) ensures that the active routes are in an ordered sequence. Here the constraints set (3.20) is not necessary, however, it is used to reduce the solution time of the model significantly since it acts as symmetry-breaking constraint.

3.3.1.4 Battery Level Tracking Constraints

As mentioned above, DBSs have a limited battery capacity and need to be recharged before the battery runs out. Accordingly, the battery level of the DBSs needs to be tracked as they provide network connectivity over the disaster area and move from one area to another along their routes. The following sets of constraints, representing the battery consumption formulations, have been developed to adequately track the endurance limit of the DBSs.

$$b_{jr} = Q - p_\alpha d_{ij} y_{ijr} - p_\beta w_{ir} + Q(1 - y_{ijr}) \qquad \forall i \in 0, \forall j \in V, \forall r \in \mathrm{R}, (i \neq j) \tag{3.21}$$

$$b_{jr} = b_{ir} - p_\alpha d_{ij} y_{ijr} - p_\beta w_{ir} + Q(1 - y_{ijr}) \qquad \forall i \in N, \forall j \in V, \forall r \in \mathrm{R}, (i \neq j) \tag{3.22}$$

$$b_{jr} + Q(1 - g_{jr}) \geq 0.2 * Q \qquad \forall j \in \{0\}, \forall r \in \mathrm{R} \tag{3.23}$$

$$b_{ir} \leq Q * g_{ir} \qquad \forall i \in V, \forall r \in \mathrm{R} \tag{3.24}$$

$$b_{ir} \leq Q * s_r \qquad \forall i \in V, \forall r \in \mathrm{R} \tag{3.25}$$

Constraints set (3.21) keep track of battery level at each hovering area starting from the charging stations. Constraints set (3.22) guarantees that the remaining battery level of a DBS is sufficient to go to its next destination. To satisfy battery safety and management, battery must be charged before it is completely run out. This safety level is offered as 20% in general for LiPo batteries. Therefore, constraints set (3.23) was constructed to satisfy that mentioned situation. Constraints sets (3.24) and (3.25) provide to track the battery level of a DBS for its route if and only if that route is an active route.

3.3.1.5 Time Tracking and Balancing Constraints

A DBS has a limited flight time due to its battery capacity, which varies between hovering and flying. To manage this, flight time and time spent at the charging station are tracked. This tracking ensures synchronized movement of the DBS, balancing hover and flight times. As a result, fair coverage is achieved across areas, with further analysis in subsection 3.4.4.

$$\Pi_{init} + d_{ij}y_{ijr} + w_{ir} - \tau_{jr} - L(1 - y_{ijr}) = 0 \qquad \forall r \in \mathrm{R}, \forall i \in \{0\}, \forall j \in V, (i \neq j) \tag{3.26}$$

$$\tau_{ir} + d_{ij}y_{ijr} + w_{ir} - \tau_{jr} - L(1 - y_{ijr}) = 0 \qquad \forall r \in \mathrm{R}, \forall i \in N, \forall j \in V, (i \neq j) \tag{3.27}$$

$$w_{jr} \leq L * g_{jr} \qquad \forall j \in \mathrm{V}, \forall r \in \mathrm{R} \tag{3.28}$$

$$\tau_{ir} \leq L * g_{ir} \qquad \forall i \in \mathrm{V}, \forall r \in \mathrm{R} \tag{3.29}$$

$$w_{jr} = 0 \qquad \forall j \in \{0\}, \forall r \in \mathrm{R} \tag{3.30}$$

$$d_{ki}y_{kir} + w_{ir} - d_{ij}y_{ijr} - w_{jr} + L(2 - y_{ijr} - y_{kir}) = 0 \quad \forall j \in \mathrm{N}, \forall r \in \mathrm{R}, \forall i, k \in \mathrm{V}, (i \neq j), (i \neq k), (k \neq j) \tag{3.31}$$

$$d_{ki}y_{kir} + w_{ir} - d_{ij}y_{ijr} - w_{jr} + L(2 - y_{ijr} - y_{kir}) - (L - \tau_{jr}) = 0 \quad \forall j \in \{0\}, \forall r \in \mathrm{R}, \forall i, k \in \mathrm{V}, (i \neq j), (i \neq k), (k \neq j) \tag{3.32}$$

$$d_{ki}y_{kir} + w_{ir} - d_{ij}y_{ijr} - w_{jr} + L(2 - y_{ijr} - y_{kir}) \geq 0 \quad \forall j, k \in \{0\}, \forall r \in \mathrm{R}, \forall i \in \mathrm{N}, (k = j) \tag{3.33}$$

Constraints sets (3.26) and (3.27) track the time spending at charging station and DBS locations, respectively. Constraints set (3.28) ensures the hovering time of a DBS do not exceed the maximum allowable cycle time of its route, while constraints set (3.29) ensures the arrival time of a DBS at an area do not exceed the maximum allowable cycle time of its route. Constraints set (3.30) ensures that a DBS do not hover

over a charging station. Through the constraints sets (3.31) and (3.32) coordination is ensured in the movements of the DBSs to the next area, and it is guaranteed continuous coverage at each area during the handoff process. Constraints set (3.33) is defined for single visit situation because of the topology. Besides, these constraints also guarantee that the maximum time (L) must not be exceed. The time balance constraints are also defined for the number of required additional DBSs at the charging station to ensure continuous coverage to be minimized. Last term of constraint set (3.32) is added to allow flexibility in returning to the charging station. Thus, the relationship between the arrival time from the last visited area and the hovering time at the first visited area is provided. This constraint set is directly related to the additional DBS constraints that will be explained in the following subsection.

3.3.1.6 Additional Drone Constraints

As stated before, this work aspires to effectively utilize the available DBSs to provide uninterrupted network connectivity in emergency conditions. Accordingly, the smaller number of DBSs backed up at the charging station the higher efficiency could be achieved in the utilization of the available DBSs. Additionally, the minimization of the backed-up DBSs directly minimizes the total number of DBSs required to provide coverage over the disaster-affected area. In each route, DBSs keep visiting the nearest neighbour area until all areas are visited in the related route. Each DBS provide network connectivity until runs out of battery and then it must return to the recharging station. When a DBS returns to the recharging station to recharge its battery, the handoff process will start between one of the backed-up DBSs at the recharging station and the DBS that covers the first area in the route. Therefore, it must be identified that how many additional DBSs are required to be backed-up at the recharging station to ensure an uninterrupted network connectivity over the disaster-affected area. The standard approach needs $\mathcal{N}$ additional DBSs to cover $\mathcal{N}$ areas, however, it is possible to guarantee to back-up only one additional DBS for each active route at the recharging station if and only if the following conditions are met simultaneously:

(i) The charging time of a DBS must be less than the travel time from the last visited area to the recharging station of a route.

(ii) Travel time from the last visited area to the recharging station of a route must be less than the hovering time at the first visited area of that route.

The rationale of these two conditions could be clarified through a small DBSDTP including one charging station and three disaster-affected areas. The charging time of a DBS lasts 5 minutes. The configuration given in Figure 3.6 does not meet the first condition while the configuration given in Figure 3.7 does not meet the second condition. In both Figures area-1 and area-3 are the first and last visited areas while area-0 is the recharging station. The hovering times at each area and the travelling times between areas and recharging station are also given.

According to the configuration given in Figure 3.6, DBSs will return to the recharging station for every 4 minutes, since the travel time from the area-3 to the recharging station equals to 4. Under these circumstances, because of 5 minutes charging time a DBS is still being charged at the recharging station and therefore at least two DBSs are at the recharging station at the same time while 3 DBSs are providing network connectivity on the air over the three disaster-affected areas.

$$0 \xrightarrow[\varsigma_{01} = 2]{} \overset{w_{11} = 5}{1} \xrightarrow[\varsigma_{12} = 3]{} \overset{w_{21} = 4}{2} \xrightarrow[\varsigma_{23} = 3]{} \overset{w_{31} = 4}{3} \xrightarrow[\varsigma_{30} = 4]{} 0$$

Figure 3.6 A DBS route does not meet condition (i)

According to the configuration given in Figure 3.7, an additional DBS must move to the first visited area to realize handoff process for every three minutes, since the hovering time of a DBS at area-1 equals to 3. On the other hand, DBSs will return to the recharging station for every 6 minutes, since the travel time from the area-3 to the charging station equals to 6. This situation reveals two additional DBS for every DBS returning to the recharging station.

Due to the 5 minutes charging time, a DBS will be ready to be a handoff process after 5 minutes after returning to the recharging station. Because of this one additional DBS is also required while a DBS is being charged. As a result, if the second condition does not meet, four additional DBSs are required at the recharging station at the same time while 3 DBSs are providing network connectivity on the air over the three disaster-affected areas.

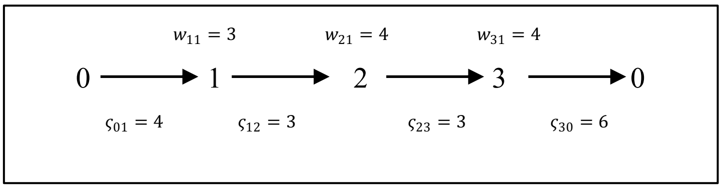

Figure 3.7 A DBs route does not meet condition (ii)

The number of additional DBSs may differ according to different route configurations and different hovering and travel times. As stated before, satisfying the above-mentioned two conditions guarantees to back-up only one DBS at the recharging station. In line with those purposes following two constraints sets were developed.

$$M * (y_{kir}) + (d_{ij} - TC) * y_{ijr} \geq 0 \qquad \forall j, k \in \{0\}, \forall i \in \mathrm{N}, \forall r \in \mathrm{R}, (j = k) \tag{3.34}$$

$$w_{ir} + L(1 - y_{kir}) \geq d_{uj} y_{ujr} \qquad \forall j, k \in \{0\}, \forall i, u \in \mathrm{N}, \forall r \in \mathrm{R}, (j = k) \tag{3.35}$$

Constraints sets (3.34) and (3.35) guarantees the above-mentioned conditions (i) and (ii), respectively. Through another small DBSDTP example given in Figure 3.8, these two conditions are further analysed.

Figure 3.8 illustrates an example route with a recharging station and five disaster-affected areas representing by DBSs. Hovering times are given into bracket above DBSs and travelling times are given with dashed lines. As shown, it is ensured one additional DBS is sufficient for the route, now it must be decided the time interval for the additional DBS movement from the recharging station to provide continuous coverage. The time interval for the additional DBS movement could be set as the hovering time at the first visited area or the travelling time from the last visited area to the recharging station.

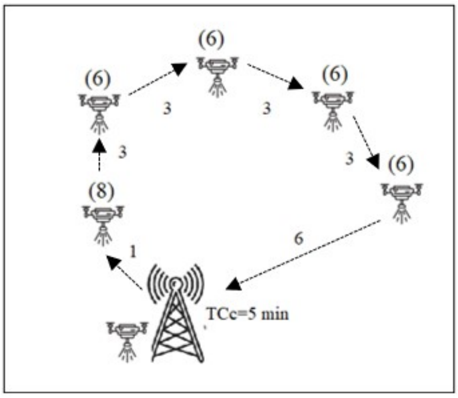

Figure 3.8 Additional DBS analysis

Table 3.1 analyses the additional DBS movement with two cycles according to the hovering time at the first visited area. First cycle starts at time *t*=0, then the second cycle starts after eight minutes based on the hovering time at the first area.

Table 3.1 Additional DBS movements according to the hovering time at the first area

Charging station	Area 1		Area 2		Area 3		Area 4		Area 5	
	Arrival	Departure	Arrival	Departure	Arrival	Departure	Arrival	Departure	Arrival	Departure
t=0	*t*=1	*t*=9	*t*=12	*t*=18	*t*=21	*t*=27	*t*=30	*t*=36	*t*=39	*t*=45
t=8	*t*=9	*t*=17	*t*=20	*t*=26	*t*=29	*t*=35	*t*=38	*t*=44	*t*=47	*t*=53

As can be obviously seen from Table 3.1, if additional DBS is released in every eight minutes, there may occur a delay for all areas except first area and therefore uninterrupted network connectivity could not be satisfied. Accordingly, Table 3.2 analyses the additional DBS movement with three cycles according to the travelling time from the last visited area to the recharging station. First cycle starts at time *t*=0, the second cycle starts at *t*=6 and then the third cycle starts at *t*=12 based travelling time from the last visited area to the recharging station.

Table 3.2 Additional DBS movements according to the travelling time from the last area to the charging station

Charging station	Area 1		Area 2		Area 3		Area 4		Area 5	
	Arrival	Departure	Arrival	Departure	Arrival	Departure	Arrival	Departure	Arrival	Departure
t=0	t=1	t=9	t=12	t=18	t=21	t=27	t=30	t=36	t=39	t=45
t=6	t=7	t=15	t=18	t=24	t=27	t=33	t=36	t=42	t=45	t=51
t=12	t=13	t=21	t=24	t=30	t=33	t=39	t=42	t=48	t=51	t=57

Table 3.2 put forwards that synchronously handoff processes between the DBSs could be satisfied for each area by backing up only one additional DBS at the recharging station. As final note from Table 3.2, the additional DBS only arrives early at the first area if the time interval for the additional DBS movement was set as the travelling time from the last visited area to the recharging station. However, this situation can be ignored rather than delay and therefore this thesis developed the MILP models of the DBSDTP variants by setting the time interval for the additional DBS movement as the travelling time from the last visited area to the recharging station to guarantee to back-up only one additional DBS for each active route.

3.3.2 Formulation of the Temporal Coverage Maximization Problem (MILP-2)

The hovering time maximization problem is a reformulation of the spatial coverage maximization problem. In this problem variant, the objective function (3.5) of the spatial coverage maximization problem is replaced with another objective function (3.36). It should also be underlined that the objective function (3.5) of the coverage maximization problem is reformulated and added to the temporal coverage maximization problem as the constraints set (3.37). Thus, the resulting below mathematical programming model constitutes the base mathematical programming model of the temporal coverage maximization problem.

$$\max \sum_{j\in N} \sum_{r\in R} w_{jr} \tag{3.36}$$

Subject to constraints (3.6) -(3.35)

$$\sum_{i\in N} \sum_{j\in N} z_{ij} \geq \vartheta * |V| \tag{3.37}$$

The objective function (3.36) maximizes the hovering time for each covered disaster-affected areas since the problem considers ensuring continuous network communication. Constraints set (3.37) ensures to fulfil the coverage threshold. Constraints set (3.6) -(3.35) are the same as above.

3.4 Experimental Analysis

This section presents the experimental analysis performed by developed MILPs. The first part outlines the methodology used for generating the instances. The second part provides the performance evaluation tests' results of MILPs on the generated instances. The third part gives pareto analysis for both objective functions. The fourth part analyses the impact of fairness for the problem by using fairness/balance constraints. Finally, the last part presents analysis on the number of drones.

3.4.1 Instance Generation

There is no standard set of benchmark instances available in the DBSDTP under disaster conditions in the literature. Since it is a newly studied area in the literature, this study executes performance analysis on a randomly generated set of test instances within range 20-180 areas. The primary features of the test instances are presented in Table 3.3. Instance group, instance no, V, N and K denote the type of topology to which the instance depends on, instance number, the total number of areas, the number of disaster-affected areas, and maximum number of available DBSs in the system, respectively. This study analyses the models for the disaster scenarios with different topologies as illustrated in Figure 3.9. The first topology (Type-A) represents an area not having a pattern made of regular shapes while second (Type-B) shows geometric features. The different size-instances belonging to a certain topology were generated by increasing the number of areas. Instances with up to 35 nodes are defined as small-scale. Those with 35-90 nodes are defined as medium-scale. Instances with more than 90 nodes are defined as large-scale. In the Table 3.3, Group A includes 7 problem instances, whereas Group B contains 6. This study partitions the given areas into different scales of problem instances. The hexagons with triangle give the charging station locations while the others represent disaster-affected areas.

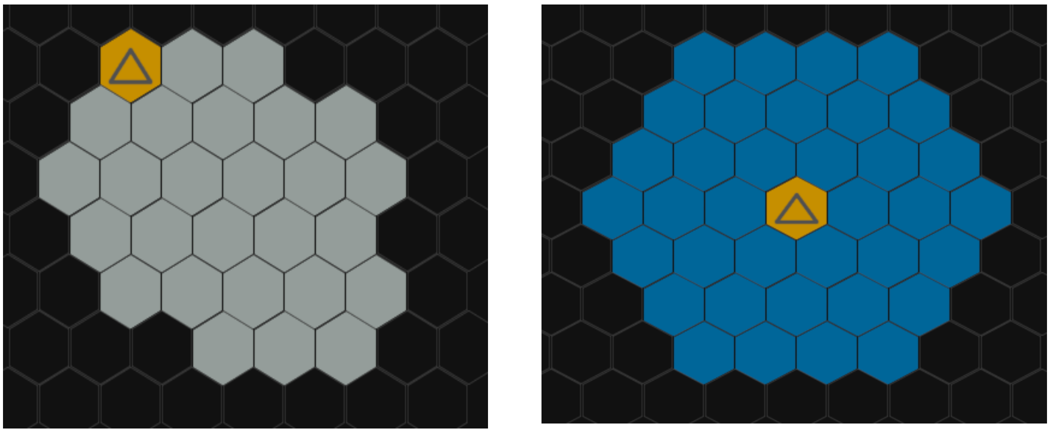

Type-A Type-B

Figure 3.9 Test instances for the experimental analysis

The DBSDTP variants have some parameters that should be tuned according to the problem size. For the spatial and temporal coverage maximization problems, it must be predetermined the maximum number of available DBSs in the system. It is set to at most 6 DBSs for the problems with up to 30 zones and increased by number of areas regarding the instance-size. Coverage threshold parameter should be determined for temporal coverage maximization problem. It is set to cover within range 60-70% of the disaster-affected areas according to the topology. Coverage matrix is set for each instance considering hexagon topology. The parameters were established based on preliminary experiments conducted on the test instances.

Rotary-wing DBS is used and its specifications from the manufacturers' websites is collected. The relevant data includes DBS battery payload as 1.30 *kg*, maximum flight time at a particular speed as $L = 55$ *minutes* and maximum speed as 17 *m/s*. Since the manufacturers provide the "Battery energy" in *Wh* or as capacity in *mAh* and voltage in $\mathcal{V}$, the Eq. 3.3 is used to calculate the energy as Q= 107.712 *Joules*. The battery consumption rates for flying and hovering that are presented as constant by using the formulations given in section 3.2.2. It is calculated α = 3,366 *Joules/minutes* for flight consumption and β = 1,965 *Joules/minutes* for hovering consumption. It should be noted that the manufacturers provide maximum flight time for only considering DBS flight in the air. On the other hand, this study aims to keep the DBSs in a hovering state as much as possible to meet the network coverage requirements. This situation leads to save time as the consumption is not entirely due to flight. This extra time should be added to the flight time. However, since the hovering time is a decision variable in our model, it is impossible to obtain the extra time deterministically at the beginning of the execution. Therefore, this study restricts the total flight and hover time by controlling the battery level at each zone and by ensuring that DBSs return to the charging stations with at least 20% battery. According to the drone manufacturers' data, charging time varies between 30-60 *min* according to the battery specification. However, this study assumes that the charging station is equipped with wireless charging technology so that the "charging time" is taken as 5 *min*.

Table 3.3 Main characteristics of the test instances

Instance Group	Instance no	V	N	K
Type-A	1	20	19	5
	2	30	29	6
	3	45	44	8
	4	55	54	8
	5	90	89	11
	6	120	119	12
	7	150	149	14
Type-B	8	19	18	5
	9	37	36	6
	10	61	60	9
	11	91	90	11
	12	127	126	13
	13	169	168	15

The experimental analysis focuses on evaluating the performance of the MILP models on the test instance set with respect to solution time. This study analyses the models on the overall each objective function and demonstrate the applicability of the proposed models to serve a disaster-affected area. All computations are performed on an Intel Core i7 with 3.40 GHz and 32 GB of RAM computer. The MILP models are implemented in Python and are solved using GUROBI 10.0.0. A time limit of one hour was imposed for each execution of the MILP models.

3.4.2 Results of MILP models

The results are presented in Table 3.4 for the two- model instances by performed under two objective functions, respectively, for the MILPs. The columns of the tables are self-explanatory. The results for the instances generated by increasing the number of nodes in a random range are reported to test the computational capability of the MILP models.

Table 3.4 Experimental results for the MILP models

Instance no	MILP-1			MILP-2		
	Opt. value	Best integer	CPU *(s)*	Opt. value	Best integer	CPU *(s)*
1	15	15	20	88.34	88.34	18
2	24	24	725.59	84.32	84.32	1947
3	29	41	3600	159.42	279.12	3600
4	No feasible solutions found			No feasible solutions found		
5	Out of memory			No feasible solutions found		
6	Out of memory			Out of memory		
7	Out of memory			Out of memory		
8	12	12	15	77.09	77.09	12
9	29	29	3133.82	127.79	320.27	3600
10	No feasible solutions found			No feasible solutions found		
11	Out of memory			No feasible solutions found		
12	Out of memory			Out of memory		
13	Out of memory			Out of memory		

As can be seen from Table 3.4, MILPs were able to solve the instance with up to 20 areas to optimality for all objectives in less than one minute. The models solved the instances with up to 37 areas to optimality within the pre-defined maximum computational time of one hour while no feasible solution found for the instances numbered 4, 5, 10 and 11. For the instance numbered 6, 7, 12 and 13, the models return an “out of memory” error. These results demonstrate the limits of the capable of generating solutions of the MILP models.

3.4.3 Pareto Analysis

In addition, the two competing objectives of maximizing the disaster areas covered (spatial) and maximizing the hover time at each visited area (temporal) were analysed, an analysis of the interaction between these two objectives is of particular interest. Figure 3.10 shows the interaction between spatial coverage and temporal coverage, when F = 37 and K = 3. The horizontal axis shows spatial coverage, and the vertical axis indicates temporal coverage. Initially, covering more areas yields significant gains in both objectives, as resources are used efficiently. However, beyond a certain point, the marginal increase in spatial coverage leads to a sharper reduction in temporal coverage, reflecting the trade-off between covering more nodes and maintaining sufficient hover time. The steep decline at higher spatial coverage shows that spreading resources too thin reduces temporal coverage, highlighting the need to balance these objectives for an effective and fair solution.

In this analysis, the epsilon-constraint method was employed because it is particularly effective in capturing both convex and non-convex regions of the pareto front, which are often missed by traditional weighted sum approaches. The results show that the non-convex parts of the pareto front - particularly the decreasing trend after a spatial coverage of 25 units - are successfully identified using this method. Consequently, both convex and non-convex areas of the pareto front are represented evenly and accurately. The analysis further shows that temporal coverage reaches its maximum at around 25 units of spatial coverage, beyond which further increases in spatial coverage led to diminishing returns and even a loss in temporal performance. Therefore, the optimal trade-off point for decision-making appears to be around 25 units of spatial coverage, where both objectives are most effectively balanced.

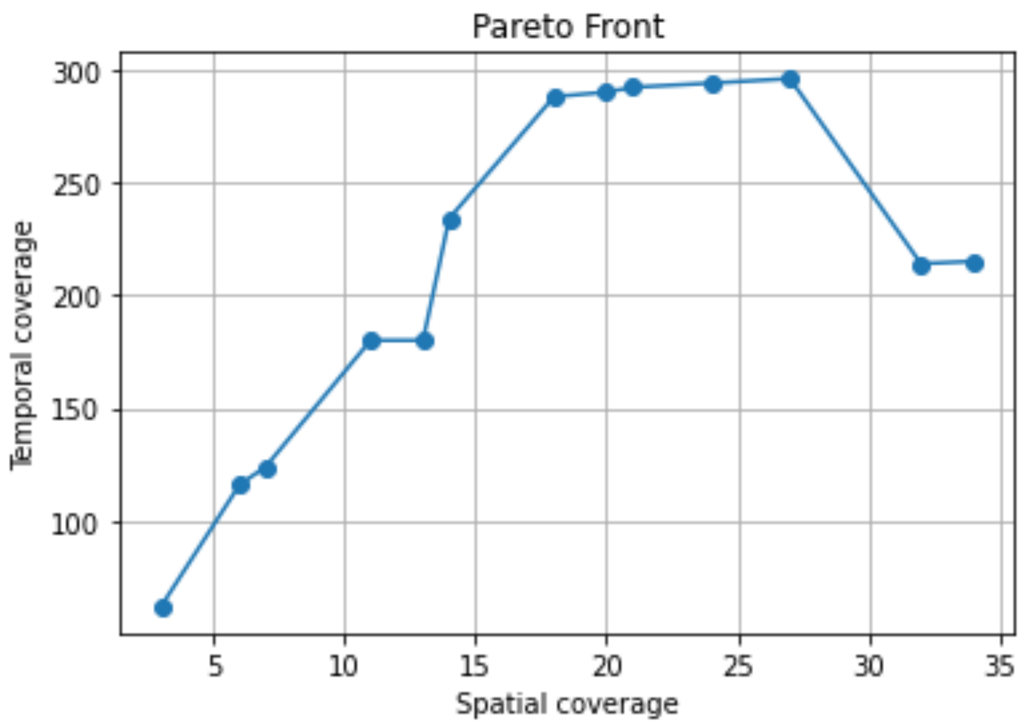

Figure 3.10 Pareto front analysis

3.4.4 Impact of Fairness

This section provides an analysis of fair coverage. The main implication of our study is to implement a fair solution. In public safety implementations, achieving a fair solution is essential to increase the effectiveness of safety measures and to promote equitable distribution of resources. This section analyses the effect of fairness on hover time by balancing it (minimizing the differences) in the areas visited on a route in the fairness constraints. Table 3.5 shows the results for a small instance, considering a recharging station and one DBS. In this table, “Visits”, “Cov. areas”, ’Hover time’ and ’Remaining energy’ represent the order of visits on the corresponding route, the number of areas covered by the visited area, the length of time spent in the visited area, and the energy remaining when a DBS arrives at an area, for both cases: the problem with balancing and the problem without balancing. However, as expected, the number of areas covered is the same in both cases, considering that equity leads to an increase in the total number of areas visited. In other words, it does not mean that the people in the area are only reached when the drone is constantly moving. The results reveal that the balancing problem gives a solution where the service reaches the people in the visited areas since there is a positive visit time for each visited area. Another finding from these experiments is that incorporating fairness has a lesser effect on hover time concerning the total area covered, total energy consumption, and overall hovering duration. It should be noted here that the results represent only one possible way of analysing the equity issue, since this study considers equity as the duration of each visited area. As fairness is a very important issue in disaster management, this study aims to ensure a fair distribution of hover time to the affected area.

Table 3.5 Comparison of visits with and without balancing

Without balancing				**With balancing**			
Objective: 49				Objective: 49			
Visits	**Cov. Areas**	**Hover time *(min)***	**Remaining energy *(J)***	**Visits**	**Cov. Areas**	**Hover time *(min)***	**Remaining energy *(J)***
1	4	-	105512	8	4	9.8	103312
12	7	49	98912	20	6	9.8	86912
26	4	-	43312	26	4	9.8	70512
20	6	-	36712	12	7	9.8	54112
8	4	-	30112	1	4	9.8	37712
0*	-	-	25712	0*	-	-	25712
Total	25	49	-	**Total**	25	49	-

0* represents the recharging station

3.4.5 Analysis on the Number of DBSs

In disaster situations, where limited resources must be allocated among the entities, the notion of fairness is crucial. Efficient use ensures that these limited resources are directed to where they are most needed, maximizing their impact. Efficient resource allocation helps ensure that the greatest number of people receive aid and that critical areas are addressed first. It is expected that the findings of this study to be valuable for decision-makers in promoting equity in public service delivery and the efficient use of available resources.

Therefore, this section provides an analysis of another crucial strategic extension of our problem, where the goal is to determine solutions with the minimum number of DBSs required to achieve a certain percentage of coverage. Identifying the optimal number of resources is vital for creating an efficient system to prepare for a potential earthquake, while avoiding overspending on the fleet. The inclusion of DBSs in the necessary fleet enhances the relevance of this extension for practitioners, given that DBSs are a relatively new technology and may not yet be widely available.

A practical approach to address this extension is to revise the mathematical formulation presented in section 3.3.1. Specifically, the objective function needs to be adjusted to minimize the number of DBSs, and a constraint must be introduced to ensure that a predetermined coverage level is satisfied. Essentially, the problem of minimizing the number of DBSs can be seen as a reformulation of the problem of maximizing coverage. The objective function (3.5) from the spatial coverage maximization problem is replaced with an objective function focused on minimizing the number of DBSs, relaxing the constraint set (3.9). Subsequently, the objective function (3.5) from the spatial coverage maximization problem is incorporated as a constraint. In other words, the restriction on the DBSs in the system was relaxed and then the resulting reformulation is designated as the objective function of the DBS minimization problem. This once, the resulting below mathematical programming model constitutes the base mathematical programming model of the DBS minimization problem.

$$\min \sum_{j \in N} x_j + \sum_{r \in R} s_r \tag{3.38}$$

Subject to

Constraints (3.6) -(3.8), (3.10) -(3.35) and (3.37)

The objective function (3.38) minimizes the total number of employed DBSs. Constraints set (3.6) -(3.8), (3.10) -(3.35) and (3.37) are the same as above.

Table 3.6 shows different scenarios based on the percentage of coverage required. Table 3.6 summarizes the values of the objective function (total number of DBSs used), the number of areas covered, and the computation times. The first column of

Table 3.6 indicates the percentage of coverage (ϑ). Further analysis of the solutions shows that as the percentage of coverage increases, the number of DBSs required increases by an average of 53.6% for each scenario. Higher coverage percentages typically result in more areas being covered. Overall, higher coverage targets significantly increase resource requirements.

Table 3.6 Result for the DBS usage with varying parameters

ϑ(%)	**Total number of DBSs used**	**Number of areas covered**	**CPU time *(s)***
70	7	29	1714.61
80	9	32	3600
95	11	36	528.33

3.5 Chapter Conclusion

This chapter introduced an optimization problem for a communication system enabled by DBSs to provide reliable connectivity under disaster conditions. New MILP formulations with different objectives for the problem have been developed. Optimal DBS allocation consists of determining the hovering locations of the DBSs over the disaster area and keeping them hovering as long as possible to provide fair coverage. Optimal routes for DBSs consist of determining the visit order of these locations and recharging station. The main aim of the problem is to maximize the total spatial-temporal coverage in all areas while ensuring that the coverage is provided within the given battery limit. The problem was first modelled as a spatial coverage maximization problem, and then its derivation as a temporal coverage maximization problem was presented. Computational experiments were performed on a generated dataset to evaluate the performance of the models, to analyse the impact of fairness concerns in the constraints, and to investigate the results under different parametric settings.

The following practical implications have been derived from extensive computational analysis: (i) the balanced hover time model improves fairness and efficiency by ensuring longer and more balanced hover times at each area, which can enhance data collection and user support in disaster areas. (ii) focusing on travel time due to short hover times, the total energy consumption is primarily impacted by travel, suggesting the need for efficient routing to minimize energy usage. The theoretical implications are as follows: (i) the comparison between spatial and temporal coverage maximization highlights the need to balance different objectives, influencing decision-making in disaster response strategies. (ii) ensuring fairness in hover time distribution between areas presents a complex optimization challenge, suggesting avenues for future research on equitable resource allocation. (iii) the solution's requirement for longer computation time indicates the need for more efficient algorithms to solve such complex problems.

In this chapter, the proposed model was developed based on the well-established MCLP from the literature. Problem-specific constraints were introduced, with a particular focus on ensuring fairness by time balancing constraints. While these constraints successfully impose fairness within the model, the overall formulation is tractable primarily for medium-sized problem instances. The time balancing constraints represent the hard constraints of the model, raising the question of whether a more efficient formulation could be achieved by incorporating fairness differently. In the subsequent chapter, we present the Fair Multi-DBS CTP, a novel formulation that incorporates fairness considerations directly into the objective function rather than as hard constraints. Building upon the classical CTP framework, this new model introduces modified constraints, and a reformulated objective function tailored to multi-DBS routing scenarios with equitable service provision.

CHAPTER FOUR

MULTI-DBS COVERING TOUR PROBLEM FORMULATION OF THE DBS-SUPPORTED COMMUNICATION NETWORKS UNDER POST-DISASTERS CONDITIONS

4.1 Chapter Introduction

This chapter introduces a novel formulation of the multi-DBS CTP, in which fairness is directly embedded into the objective function rather than being imposed through hard constraints. The model is designed to evaluate and compare three distinct fairness criteria within a maximal temporal coverage framework: Total Pairwise Absolute Difference (Total Pairwise), Rawlsian Maximin (MaxiMin), and Time Distribution Balance (Distribution). To operationalize these objectives, new mathematical formulations and supporting constraints are developed, enabling service time allocations that reflect population density across affected areas.

A formal evaluation methodology is established to systematically assess how effectively each model achieves temporal fairness. This methodology employs a normalized performance comparison across the three fairness measures, ensuring a consistent basis for evaluation. Empirical studies are conducted using small- and medium-scale instances to examine the solution quality and behaviour of each fairness objective under varying conditions.

4.2 Model with Multiple Visits and Fairness Measures

This section introduces an alternative modelling approach that builds upon and extends the limitations observed in the previous formulation in Chapter Three. While the earlier model focused on fairness through hard constraints the current formulation embeds fairness directly into the objective function. Decisions now include not only which areas to visit and how long to serve at each location but also in what sequence, reflecting more realistic operational constraints and priorities. The previous model focused on covering fixed clusters of areas through hard constraints, with fairness enforced via strict time balancing. Routes were designed based on predefined cluster heads and limited by DBS endurance, considering both flight and hover energy consumption. In contrast, the current model introduces demand heterogeneity and integrates fairness directly into the objective function. It allows for flexible selection of service locations and durations, shifting the problem structure towards a CTP variant, allowing for more nuanced control over equity and efficiency in service delivery. The new model also considers hexagonal structure and energy consumption models as presented in subsections 3.2.1 and 3.2.2.

The CTP was firstly introduced by Gendreau, Laporte, & Semet, (1997). They described the set of vertices divided into two groups (i.e. $N=N_1 \cup N_2$). Set N_1 consists of vertices that may be visited and includes a subset T of vertices required to be visited. Moreover, set N_2 contains vertices that need to be covered during the tour. The CTP seeks to construct a minimum-length Hamiltonian cycle traversing all vertices in T and possibly a subset of vertices in $N_1 \backslash T$, ensuring that all vertices in N_2 are covered. Naji-Azimi, Renaud, Ruiz, & Salari, (2012) developed a generalized model of the CTP wherein humanitarian aid to affected populations is delivered through satellite distribution centers located within a predefined distance from their residences. Davoodi & Goli, (2019) proposed a model addressing relief operations that encompasses the determination of relief center locations within the affected area as well as the allocation and routing of commodities.

This section presents a tour planning problem for a fleet of DBSs with energy limitations, in which a set of nodes including a central depot and a set of areas are given. Each area can serve other areas within its defined coverage radius. The system aims to make efficient use of DBSs, in the sense of increasing the number of areas to be covered and ensuring a fair service time under the battery limitations. Fair service time refers to the equitable allocation of operational time across all covered areas, ensuring that each area receives a comparable amount of service under battery life limitations. Unlike the previous MILPs, decisions include the selection of the subset of areas to be visited, the optimal service time of each DBS over the areas, and the scheduling of the sequence of visits to the areas. Since the visits occur between the selected stops and other areas within the coverage radius are covered by those, our problem can be classified as a variant of the CTP. Traditional location coverage problems focus on locating facilities to achieve maximum spatial coverage, intentionally ignoring how the service time is allocated to the locations covered. In the previous model service was tracked only at visited nodes, and each area could be covered by at most one DBS at a time. In contrast, the new model generalizes the concept of service by introducing continuous service time as a decision variable for all covered areas, not just those directly visited. To enable this, the model allows for multiple coverage of the same area, capturing the cumulative service received from different routes. Thus, the CTP is extended to maximize the spatial and temporal coverage simultaneously. In many applications, population density is a key to prioritizing service needs, with densely populated areas often requiring more frequent monitoring. In dynamic settings, such as urban or emergency management, these areas benefit from intensive coverage, ensuring timely detection of changes and efficient resource allocation (Church & Murray, 2008). The new model addresses this need by allocating service levels proportionate to population density, allowing for more intensive coverage in densely populated areas. Additionally, fairness objectives within the model ensure equitable service distribution considering a minimum threshold for spatial coverage and population differences of areas served. This approach promotes balanced resource allocation, maintaining both priority coverage and a fair distribution of services across areas.

Figure 4.1 illustrates the problem on a 1000 x 1000 grid with a depot located in the centre and 18 areas that follow the positioning with adjacent neighbours starting from the depot. These neighbours are units that share two corner points or boundary segments, also called ‘honeycomb’ adjacencies. The network includes two DBSs that serve the areas starting from the depot and ending at the depot. Two routes are shown for a coverage plan. In the first route, one DBS follows a dotted path to two areas and returns to the depot. In the second route, another DBS visits two areas. The circles show the coverage areas in the network. These two routes represent a trade-off in terms of service time. The first route minimizes the flight distance, enabling longer service times, while the second route involves a longer flight distance, reducing the service time available for each area visited or covered. Two adjacent neighbours were visited on different routes and their coverage areas appear to overlap. However, as the visits to these neighbours were made at different times, there was no actual simultaneous overlap.

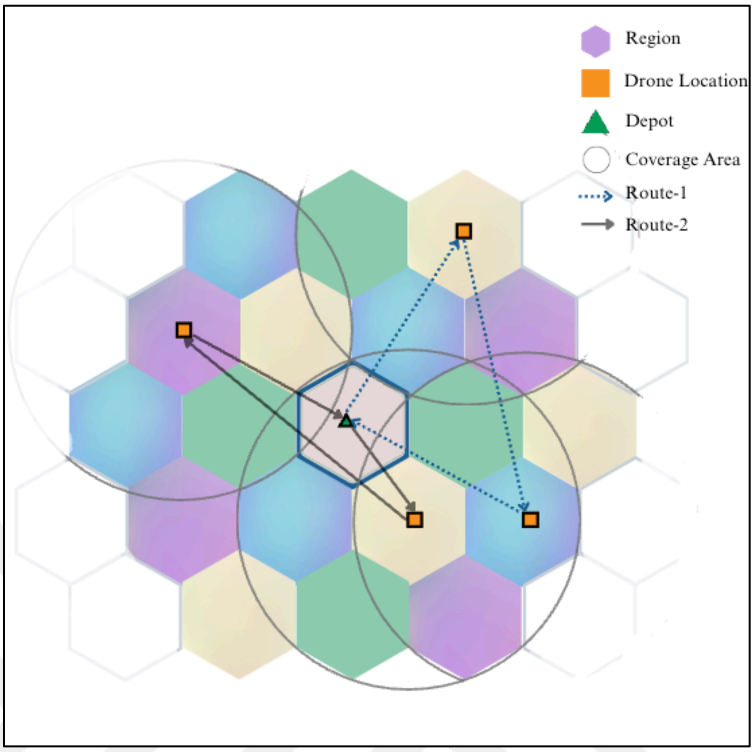

Figure 4.1 Illustrative example for the multi-DBS CTP

4.3 Formulation of the multi-DBS CTP

This section presents the extended CTP model, which allows multiple coverage in each area aimed at maximizing temporal coverage and spatial coverage. This section first introduces the multi-DBS CTP. Subsequently, various fairness measures are examined, followed by the presentation of model formulations that integrate these measures.

This formulation follows the approach proposed for the CTP in Sinnl, (2021). Unlike the classical CTP, in this current variant, all areas can be visited. The constraint on the number of areas on each route is relaxed while the restriction on the length of each route is ensured by battery limitations. Considering the following notation, a MILP formulation for the problem is described. A directed graph $G = (V, A)$ is given where $V = \{0\} \cup N$ is the set of vertices. The vertex 0 represents the central depot and

N represents the set of areas. K is the set of homogeneous drones. The arc set $A = A_{0N} \cup A_{NN}$ is defined as a set of routing arcs $A_{0N} = \{(i,j) : i,j \in \{0\} \cup N\}$ and assignment arcs for areas that are within the coverage range $A_{NN} \subseteq \{(i,j): i,j \in N\}$. A subset $S \subseteq \{0\} \cup N$, let $\delta^{+}(S) = \{(i,j) \in A_{0N} \mid i \in S, j \notin S\}$ and $\delta^{-}(S) = \{(i,j) \in A_{0N} \mid i \notin S, j \in S\}$ be the set of outgoing and incoming arcs of the cut induced by S as in Sinnl (2021). Each arc $(i,j) \in A_{0N}$ has a travel time $d_{ij} > 0$ with a time limit denoting by L (seconds). h_i indicates the weight of each area based on population density. As the energy consumption of the DBS depends on the travel time and hovering time, it is important to track the energy consumption in each area. The battery consumption rates for flying, α, and hovering, β, and the battery level of the DBS, Q are calculated as in Section 3, respectively. The parameter ϑ specifies the minimum desired percentage of coverage of the disaster-affected areas. Finally, M is a very large number.

Let binary variables $y_{ijk} = 1$, if arc $(i,j) \in A_{0N}$ is traversed by a DBS $k \in K$ and 0 otherwise. Binary variables $x_{ik} = 1$, if area $i \in N$ visited by DBS $k \in K$ and 0 otherwise. Binary variables $z_j = 1$, if area $i \in N$ is covered and 0 otherwise. Binary variables $u_{ijkg} = 1$, if arc $(i,j) \in A_{NN}$ is visited by DBS $g \in K$ after DBS $k \in K$ and 0 otherwise. Let continuous variables f_{ijk} for $(i,j) \in A_{0N}$ indicate the battery level from the central depot at area $j \in N$ for vehicle $k \in K$ arriving from $i \in N$. Continuous variables w_{ik} indicate the hover time of DBS $k \in K$ at visited area $i \in N$. Continuous variables τ_{ik} indicate the arrival time of DBS $k \in K$ at visited area $i \in N$. Continuous variables σ_i indicate the service time at area $i \in N$.

A brief description of the sets and indices, parameters, and decision variables is provided next, followed by the mathematical formulation.

Sets and indices

N: Set of disaster-affected areas indexed by *i, j, and k*

V : Set of nodes including disaster-affected areas and battery recharging station, i.e., $V = N \cup 0$

Parameters

L: Maximum allowable cycle time for each route

K : Maximum number of DBSs available

ϑ : Minimum desired percentage of coverage

TC : Charging time at the recharging station

α : Unit energy consumption rate for flight

β : Unit energy consumption rate for hovering

Q: Battery capacity of a DBS

d_{ij}: Travelling time required by a DBS through arc $(i, j)\epsilon\ V|i \neq j$

h_i weight of each area

M : A very large number

Decision variables

$x_{ik} \in \{0,1\}$: Equals 1 if area $i \in N$ visited by DBS $k \in K$ and 0 otherwise

$z_j \in \{0,1\}$: Equals 1 if area $i \in N$ is covered and 0 otherwise

$y_{ijk} \in \{0,1\}$: Equals 1 if arc $(i, j) \in A_{0N}$ is traversed by a DBS $k \in K$ and 0 otherwise

$u_{ijkg} \in \{0,1\}$: Equals 1 if arc $(i, j) \in A_{NN}$ is visited by DBS $g \in K$ after DBS $k \in K$ and 0 otherwise

$f_{ijk} \in [0, Q]$: Battery level from the central depot at area $j \in N$ for vehicle $k \in K$ arriving from $i \in N$

$\tau_{ik} \in [0, L]$: Arrival time of DBS $k \in K$ at visited area $i \in N$

$w_{ik} \in [0, L]$: Hovering time of DBS $k \in K$ at visited area $i \in N$

$\sigma_i \in [0, M]$: Service time at area $i \in N$.

Using this notation, the multi-DBS CTP can be structured as follow.

$$maximize \ \sum_{i \in N} h_i \sigma_i \tag{4.1}$$

Subject to

$$\sum_{k \in K} \sum_{(i,j) \in A_{NN}} x_{ik} \geq z_j \qquad \forall j \in N \tag{4.2}$$

$$\sum_{(i,j) \in A_{0N}} y_{ijk} = x_{ik} \qquad \forall i \in N, \forall k \in K \tag{4.3}$$

$$\sum_{(j,i) \in A_{0N}} y_{jik} = x_{ik} \qquad \forall i \in N, \forall k \in K \tag{4.4}$$

$$\sum_{(0,i) \in A_{0N}} y_{0ik} = 1 \qquad \forall k \in K \tag{4.5}$$

$$\sum_{(i,0) \in A_{0N}} y_{i0k} = 1 \qquad \forall k \in K \tag{4.6}$$

$$f_{0ik} = \alpha d_{0i} y_{0ik} \qquad \forall i \in N, \forall k \in K \tag{4.7}$$

$$\sum_{j \in \delta^+(i)} f_{ijk} - \sum_{j \in \delta^-(i)} f_{jik} = \sum_{(i,j') \in A_{0N}} \alpha d_{ij'} y_{ij'k} + \beta w_{ik} \qquad \forall i \in N, \forall k \in K \tag{4.8}$$

$$f_{ijk} \leq (Q - d_{j0}\alpha) y_{ijk} \qquad \forall (i,j) \in A_{0N}, j \neq 0, \forall k \in K \tag{4.9}$$

$$f_{ijk} \geq (d_{0i} + d_{ij}) \alpha y_{ijk} \qquad \forall (i,j) \in A_{0N}, i \neq 0, \forall k \in K \tag{4.10}$$

$$\tau_{ik} + d_{ij} y_{ijk} + w_{ik} - M(1 - y_{ijk}) \leq \tau_{jk} \qquad \forall (i,j) \in A_{0N}, j \neq 0, \forall k \in K \tag{4.11}$$

$$\tau_{ik} + d_{ij} y_{ijk} + w_{ik} \leq L \qquad \forall (i,j) \in A_{0N}, j = 0, \forall k \in K \tag{4.12}$$

$$\tau_{ik} \leq L x_{ik} \qquad \forall i \in N, \forall k \in K \tag{4.13}$$

$$u_{ijkg} + u_{ijgk} \leq x_{ik} \qquad \forall i,j \in A_{NN}, \forall k,g \in K, g > k \tag{4.14}$$

$$u_{ijkg} + u_{ijgk} \leq x_{jg} \qquad \forall i,j \in A_{NN}, \forall k,g \in K, g > k \tag{4.15}$$

$$u_{ijkg} + u_{ijgk} \geq x_{ik} + x_{jg} - 1 \qquad \forall i,j \in A_{NN}, \forall k,g \in K, g > k \tag{4.16}$$

$$\tau_{ik} + w_{ik} - \tau_{ig} - M(1 - u_{ijkg}) \leq 0 \qquad \forall i,j \in A_{NN}, \forall k,g \in K, g > k \tag{4.17}$$

$$\tau_{ig} + w_{ig} - \tau_{ik} - M(1 - u_{ijgk}) \leq 0 \qquad \forall i,j \in A_{NN}, \forall k,g \in K, g > k \tag{4.18}$$

$$\sigma_i = \sum_{k \in K} \sum_{(i,j) \in A_{NN}} w_{jk} \qquad \forall i \in N \tag{4.19}$$

$$w_{0k} = 0 \qquad \forall k \in K \qquad (4.20)$$

$$w_{ik} \geq x_{ik} \qquad \forall i \in N, \forall k \in K \qquad (4.21)$$

$$\sum_{i \in N} z_i \leq \vartheta |N| \qquad (4.22)$$

$$y_{ijk} \in \{0, 1\} \qquad \forall (i, j) \in N, \forall k \in K \qquad (4.23)$$

$$x_{ik} \in \{0, 1\} \qquad \forall i \in N, \forall k \in K \qquad (4.24)$$

$$u_{ijkg} \in \{0, 1\} \qquad \forall (i, j) \in N, \forall k, g \in K \qquad (4.25)$$

$$z_i \in \{0, 1\} \qquad \forall i \in N \qquad (4.26)$$

$$f_{ijk} \geq 0 \qquad \forall (i, j) \in N, \forall k \in K \qquad (4.27)$$

$$w_{ik} \geq 0 \qquad \forall i \in N, \forall k \in K \qquad (4.28)$$

$$\tau_{ik} \geq 0 \qquad \forall i \in N, \forall k \in K \qquad (4.29)$$

$$\sigma_i \geq 0 \qquad \forall i \in N \qquad (4.30)$$

The objective function (4.1) maximizes the temporal coverage based on the weights. As service time is a decision variable, there is no restriction on the distribution of service time between the covered areas. The potential consequence is that imbalanced service times between areas may result. Therefore, the most common and problem-specific fairness measures are discussed in the next section.

Constraints (4.2) ensure that an area is only counted in the objective function if an area covered is visited in the solution. Constraints (4.3) and (4.4) imply the connectivity of each route with the visited areas while imposing flow conservation for each visited area. Constraints (4.5) and (4.6) make sure that there are exactly *K* DBSs leaving and entering the depot. The solution defined by the constraints (4.3) -(4.6) (plus the integrality of the variables) will consist of cycles containing the central depot. Potential subtours are prohibited by flow conservation constraints (4.7) and (4.8). Moreover, together with constraints (4.9) and (4.10), these constraints also model the battery limit of a tour: For each area, *i*, in the solution, the remaining energy in the battery must allow to return from area *i* to the central depot. Time tracking constraints (4.11) -(4.13) keep track of time and ensure that the maximum tour duration is not exceeded. The scheduling constraints (4.14) -(4.18) ensure that if multiple DBSs are present in the same area, they must visit consecutively (Keskin, Li, Steil, & Spiller, 2012). Constraints (4.17) and (4.18) track a situation of arrival time of two areas i and j: if both visited, i.e. $x_{ik} = 1$ and $x_{jg} = 1$, arrival times of areas are sequenced as $\tau_{jg} \geq \tau_{ik} + w_{ik}$ or $\tau_{ik} \geq \tau_{jg} + w_{jg}$. Constraints (4.19) refer to the time taken to visit one area and to cover the same area when a different area is visited. Constraints (4.20) ensure that there is no hovering action in the depot. Constraint (4.21) links the decision variables. Since there is a trade-off between temporal and spatial coverage, spatial coverage is added to the model as a $epsilon$ constraint, as in constraint (4.22). Constraints (4.23) -(4.30) are integrality definitions of decision variables.

4.3.1 Fairness Measures

In this section, various measures of fairness that will be included in the modelling framework above are discussed. A significant limitation of coverage models that aim to maximize overall coverage is that they often concentrate more service agencies in densely populated areas, overlooking suburban areas with fewer emergencies (Zhou, Chen, Li, Liu, & Yu, 2023). This leads to uneven spatial coverage, which can be perceived as unfair. Thus, the coverage models to provide fairer solutions for service times while maximizing overall coverage are extended. Several approaches to measuring fairness have appeared in the location literature, such as total absolute deviation and maximin (minimax) (Marsh & Schilling, 1994; Xu, Murray, Church, & Wei, 2023). Some of these, which can be incorporated in a way that preserves linearity, are used in this study for evaluation and comparison. In addition, a new fairness measure for the problem is also proposed. These approaches are presented in Table 4.1 to characterize service time fairness and are explained in the rest of the section.

Table 4.1 Fairness measures to account for service time distribution

Measures	**Mathematical Expression**	**Reference**
Total pairwise absolute differences	$\sum_{i \in N} \sum_{j \in N} \lvert \sigma_i - \sigma_j \rvert$	(Church & Murray, 2008)
The Rawlsian approach	$\max \min_{i \in N} \sigma_i$	(Rawls, 2017)
Time budget distribution	$\max t$	This study

4.3.1.1 Total Pairwise Absolute Differences

The total pairwise absolute difference metric evaluates the service time-based coverage between each pair of areas, aiming to minimize their absolute differences (Church & Murray, 2008) following objective function (4.31).

$$minimize \sum_{i\in N}\sum_{j\in N}\left|\sigma_i - \sigma_j\right| \tag{4.31}$$

To define the absolute differences between any two areas in terms of temporal coverage, T_{ij} is used. Above equation becomes $\sum_{i\in N}\sum_{j\in N}\left|\sigma_i - \sigma_j\right| = \sum_{i\in N}\sum_{j\in N} T_{ij}$. In addition, a situation regarding the temporal coverage of two areas i and j are considered by defining new binary variable p_{ij}, 1 if $\left(\sigma_i - \sigma_j\right) > 0$; 0 otherwise, ensuring that the minimum value of T_{ij} is obtained to accurately account for temporal coverage difference. Additional constraints are introduced to track this situation. A balancing model that minimizes the total pairwise absolute difference through integrating of the multi-DBS CTP, which we call Total Pairwise, is formulated as follows:

$$minimize \sum_{i\in N}\sum_{j\in N} T_{ij} \tag{4.32}$$

Subject to (4.2) -(4.30)

$$0 \le h_i\sigma_i \le M \qquad \forall i \in N \tag{4.33}$$

$$0 \le T_{ij} - \left(h_i\sigma_i - h_j\sigma_j\right) \le 2M(1 - p_{ij}) \qquad \forall (i,j) \in A_{0N},\ i \ne 0, j \ne 0 \tag{4.34}$$

$$0 \le T_{ij} - \left(h_j\sigma_j - h_i\sigma_i\right) \le 2Mp_{ij} \qquad \forall (i,j) \in A_{0N},\ i \ne 0, j \ne 0 \tag{4.35}$$

$$p_{ij} \in \{0,1\} \qquad \forall (i,j) \in N \tag{4.36}$$

$$T_{ij} \ge 0 \qquad \forall (i,j) \in N \tag{4.37}$$

The objective function (4.32) maximizes T_{ij}, which is the absolute differences between any two areas in terms of temporal coverage. Constraint (4.33) ensures that service time takes a positive value for each area. Constraint (4.34) and (4.35) ensure a non-negative outcome for each pairwise comparison indicating that either the service time of area i or that of area j is greater. Constraints (4.36) and (4.37) are integrality constraints.

4.3.1.2 The Rawlsian Approach

The Rawlsian approach focuses on maximizing the minimum (or vice versa) outcome level that is worst-off entity (Rawls, 2017). Due to its ease of implementation and widespread adoption, this approach has been employed in numerous classical optimization problems—including location, assignment, and scheduling—to integrate fairness considerations into the models (Karsu & Morton, 2015). For example, well-known *p-centre* facility location problems which is widely considered in public sector applications, minimizes the maximum distance between any demand point and its closest facility. An alternative to objective function (4.31) is to maximize the minimum equity value rather than the sum. A new decision value ζ is introduced to represent the minimum equity overall. Therefore, the objective function (4.31) will be replaced by (4.38), and constraints (4.39) -(4.41) are added to the model. These constraints represent a relaxed adaptation of the original maximin constraint, tailored to the specific problem context. Unlike the original constraint, which ensures a minimum value for all areas, the relaxed version accounts for partial coverage, guaranteeing a minimum value exclusively for the areas that are covered. Then the MaxiMin model is formulated as follows:

$$maximize\ \zeta \tag{4.38}$$

Subject to (4.2) -(4.30)

$$h_i \sigma_i \geq \zeta - M(1 - z_i) \qquad \forall i \in N \tag{4.39}$$

$$h_i \sigma_i \leq M(z_i) \qquad \forall i \in N \tag{4.40}$$

$$\zeta \geq 0 \tag{4.41}$$

The objective function (4.38) maximizes ζ, which is the minimum equity value. Constraints (4.39) and (4.40) guarantee a minimum value for the areas for partial coverage. Constraint (4.41) represents the integrality constraint.

4.3.1.3 Service Time Distribution

Another approach is to fairly distribute the remaining time from the traveling time in the system among the areas covered. The total time available in the system is calculated by $|K|L$ and the time is spent on travel, represented by $\sum_{(i,j)\in A_{0N}} \sum_{k\in K} d_{ij} y_{ijk}$, results in $|K|L - \sum_{(i,j)\in A_{0N}} \sum_{k\in K} d_{ij} y_{ijk}$ units of time left for the service. To distribute this time as equally as possible across the areas covered, the following nonlinear expression $(|K|L - \sum_{(i,j)\in A_{0N}} \sum_{k\in K} d_{ij} y_{ijk}) / \sum_{i\in N} z_i$ is introduced. To linearize it, a continuous variable *t*, is introduced to represent the average remaining service time per area covered, as follows.

$$t = (|K|L - \sum_{(i,j)\in A_{0N}} \sum_{k\in K} d_{ij} y_{ijk}) / \sum_{i\in N} z_i \tag{4.42}$$

As the denominator depends on a decision variable, the expression $t \sum_{i\in N} z_i$ must be linearized by introducing another continuous variable *r* as follows.

$$r - \left(t - L(1 - \sum_{i\in N} z_i)\right) \leq 0 \tag{4.43}$$

$$r \geq 0 \tag{4.44}$$

$$r \leq t \tag{4.45}$$

$$r - L \sum_{i\in N} z_i \leq 0 \tag{4.46}$$

With the linearization, the resulting model which we call Distribution is given as follows.

$$maximize\ t \tag{4.47}$$

Subject to (4.2) -(4.30), (4.43) -(4.46)

$$h_i \sigma_i \geq t - M(1 - z_i) \qquad \forall i\ \in N \tag{4.48}$$

$$h_i \sigma_i \leq M(z_i) \qquad \forall i\ \in N \tag{4.49}$$

$$|K|L - \sum_{(i,j)\in A_{0N}} \sum_{k\in K} d_{ij} y_{ijk} \geq r \tag{4.50}$$

The objective function (4.47) maximizes *t,* which is the average remaining service time per area covered. Constraints (4.48) and (4.49) ensure that the service time is at least t while constraints (4.50) represent the minimum value of the remaining time after travel.

4.3.2 Comparison of Fairness Measures

This section proposes an empirical assessment to evaluate and compare the fairness objectives in terms of solution quality and computational effort. The mathematical models are coded in Python and GUROBI is used to solve the MILP models with a time limit of one hour. The experiments are run on a laptop with Intel Core i7 with 3.40 GHz and 32 GB of RAM. The following analyses consider the small and medium size and regular-structured instances with 19 and 37 areas including a depot. The instances are based on a homogeneous fleet by varying the number of drones $|K| = \{2, 3, 4\}$. The spatial coverage threshold (in percentage) is set to $\vartheta = \{50, 80, 100\}$. The travel distance between areas was calculated according to the Euclidean norm. For each DBS, the flight time limit is $L = 55$ *minutes*. The battery energy is Q = 107.712 *Joules*. It is calculated as α = 3,366 *Joules/minutes* for flight consumption and β = 1,965 *Joules/minutes* for hovering consumption.

Table 4.2 shows the normalized performance of three fairness measures —Total Pairwise, MaxiMin, and Distribution —under varying configurations, with each row normalized according to the measure in the corresponding column. Total Pairwise minimizes differences in service time across areas, so lower values in the Total Pairwise column indicate better performance. Conversely, MaxiMin and Distribution maximize the minimum service time for an area, so higher values in their respective columns indicate better fairness results.

Table 4.2 Comparison of Total Pairwise, MaxiMin, and Distribution for different variants

Number of nodes	Number of DBSs	Coverage Threshold	Model	Total Pairwise	MaxiMin	Distribution
			Total Pairwise	0.00	0.68	0.68
		50	MaxiMin	2.36	0.00	0.00
			Distribution	1.97	0.00	0.00
			Total Pairwise	0.00	-0.45	-0.50
	2	80	MaxiMin	-0.49	0.00	-0.10
			Distribution	-0.51	0.11	0.00
			Total Pairwise	0.00	0.79	0.79
		100	MaxiMin	0.27	0.00	0.00
			Distribution	0.10	0.00	0.00
			Total Pairwise	0.00	0.09	0.09
		50	MaxiMin	-0.18	0.00	0.00
			Distribution	-0.18	0.00	0.00
			Total Pairwise	0.00	1.68	1.68
19	3	80	MaxiMin	0.41	0.00	0.00
			Distribution	0.13	0.00	0.00
			Total Pairwise	0.00	1.80	1.80
		100	MaxiMin	0.65	0.00	0.00
			Distribution	0.65	0.00	0.00
			Total Pairwise	0.00	0.15	0.08
		50	MaxiMin	-0.42	0.00	-0.06
			Distribution	-0.46	0.06	0.00
			Total Pairwise	0.00	1.00	1.00
	4	80	MaxiMin	-0.23	0.00	0.00
			Distribution	-0.23	0.00	0.00
			Total Pairwise	0.00	-0.29	-0.29
		100	MaxiMin	-0.02	0.00	0.00
			Distribution	-0.03	0.00	0.00
			Total Pairwise	0.00	-1.00	-1.00
		50	MaxiMin	0.42	0.00	0.00
			Distribution	0.37	0.00	0.00
			Total Pairwise	0.00	2.00	2.00
	2	80	MaxiMin	-0.17	0.00	0.00
			Distribution	-0.17	0.00	0.00
			Total Pairwise	0.00	18.73	16.00
		100	MaxiMin	1.94	0.00	-0.14
			Distribution	1.90	0.16	0.00
			Total Pairwise	0.00	0.89	0.16
		50	MaxiMin	0.76	0.00	-0.39
			Distribution	0.47	0.63	0.00
			Total Pairwise	0.00	2.77	2.77
37	3	80	MaxiMin	0.05	0.00	0.00
			Distribution	0.05	0.00	0.00
			Total Pairwise	0.00	18.60	18.60
		100	MaxiMin	1.40	0.00	0.00
			Distribution	1.40	0.00	0.00
			Total Pairwise	0.00	0.65	0.65
		50	MaxiMin	-0.28	0.00	0.00
			Distribution	-0.28	0.00	0.00
			Total Pairwise	0.00	1.05	1.05
	4	80	MaxiMin	0.93	0.00	0.00
			Distribution	0.88	0.00	0.00
			Total Pairwise	0.00	24.51	15.34
		100	MaxiMin	1.01	0.00	-0.36
			Distribution	0.94	0.56	0.00

In general, MaxiMin and Distribution demonstrate superior performance on service time disparities in configurations with a smaller number of nodes. For instance, in the configuration of 19 nodes and 4 drones, when normalized to Total Pairwise, both MaxiMin and Distribution show negative values, reflecting superior fairness performance compared to Total Pairwise. However, as the problem size increases (e.g., 37 nodes, 3 DBSs, 100% coverage threshold), both face greater challenges in maintaining their superiority, as evidenced by higher values when normalized to Total Pairwise.

For Total Pairwise, larger configurations (e.g., 37 nodes, 4 DBSs, 100% coverage threshold) generally allow the measure to achieve lower values, showing its effectiveness in minimizing service time disparities. Similarly, in the same configurations, when normalized to MaxiMin and Distribution, it achieves strongly positive deviations (24.51 and 15.34), indicating a relatively good performance.

MaxiMin model shows an average performance, while Distribution model demonstrates its strengths in maintaining fairness in service time, especially in larger configurations. For example, with 19 nodes, 2 DBSs, 80% coverage threshold, Distribution model achieves the best normalized performance in its column, outperforming both Total Pairwise and MaxiMin. In other configurations, however, there is very little difference between MaxiMin and Distribution models.

Figures 4.2 and 4.3 show the comparison of the solution time of Total Pairwise, MaxiMin, and Distribution on instances with n = {19, 37} for ϑ = {50, 80, 100} in percentage, which are solved to optimality by all models. The sub-figures show the computation times for different numbers of DBSs (k = 2, 3, 4), and the title of each figure is given as “number of nodes-number of DBSs”. In Figure 4.2, for instances of 2 and 3 DBSs, Distribution generally gives the shortest solution time, while other models require longer solution times. However, for instances with 4 DBSs, Total Pairwise has the shortest solution time. Furthermore, the differences between the MaxiMin and Distribution models are not significant.

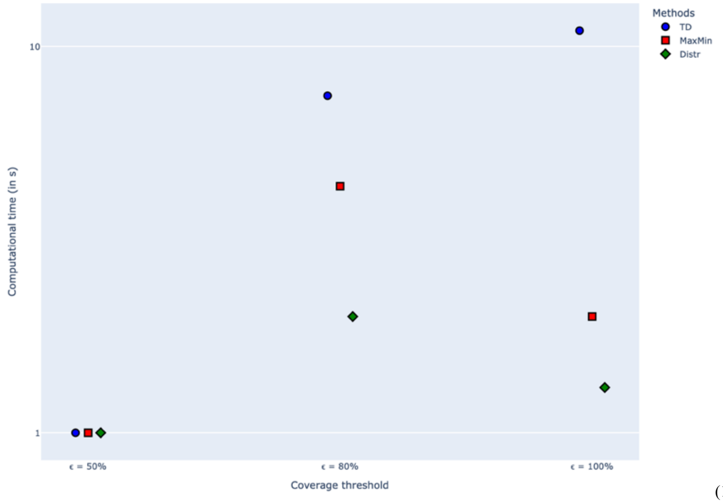

(19-2)

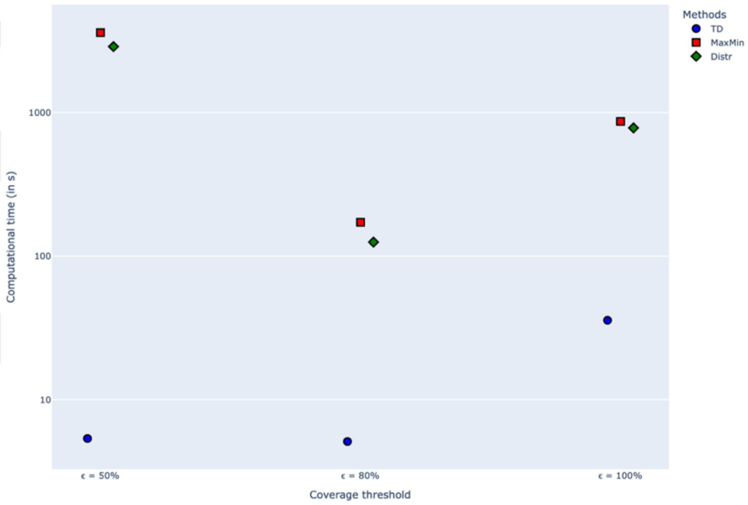

(19-3)

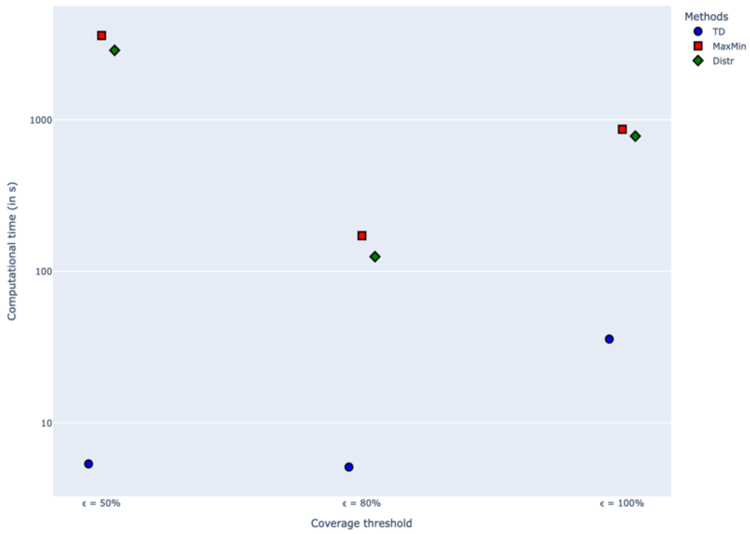

(19-4)

Figure 4.2 Computational time comparisons for n = 19 solved by all models

In Figure 4.3, for medium size instances with 2 and 3 DBSs, Distribution model shows superior computational efficiency across all coverage levels, making it a robust choice for medium size problems where solution time is a critical factor. Total Pairwise and MaxiMin require longer solution times, generally at low and moderate coverage thresholds. However, with 4 DBSs instances, Total Pairwise is the most computationally efficient model. In addition, MaxiMin and Distribution behave similarly at high coverage thresholds, indicating that fairness constraints drive their complexity in a similar manner.

Higher coverage thresholds lead to increased computation time for all models. Distribution has relatively efficient performance but still increases computation time at higher coverage levels and numbers of DBSs.

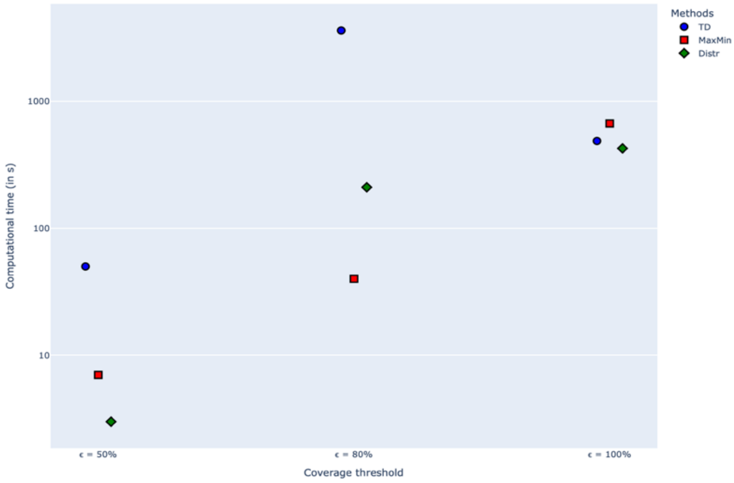

(37-2)

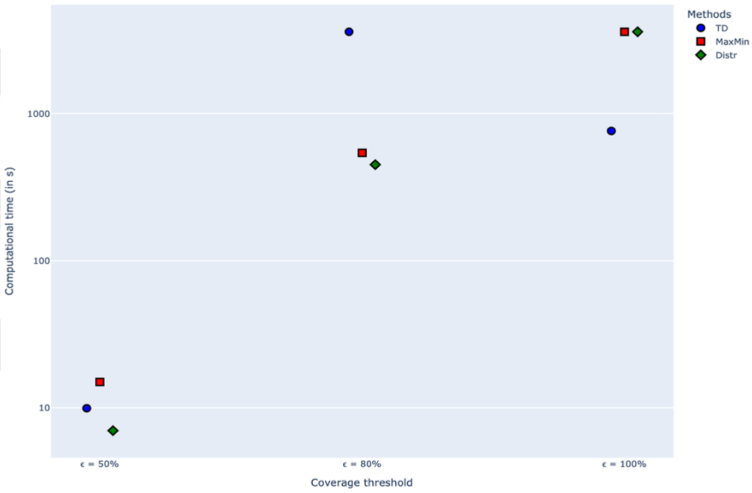

(37-3)

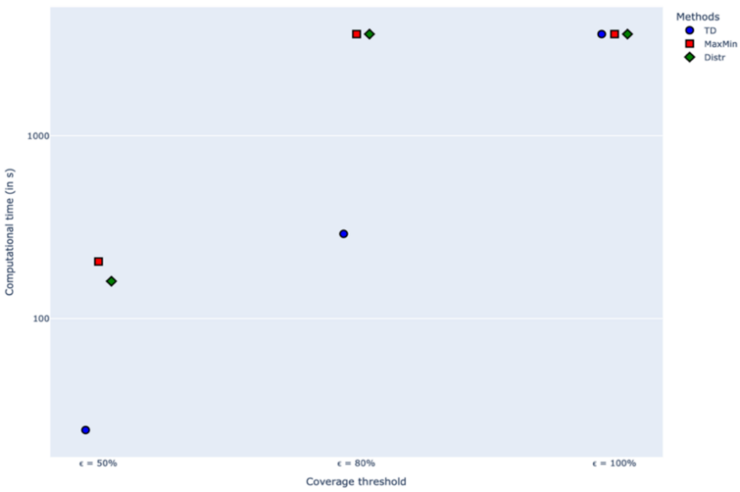

(37-4)

Figure 4.3 Computational time comparisons for n = 37 solved by all models

Figure 4.4 shows the gaps across instances. For small size instances, Total Pairwise and Distribution have similar patterns while MaxiMin has larger gaps. However, for medium size instances, Total Pairwise has the largest gaps. The average gaps for medium size instances are 1.87% for Distribution, 2.67% for MaxiMin, 24.48% for Total Pairwise. In summary, Distribution model is the most effective in reducing the gap, as evidenced by its consistently lower gap values across both instances. Total Pairwise model, with the largest gaps, is the least effective, while MaxiMin model is in between.

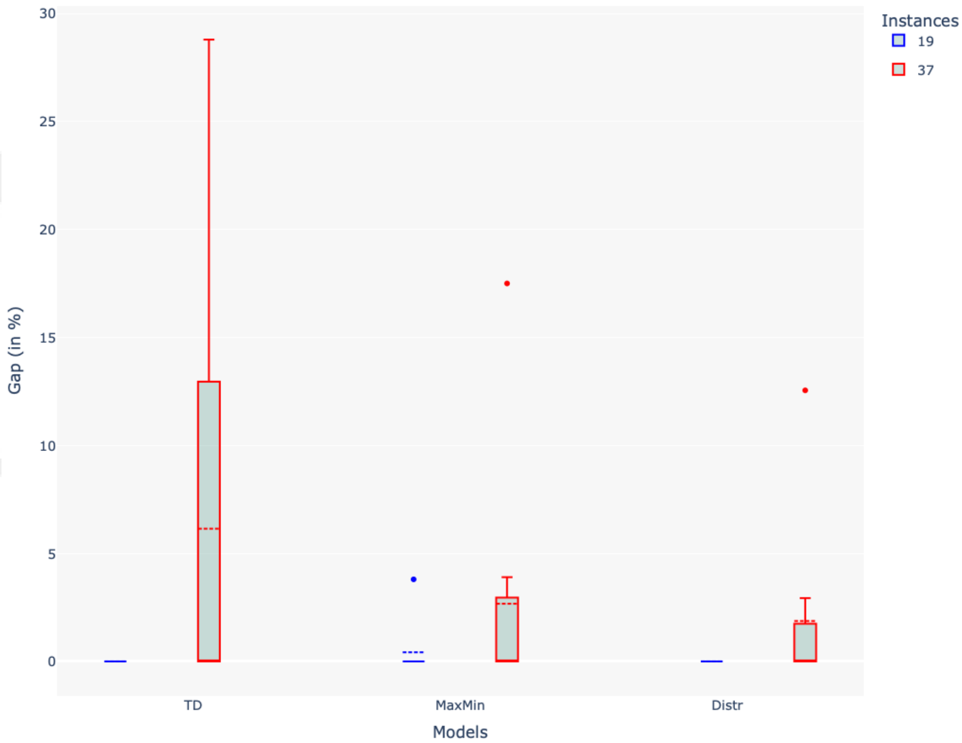

Figure 4.4 Gap for optimality for instances solved by all models

Overall, Total Pairwise performs better in larger scenarios and excels at reducing disparities, while MaxiMin and Distribution generally perform better in smaller configurations, where ensuring equity in minimum service times is more difficult, but crucial. This highlights the complementary strengths of the measures, with Total Pairwise prioritizing equity across areas and MaxiMin and Distribution focusing on guaranteeing minimum service levels for the most underserved areas.

Empirical studies were conducted to compare different fairness-oriented objective functions across various problem configurations. Among these, the Distribution objective—which prioritizes fair service times for the least served areas—demonstrated strong and consistent performance across a wide range of scenarios. Unlike Total Pairwise, which focuses on overall balance, or MaxiMin, which emphasizes only the minimum service value, Distribution proved to be more effective in achieving equitable outcomes, particularly in heterogeneous service demand settings. These results underline the practical advantages of the Distribution formulation. Therefore, in the next section, the outcomes of a mathematical model built upon the Distribution objective function is analysed. In this analysis, the model's capability to generate solutions within a defined time limit is also evaluated.

4.4 Performance Evaluation of the CTP Model with the Distribution Objective

This section presents the computational performance of the CTP model where fairness is integrated directly into the objective function via the Distribution formulation. The instances used for testing are the same of those generated in section 3.4.1, allowing for consistent benchmarking. All experiments were conducted using the same computational environment previously described. Unlike earlier models where multiple DBSs could share a route, this analysis assumes one DBS per route, enabling clearer evaluation of individual DBS performance. Table 4.3 reports key performance metrics—including total service time, spatial coverage rates, optimality gaps and CPU times—providing a comprehensive assessment of the model's practical effectiveness under the Distribution -based fairness criterion. The GAP (%) column presents the average relative difference between the best solution and the model's best integer bound.

Table 4.3 Performance analysis for the Distribution-based CTP model

Instance no	Total Service Time *(min)*	Coverage (%)	GAP (%)	CPU Time *(s)*
1	675.59	90	0.00	15
2	789.609	86	0.00	1532
3	1043.28	75	24.50	3600
4	1066.77	76	39.90	3600
5	2386.44	62	190.00	3600
6	139.57	56	Unreliable GAP[1]	3600
7	No feasible solutions found			
8	682.42	100	0	20
9	1487.92	75	20.00	3600
10	1801.84	65	28.70	3600
11	1843.26	60	212.05	3600
12	357.13	63	Unreliable GAP[1]	3600
13	No feasible solutions found			

[1] A feasible solution was found, but the optimality gap is excessively large due to weak or undefined bounds. This may indicate numerical instability or time limit exhaustion before improving dual bounds.

The results of the Distribution-based CTP model show its performance on the generated instances especially in terms of scalability and feasibility.

For irregular structured instances (1-7), feasible solutions were found up to 120 nodes. However, performance starts to decline from 45 nodes onwards, with decreasing coverage and increasing optimality gaps. For instances larger than 30 nodes, the model often hits the time limit (3600 seconds), and no feasible solution could be found for the 150 nodes. This indicates that irregular layouts create routing difficulties and overlapping coverage, making it harder for the model to allocate service time effectively under the Distribution objective.

In regular structured instances (8-13), small-scale problems are solved efficiently with full coverage and zero gap. But as the size increases, both CPU time and gap values grow significantly. By 91 nodes, the gap exceeds 200%, and no feasible solution is found for the largest instance. The extremely high gap observed in the 127-node instance suggests numerical issues or that the solver struggled to compute valid bounds within the time limit.

In summary, the Distribution-based CTP model works well for small-scale problems, providing fair service distribution. However, as the instance size or spatial complexity increases, solution quality and feasibility decline, highlighting the need for more scalable methods or heuristics-based approaches for larger applications.

4.5 Comparison Between the MCLP model and the CTP Model

In this section, the results obtained from the CTP-based model with the Distribution objective are compared against those generated by the MILP formulation introduced in section 3, which is based on the MCLP with the temporal coverage maximization. The comparison is conducted using the same set of benchmark instances to ensure consistency. Due to the different objective functions of the two models, the evaluation focuses on performance indicators such as overall coverage and the minimum service time achieved. This comparison aims to assess how effectively each model achieves coverage optimization with temporal service fairness, thereby highlighting the trade-offs inherent to each modelling approach.

Table 4.4 presents a comparative analysis between the MCLP-based MILP model and the proposed CTP model across a range of problem instances, evaluated in terms of total coverage, minimum service time provided, and the resulting optimality GAPs.

Table 4.4 Comparative analysis between the MCLP-based MILP-based model and the CTP-based model

Instance no	**MCLP-*based* Model**			**CTP-*based* Model**		
	Coverage (%)	**Minimum service time *(min)***	**GAP (%)**	**Coverage (%)**	**Minimum service time *(min)***	**GAP (%)**
1	74	34.69	0.00	90	32.17	0.00
2	62	19.77	0.00	86	27.23	0.00
3	60	47.51	82.00	75	26.62	24.50
4	No feasible solutions found			76	19.61	39.90
5	Out of memory			62	89.78	190.00
6	Out of memory			56	1	N/A
7	Out of memory			No feasible solutions found		
8	67	38.55	0.00	100	37.91	0
9	78	30.93	151.00	75	42.51	20.00
10	No feasible solutions found			65	37.55	28.70
11	Out of memory			60	19.09	212.05
12	Out of memory			63	1	N/A
13	Out of memory			No feasible solutions found		

The results in the Table 4.4 are also visualized in Figure 4.5 and Figure 4.6. As the table and figures illustrate, the CTP model demonstrates significantly higher robustness and scalability, particularly as instance size increases. While the MCLP model performs competitively for small instances (e.g., 20, 30 nodes) in terms of coverage and service time—with both models yielding optimal GAP values of 0%—it quickly becomes computationally intractable for larger instances, frequently resulting in infeasibility or memory exhaustion.

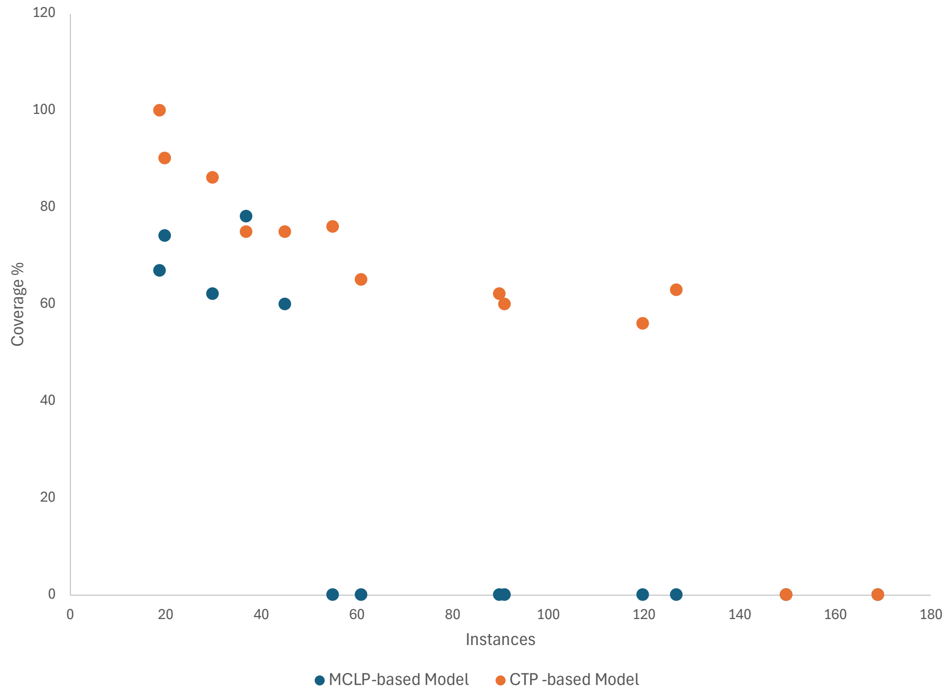

Figure 4.5 Comparison for total coverage

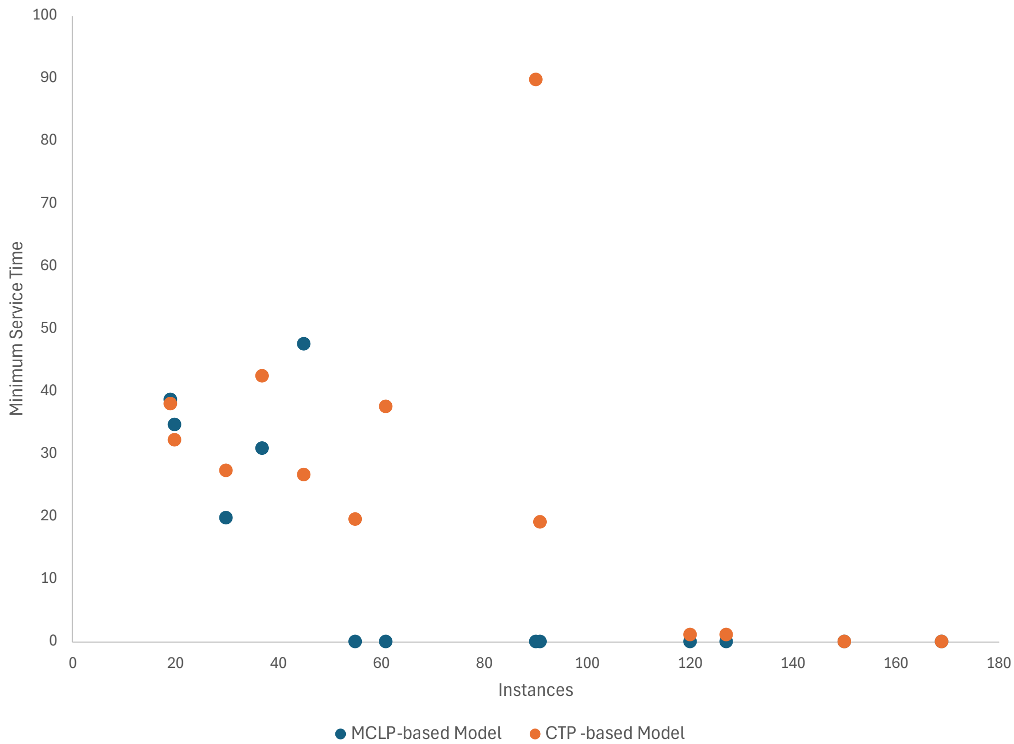

Figure 4.6 Comparison for minimum service time provided

In contrast, the CTP model consistently produces feasible solutions for a broader range of problem sizes, including instances where the MCLP model fails entirely (e.g., instances 55, 61, 91, 127). Moreover, the CTP model achieves higher total coverage values in nearly all comparable instances. For example, in the 19-node instance, the CTP model achieves full coverage (100%) compared to only 67% for the MCLP model. Although the minimum service time values are sometimes slightly lower for CTP (e.g., instance 20), its ability to provide solutions with superior spatial-temporal coverage suggests a favourable trade-off between fairness and coverage efficiency.

From a GAP perspective, the MCLP model maintains optimality (GAP = 0%) in instances where it can compute solutions. However, its overall applicability is hindered by limited scalability. Conversely, the CTP model demonstrates competitive or superior GAP values (e.g., 20% or lower in several mid-sized instances) while maintaining feasibility, which is critical for real-world deployment where timely and scalable solution generation is essential.

These findings support the conclusion that the CTP model offers a more practical and scalable framework for coverage-based planning problems, especially under constraints involving neighbourhood exclusivity and time limits. Its superior performance in terms of solution viability and spatial reach underlines its suitability for larger, more complex routing scenarios.

4.6 Chapter Conclusion

This section introduced a new formulation of the multi-DBS CTP, in which fairness is explicitly modelled within the objective function rather than as a set of hard constraints. The model was extended to evaluate and compare three distinct fairness measures—Total Pairwise, MaxiMin, and Distribution—within a maximal coverage framework. To support these objectives, new formulations and supporting constraints were developed, enabling the allocation of service times in proportion to population density. A formal evaluation methodology was proposed to measure the models' effectiveness in achieving temporal fairness, using a normalized comparison across the three fairness objectives. A formal evaluation approach is developed to assess how effectively the proposed models achieve balance in maximum temporal coverage. This approach used a normalized performance of three fairness measures against each other. Empirical studies using small and medium instances are carried out to evaluate the solution quality of these models. Total Pairwise performs better in larger scenarios by reducing inequalities in service times, while MaxiMin and Distribution perform better in smaller configurations by emphasizing fairness in minimum service times. These results highlighted the complementary nature of the measures, with Total Pairwise focusing on overall fairness across areas and MaxiMin and Distribution prioritizing fair service times for the least served areas.

Among the three formulations, the version utilizing the Distribution objective function was selected for further computational evaluation due to its consistent performance in balancing fairness across underserved areas. This version of the model was tested using the previously generated instances to assess its solution capability compared to the MCLP-based formulation. The comparative results show that while the MCLP model performs well for small instances, it lacks scalability and fails to provide solutions for larger problems. In contrast, the proposed CTP model demonstrates greater robustness, achieving higher coverage and feasibility across a wider range of instances, making it more suitable for real-world, large-scale applications.

Results indicated that the Distribution CTP-based model was generally more effective in producing equitable service allocations and showed improved feasibility across a broader range of instance sizes. However, its performance declined as problem size increased, with the solver often failing to find optimal or even feasible solutions within the predefined time limit for large-scale instances. To address this limitation, a metaheuristic approach based on the GRASP was developed to generate high-quality solutions in larger problem settings. The following section presents the GRASP-based algorithms designed specifically for the proposed models and evaluates their effectiveness in tackling the scalability challenge.

CHAPTER FIVE
GREEDY RANDOMIZED ADAPTIVE SEARCH PROCEDURES FOR THE DBS-SUPPORTED COMMUNICATION NETWORKS UNDER POST-DISASTERS CONDITIONS

5.1 Chapter Introduction

As demonstrated by the computational results in Section 4, the developed exact models fail to achieve optimal or even feasible solutions for the majority of the tested instances. A constructive algorithm was proposed for this problem since the size of the solution representation is not known a priori, making it impractical to define it as an input parameter. Instead, the solution must be incrementally built. This approach enables more effective handling of neighbourhood structures during the solution improvement phase, which is crucial for guiding the search process. Given these characteristics, the use of a constructive heuristic was deemed more appropriate, and the Greedy Randomized Adaptive Search Procedure (GRASP) metaheuristic was selected as a suitable framework for addressing the problem. Within this context, a GRASP algorithm employed some of the features of the variable neighbourhood search (VNS) and simulated annealing algorithms is proposed to achieve high-quality results within acceptable computational times for the handled problem. This chapter presents the proposed GRASP algorithm in detail, the performance evaluation on generated instances, and the computational results. Two GRASP algorithms are specifically developed for both the MCLP-based problem formulation with a temporal coverage objective and the CTP-based formulation incorporating the Distribution fairness objective. These algorithmic solutions are then evaluated and benchmarked against their corresponding mathematical models to assess solution quality, scalability, and computational efficiency.

The proposed GRASP algorithm is explained in the next section (5.2). In section 5.3, the performance of the proposed metaheuristic is tested on generated instances for the specific problem.

5.2 Greedy Randomized Adaptive Search Procedure

GRASP is a multi-start metaheuristic algorithm introduced by Feo & Resende, (1995) to address combinatorial optimization problems. Each GRASP iteration comprises two main phases: a construction phase, which generates an initial feasible solution, and a local search phase, which attempts to refine this solution by exploring its neighbourhood.

In the construction phase, GRASP combines greedy selection criteria with a randomized decision process to incrementally build a solution. At each step, candidate elements are ranked based on a greedy function, and the most promising ones form a Restricted Candidate List (RCL). One element from the RCL is then chosen at random, rather than deterministically selecting the top-ranked candidate. This probabilistic mechanism ensures that different solutions can be constructed across iterations. The method is adaptive, as the utility of each candidate is updated in response to previous selections, dynamically influencing future choices (Feo & Resende, 1995; Resende & Ribeiro, 2003).

Following the construction phase, a local search procedure explores the solution's neighbourhood to find improved alternatives. This iterative improvement continues until no better neighbour can be found, i.e., a local optimum is reached. The best solution obtained across all iterations is retained as the result. Common termination criteria include a fixed iteration count, a maximum number of iterations lacking improvement, or imposed time limits.

GRASP's strength lies in its ability to explore diverse regions of the solution space via randomization while still maintaining a greedy focus to guide search efficiency. The modular nature of GRASP makes it particularly suitable for tailoring to specific problem contexts and hybridization with other metaheuristics. Furthermore, GRASP has been extended through hybrid approaches. For instance, GRASP-VNS incorporates ideas from SA by allowing the acceptance of non-improving or degraded solutions under certain probabilistic thresholds. This addition helps the algorithm escape local minima and improves the exploration of the global search space.

Due to its simplicity, flexibility, and strong empirical performance, GRASP has been successfully applied in various domains such as scheduling (Aiex, Binato, & Resende, 2003), routing (Prins, 2009), network design (Resende & Ribeiro , 2003), assignment problems, partitioning, and resource allocation.

Algorithm 5.1 presents a basic framework for the proposed GRASP algorithm. The method consists of $GRASP_{iter}$ iterations of the GRASP algorithm. At each iteration, an initial feasible solution (S) is created by the construction procedure and an improvement solution (S_{neigh}) is found by local search procedure. If the solution (S_{neigh}) is accepted by local search procedure as a best solution, S_{best} is updated. Following subsections present further details for the construction and local search prodecures.

Algorithm 5.1: The framework of the proposed *GRASP* algorithm

Input: $GRASP_{iter}$: number of GRASP iterations;
Output: S_{best};
$S_{best} \leftarrow \emptyset$;
Obj(S_{best}) $\leftarrow \infty$;
$Out_{iter} \leftarrow 0$;
while ($Out_{iter} \leq GRASP_{iter}$) **do**
    $Out_{iter} \leftarrow Out_{iter} + 1$;
    $S = construction()$;
    $S_{neigh} = localsearch(S)$;
    if (Obj (S_{neigh}) > Obj (S)) **then**
        $S_{best} \leftarrow S_{neigh}$;
    end
end
Return S_{best}.

5.2.1 Construction Phase

The detailed description of generating an initial feasible solution is as follows. Each route begins at a central depot at time zero and progressively visits nodes in a randomized order. Candidate nodes are selected based on their feasibility within the given battery limit and their contribution to spatial coverage, considering neighbourhood relations derived from a coverage matrix.

To ensure fairness in time allocation across visited nodes, a dynamic service time is computed at each iteration by equally distributing the remaining available time. Since two problem formulations (see sections 3 and 4) have different assumptions, initial solution and feasibility check functions are constructed according to these specialties. For the MCLP-based problem formulation, a node is feasible for a route if it has not been visited or covered before, meets strict neighbourhood relations and the battery limits. For the CTP-based problem formulation, a node is deemed feasible for a DBS if its service and travel times do not overlap with already visited nodes' time windows—ensuring no temporal conflicts across DBSs. This is enforced via a validation routine that cross-checks arrival and departure intervals across all previously scheduled nodes and their neighbours. Once a valid node is added to the route, its associated neighbours are marked as covered. This iterative process continues until a predefined coverage threshold is achieved or no further feasible nodes can be added. The design effectively balances greedy coverage expansion with randomized selection, while maintaining strict adherence to global battery constraints. This makes it a robust and adaptable construction strategy within the GRASP metaheuristic framework. Algorithm 5.2 presents the solution construction phase of the proposed GRASP algorithm.

Algorithm 5.2: Solution construction.

Input: K, coverage_matrix, Q, L, Ω: size of the RCL, ϑ

Output: S

repeat

$l \leftarrow 1$ // drone index

$S \leftarrow \emptyset$ // solution

add ← 0 // next node

route ← {add} // route

covered_nodes ← ∅

set_time ← 0

while size(*covered_nodes*) < Threshold **do**

$RCL \leftarrow generateRCL(\Omega)$;

add ← RandomChoice(*RCL*);

set_time ← *set_time* + compute_time(*add*)

if set_time < L & $l < K$ **then**

$route \leftarrow route \cup \{add\}$;

$RCL \leftarrow RCL - \{add\}$;

covered_nodes ← *covered_nodes* ∪ get_neighbor (coverage_matrix(*add*)==1)

$l \leftarrow l + 1$;

$S \leftarrow S \cup\ route$;

end

end

until *S is feasible*;

return *S;*

To illustrate the solution process of the proposed GRASP algorithms, a series of figures were generated to demonstrate the construction phase for each problem formulation. Each figure presents the step-by-step addition of nodes during the construction phase. These visualizations aim to provide deeper insight into the structural distinctions and decision-making mechanisms underlying the initial solution procedures of the two GRASP variants. Figure 5.1 illustrates the construction steps and resulting solution of the GRASP algorithm developed for the MCLP-based problem formulation, which is called $\text{GRASP}_{\text{MCLP}}$. It highlights how candidate nodes are selected, added to the solution, and evaluated based on coverage and feasibility at each step.

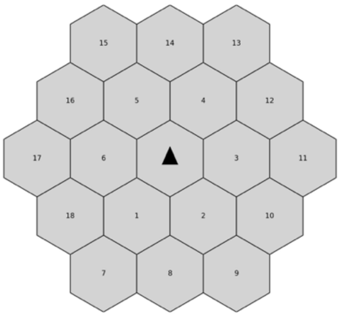

(a) Solution $S = \{\}$
$RCL = \{1, .. F\}$
$K = 6$
$\vartheta = 75\%$
$coveredNodes = \{\}$

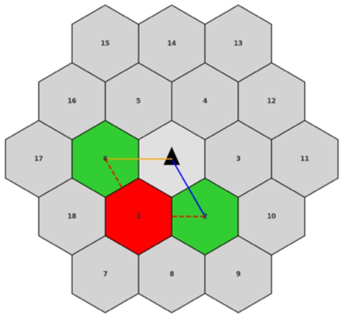

(b) $randomRCL = \{2\}$
$coveredNodes = \{1,2,3,8,9,10\}$
$K = K - 1$
$\textbf{while } K \geq 0 \textbf{ do}$
$\textbf{while } length(coveredNodes) \leq \vartheta F \textbf{ do}$
$S = \{0,2\}$
$RCL = RCL\ /\{2\}$
$randomRCL = \{6\}$
$coveredNodes = coveredNodes\ \cup \{1, 5,6,16,17,18\}$
Infeasible
$RCL = RCL\ /\{6\}$
$coveredNodes = \{1,2,3,8,9,10\}$

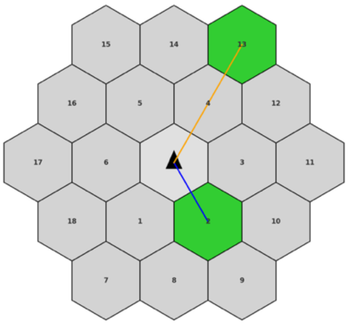

(c) $randomRCL = \{13\}$
$coveredNodes = coveredNodes\ \cup \{4,12,13,14\}$
$\textbf{while } K = K - 1 \textbf{ do}$
$\textbf{while } length(coveredNodes) \leq \vartheta F \textbf{ do}$
$S = \{0,2,0,13\}$
$RCL = RCL\ /\{13\}$

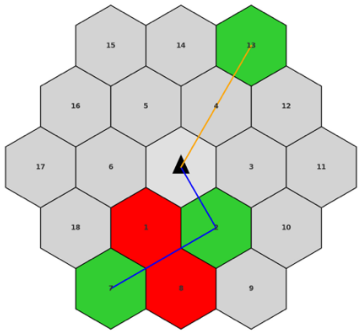

(d) $randomRCL = \{7\}$
$coveredNodes = coveredNodes\ \cup \{1,7,8,18\}$
Infeasible
$RCL = RCL\ /\{7\}$
$coveredNodes = \{1,2,3,8,9,10,4,12,13,14\}$

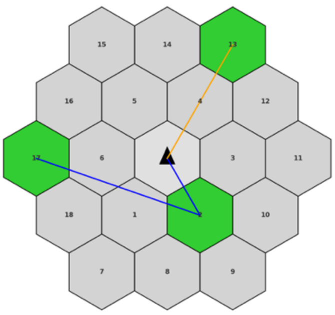

(e) $randomRCL = \{17\}$
$coveredNodes = coveredNodes\ \cup \{6,16,17,18\}$
$length(coveredNodes) > \vartheta F \textbf{ break}$
$S = \{0,2,17,0,13\}$

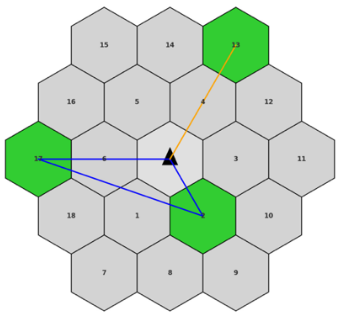

(f) Final $S = \{0,2,17,0,13\}$
$coveredNodes = \{1,2,3,8,9,10,4,12,13,14,6,16,17,18\}$

Figure 5.1 Solution construction for GRASP$_{MCLP}$

The step-by-step construction of the initial solution is illustrated through stages (a) to (f). In step (a), the solution set S is initialized as empty, with the RCL including all areas, a coverage threshold ϑ set at 75%, and the number of available DBSs $K = 6$. At this point, no nodes are covered. In step (b), a candidate (node 2) is randomly selected from the RCL, and the nodes it covers are added to the *coveredNodes* set. After updating K, the algorithm proceeds to select node 6, but the resulting configuration is deemed infeasible, prompting the algorithm to discard node 6 and revert the coverage set. In step (c), node 13 is added, extending the coverage, and the route is updated accordingly. In step (d), node 7 is selected but also leads to an infeasible configuration and is therefore removed. In step (e), node 17 is added successfully, significantly increasing the coverage. At this point, the algorithm verifies that the coverage exceeds the defined threshold ϑF, and terminates the construction. Step (f) presents the final solution $S = \{0, 2, 17, 0, 13\}$, which collectively covers a sufficiently large subset of nodes to satisfy the problem's initial feasibility requirements.

Figure 5.2 presents the construction phase of the GRASP algorithm tailored for the CTP-based problem formulation, which is called $GRASP_{CTP}$. Unlike the previous approach, this version incorporates temporal dynamics by accounting for both arrival and departure times at each node during solution construction. Although both construction procedures utilize the same initial candidate set, sampling instance, and parameter settings—such as RCL size and selection thresholds—certain adjustments were required for the $GRASP_{CTP}$ due to its temporal structure. Since the problem formulation allows multiple visits to nodes at different times, a higher coverage threshold (approximately 90%) was adopted to better reflect the extended service capacity of the system. This modification ensures that the temporal flexibility inherent in the CTP formulation is fully leveraged during the solution construction process. Figure 5.2 sequentially displays how nodes are added to the tour while respecting time-dependent feasibility constraints.

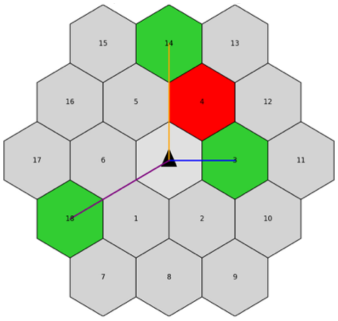

(a) $randomRCL = \{3\}$
$ArrivalTimes = \{3{:}\,1.73\}$
$coveredNodes = \{2,3,4,10,11,12\}$
$\boldsymbol{while}\ length(coveredNodes) \leq \vartheta F\ \boldsymbol{do}$
$S = \{0,3\}$
$RCL = RCL\ /\{3\}$
$randomRCL = \{18\}$
$ArrivalTimes = \{3{:}\,1.73, 18{:}\,3.00\}$
$coveredNodes = coveredNodes\ \cup \{1,6,7,17,18\}$
$\boldsymbol{while}\ length(coveredNodes) \leq \vartheta F\ \boldsymbol{do}$
$RCL = RCL\ /\{18\}$
$S = \{0,3,0,18\}$
$randomRCL = \{14\}$
$ArrivalTimes = \{3{:}\,1.73, 18{:}\,3.00, 14{:}\,3.00\}$ AND
$coveredNodes = coveredNodes\ \cup \{4,5,13,14,15\}$
Infeasible
$RCL = RCL\ /\{14\}$
$coveredNodes = \{2,3,4,10,11,12,1,6,7,17,18\}$

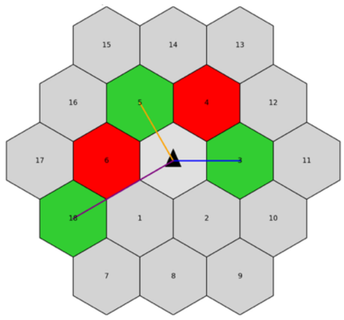

(b) $randomRCL = \{5\}$

$ArrivalTimes = \{3{:}\,1.73, 18{:}\,3.00, 5{:}\,1.73\}$ AND

$coveredNodes = coveredNodes\ \cup \{4,5,6,14,15,16\}$

Infeasible

$RCL = RCL\ /\{5\}$

$coveredNodes = \{2,3,4,10,11,12,1,6,7,17,18\}$

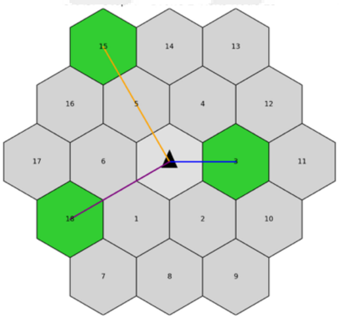

(c) $randomRCL = \{15\}$

$ArrivalTimes = \{3{:}\,1.73, 18{:}\,3.00, 15{:}\,3.46\}$

$coveredNodes = coveredNodes\ \cup \{5,14,15,16\}$

$\boldsymbol{while}\ length(coveredNodes) \leq \vartheta F\ \boldsymbol{do}$

$RCL = RCL\ /\{15\}$

$S = \{0,3,0,18,0,15\}$

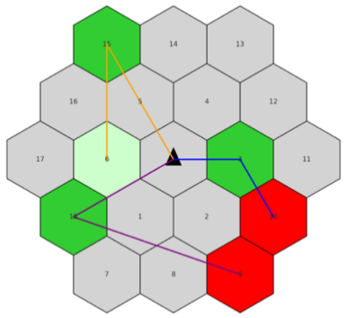

(d) $randomRCL = \{6\}$
$ArrivalTimes = \{6{:}\,34.73\}$
$DepartureTimes = \{18{:}\,31.50\}$
$coveredNodes = coveredNodes\ \cup \{\}$
$\boldsymbol{while}\ length(coveredNodes) \leq \vartheta F\ \boldsymbol{do}$
$RCL = RCL\ /\{6\}$
$S = \{0,3,0,18,0,15,6\}$
$randomRCL = \{9\}$
$ArrivalTimes = \{9{:}\,36.08\}$
$DepartureTimes = \{3{:}\,30.87\}$
$coveredNodes = coveredNodes\ \cup \{8,9\}$
$\boldsymbol{while}\ length(coveredNodes) \leq \vartheta F\ \boldsymbol{do}$
$RCL = RCL\ /\{9\}$
$S = \{0,3,0,18,9,0,15,6\}$
$randomRCL = \{10\}$
$ArrivalTimes = \{9{:}\,36.08, 10{:}\,32.59\}$
Infeasible
$RCL = RCL\ /\{10\}$

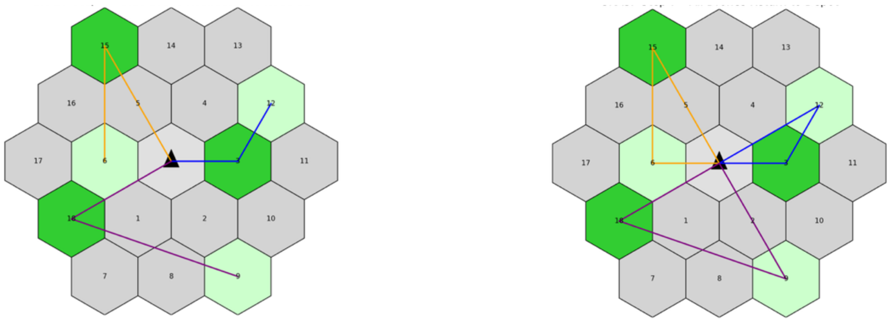

(e) $randomRCL = \{12\}$

$ArrivalTimes = \{12{:}\ 32.59\}$

$length(coveredNodes) > \vartheta F$ $\boldsymbol{break}$

$S = \{0,3,12,0,18,9,0,15,6\}$

(f) $S = \{0,3,12,0,18,9,0,15,6\}$

Arrival Times: {15: 3.46, 6: 34.73, 3: 1.73, 12: 32.59, 18: 3.0, 9: 36.08} Departure Times: {15: 31.73, 6: 52.57, 3: 30.86, 12: 51.44, 18: 31.50, 9: 53.55}

Final Service Times: {15: 28.26, 6: 46.34, 3: 47.97, 12: 47.97, 18: 46.34, 9: 17.47, 5: 46.11, 14: 28.26, 16: 46.11, 0: 46.97, 1: 46.34, 17: 46.34, 2: 46.60, 4: 47.97, 10: 46.60, 11: 47.97, 13: 18.84, 7: 28.50, 8: 17.47}

Figure 5.2 Solution construction for $\text{GRASP}_{\text{CTP}}$

The construction process of the $\text{GRASP}_{\text{CTP}}$ is depicted through steps (a) to (f), highlighting both spatial coverage and temporal feasibility. In step (a), node 3 is selected as the first area visited, covering a subset of areas and yielding an initial arrival time. Another tour is started to node 18, and subsequently to node 14; however, the latter results in a temporal infeasibility due to overlap constraints and is thus removed. In step (b), node 5 is selected but again leads to an infeasible configuration, likely due to arrival-departure time conflicts. In step (c), node 15 is chosen, and its addition maintains temporal feasibility while increasing coverage. The tours are further extended in step (d) by attempting to add nodes 6, 9, and 10. Among these, nodes 6 and 9 are feasible, while node 10 is excluded due to infeasibility. In step (e), node 12 is successfully added, and the coverage threshold is satisfied, prompting the termination of the construction process. Finally, step (f) summarizes the complete solution sequence and presents detailed arrival and departure times, along with the computed service times for each visited and indirectly covered node. This detailed temporal accounting reflects the algorithm's ability to construct a feasible tour under time-dependent constraints while maximizing spatial coverage.

5.2.2 Local Search Phase

The local search component of the proposed GRASP framework integrates multiple neighbourhood structures and a strict feasibility validation mechanism to refine constructed solutions. The procedure leverages a VNS approach, combined with SA-based acceptance criteria to balance intensification and diversification. VNS framework originally proposed by Mladenović & Hansen, (1997). It relies on the systematic modification of neighborhood structures during the search procedure. The VNS starts by exploring the random-selected neighbourhood given a number of inner-iterations, and if a better solution is found returning as a best solution. Until the inner iterations completed, it explores the neighbourhood structures randomly. To enhance the exploitation of solutions, the proposed VNS procedure perturbs the current solution using the following inter-route and intra-route neighbourhoods, swap, insertion, two-opt, replacement, and inversion, that are applied to the given solution:

- Swap: swap of the nodes visited in different routes.
- Insertion: a node is removed from one route and inserted into another route.
- 2-opt: a sequence of nodes within a specified segment of a route is reversed.
- Replacement: substitute a node with a non-visited one.
- Inversion: reverse the route direction.

These operators are selected probabilistically and designed to investigate diverse regions of the solution space. The replacement operator incorporates a custom feasibility filter that restricts substitutions to those that do not violate neighbourhood overlaps among nodes.

After each move, the feasibility of the modified solution is rigorously checked. The solution feasibility check function ensures that:

- DBS routes do not exceed the battery limit,
- There are no temporal overlaps between neighbouring nodes served by different DBSs,
- The number of DBSs used does not exceed the allowed limit,

- The coverage threshold (based on a defined matrix of neighbourhood relationships) is met.

Only if a solution passes all these constraints is it considered for acceptance. Improvements are always accepted, while worse solutions may still be accepted probabilistically based on a decreasing temperature parameter, akin to SA. This adaptive mechanism allows the algorithm to avoid local optima and explore various areas within the search space. The local search procedure is detailed in the pseudo-code of Algorithm 5.3.

Algorithm 5.3: Local search.

Input:

VNS_{iter}: number of VNS iterations;

$\mathcal{T}_{ini}$: initial temperature;

$\mathcal{T}_{fin}$: final temperature;

ϱ: cooling rate;

Initial solution S;

Output: S_{best};

$S_{best} \leftarrow \emptyset$;

Obj(S_{best}) $\leftarrow \infty$;

$S_{cur} \leftarrow S$;

$\mathcal{T}_{cur} \leftarrow \mathcal{T}_{ini}$;

while ($\mathcal{T}_{cur} \geq \mathcal{T}_{fin}$) **do**

  for ($In_{iter} = 1, \ldots, VNS_{iter}$) **do**

    $S_{imp} = Neighborhood(S_{cur})$; // Randomly choice

    if (feasibility_check(S_{imp})==1) **then**

      if (Obj(S_{imp})>Obj (S_{best})) **then**

        $S_{best} \leftarrow S_{imp}$;

      end

      if (Obj(S_{imp})>Obj (S_{cur})) **then**

        $S_{cur} \leftarrow S_{imp}$;

      end

      else

        $\nabla S = 100 \cdot ((Obj(S_{cur}) - Obj(S_{imp}))/Obj(S_{imp}))$;

        if ($U(0,1) \leq \exp(-\nabla S/\mathcal{T}_{cur})$) **then**

          $S_{cur} \leftarrow S_{imp}$;

        end

        else

          $S_{cur} \leftarrow S$;

        end

      end

      $\mathcal{T}_{cur} = \varrho \cdot \mathcal{T}_{cur}$;

    end

  end

end

Return S_{best}, Obj(S_{best})

5.3 Computational Results

Extensive computational tests are performed to evaluate the performance of the proposed GRASP algorithms. Subsection 5.3.1 provides the discussion about the parameters tuning. Subsection 5.3.2 compares the performance of the proposed GRASP algorithms against two MILP models (MCLP and CTP). The algorithms were coded in Python. All tests were run using an Intel Core i7 with 3.40 GHz and 32 GB of RAM computer.

5.3.1 Parameter Tuning

To determine suitable values for the algorithm's parameters, we varied one parameter at a time while keeping the others constant. For each configuration, the algorithm was executed five times on a collection of generated instances. The configuration that achieved the best overall performance gap was chosen as the optimal setting. The parameter values used in the final experiments are summarized in Table 5.1.

Table 5.1 Parameter setting for the GRASP algorithm

Parameter	$GRASP_{iter}$,	VNS_{iter}	$\mathcal{T}_{ini}$	$\mathcal{T}_{fin}$	ϱ	Ω
Value	10	100	5	1	0.999975	[15,150]

The initial temperature is deliberately set to a low value to reinforce the intensification mechanism during the local search phase, thereby reducing the likelihood of accepting inferior solutions.

5.3.2 Comparison of GRASP Algorithms against the MILPs

This section gives the experimental results and analysis of the algorithm-based solution approach for the problem, which is explained in detail in the previous sections. Previously generated instances were used to evaluate the performance of the proposed GRASP algorithms.

The first part of the computational study compares the performances of MCLP-based problem formulation against the $GRASP_{MCLP}$. In the second part of the study, CTP-based problem formulation is compared against the $GRASP_{CTP}$. The comparison criteria are the objective values achieved within a given time for each model (total hover time for the MCLP-based problem formulation and total service time for the CTP model). In addition, the column labelled “Total Coverage” reports the percentage of the area covered, while the “Standard Deviation” column indicates the variability in service times across the visited or covered locations. The “Max-Min Time” column shows the range between the maximum and minimum service times provided, and the “CPU Time” column presents the computational time in seconds, measured within a 3600-second time limit for both the problem formulations and the algorithms. Furthermore, for the GRASP algorithm, the best, average, and worst results obtained over a predefined number of iterations are reported. Since the algorithm is stochastic in nature and executed multiple times, presenting a range of outcomes—rather than a single result—provides a more comprehensive and reliable evaluation of its performance. For the GRASP algorithm, the reported CPU time corresponds to the average runtime over all iterations, reflecting the typical computational effort required by the heuristic.

The results of the first computational study are summarized in Table 5.2. The comparative analysis reveals that the $GRASP_{MCLP}$ algorithm consistently outperforms the MCLP-based MILP model across multiple performance metrics, particularly as problem size increases. The performance of the $GRASP_{MCLP}$ algorithm and the MCLP-based MILP model was first examined on the irregular instance set (1-7). Here, $GRASP_{MCLP}$ consistently achieved higher total coverage—peaking at 89 % in the worst run for the 45-node case versus the MILP’s 60 %. Moreover, $GRASP_{MCLP}$’s service-time variability remained substantially lower (standard deviation between 1.03 and 2.16) than the MILP’s 5.73 on the same instance, indicating a more equitable temporal allocation.

Table 5.2 Computational analysis for MCLP-based problem formulation and $GRASP_{MCLP}$

Instance no	MCLP-based Model					$GRASP_{MCLP}$												
						Best				Average				Worst				Average CPU time *(s)*
	Objective *(min)*	**Coverage (%)**	**Standard Deviation**	**Max-Min time**	**CPU time *(s)***	**Objective *(min)***	**Coverage (%)**	**Standard Deviation**	**Max-Min time**	**Objective *(min)***	**Coverage (%)**	**Standard Deviation**	**Max-Min time**	**Objective *(min)***	**Coverage (%)**	**Standard Deviation**	**Max-Min time**	
1	83.66	74	10.09	48.97-34.69	18	83.30	74	5.84	34.0-22.39	65.00	63	0.00	32.5-32.5	54.94	89	1.43	15.87-13.02	55
2	84.32	62	9.56	38.55-19.77	1947	84.30	79	2.55	20.00-14.30	79.30	72	1.86	22.06-17.51	66.73	69	4.68	27.5-18.51	126
3	159.42	60	5.73	56.54-47.51	3600	110.77	82	2.16	19.49-13.78	106.98	68	1.74	20.39-16.22	68.69	89	1.03	10.94-8.09	178
4	No feasible solutions found					136.89	71	4.24	28.02-14.05	111.48	72	2.36	18.99-12.45	80.64	61	9.73	32.5-5.54	145
5	Out of memory					104.53	64	5.33	19.05-1.00	94.97	60	6.41	22.79-2.99	89.29	60	8.50	32.5-1.97	280
6	Out of memory					106.29	56	5.94	20.97-1.00	98.53	50	5.68	22.43-2.58	90.63	52	8.49	32.5-2.05	395
7	Out of memory					143.39	48	3.40	16.79-5.69	103.92	45	4.76	15.91-3.12	97.30	41	5.68	20.09-1.00	476
8	77.09	67	0	38.55-38.55	12	76.04	83	6.36	32.5-20.34	65.00	67	0.00	32.5-32.5	51.42	98	0.79	14.04-12.46	22
9	127.79	78	1.19	32.99-30.93	3600	170.29	81	23.35	52.61-16.18	114.13	78	24.44	53.54-11.44	93.28	76	21.62	53.61-5.41	60
10	No feasible solutions found					221.25	78	12.53	54.14-17.75	156.84	77	18.04	53.51-6.84	100.84	77	21.79	53.54-4.38	164
11	Out of memory					129.71	82	3.08	13.68-1.00	117.98	56	0.71	16.08-13.54	89.57	71	20.27	53.54-1	240
12	Out of memory					132.15	63	3.08	13.15-1	78.75	63	4.87	14.04-1.00	69.01	65	7.11	17.75-1	282
13	Out of memory					196.77	62	4.66	17.42-1	118.01	63	9.46	33.27-1	96.29	61	9.39	31.13-1	370

In the structured hexagonal instances (8-13), the MILP model provided feasible solutions only for the smallest layouts (19 and 37 nodes), achieving 67 % and 78 % coverage, respectively. By contrast, $GRASP_{MCLP}$ produced feasible routes across all sizes, with average coverage ranging from 83 % (19 nodes) down to 63 % (169 nodes). Although the maximum–minimum service-time range widened in larger instances (e.g., 53.61–5.41 for 37 nodes and 33.27–1.00 for 169 nodes), the standard deviation remained below 10 in all experiments, reflecting acceptable fairness given the instance scale.

In terms of total coverage, GRASP achieves higher or comparable values in almost all instances, which is a desirable outcome for coverage-centric problems. Moreover, although the total hover time for $GRASP_{MCLP}$ is sometimes higher, it reflects the algorithm's ability to extend service reach rather than inefficiency, especially in instances where MCLP fails to provide any solution.

From a standard deviation perspective, $GRASP_{MCLP}$ generally maintains lower variability in service times across covered locations, which is crucial for ensuring fairness and consistency in temporal allocation. This is especially notable in larger instances, where $GRASP_{MCLP}$'s deviation remains moderate despite the complexity of the solution space, while MCLP either fails to compute or returns more irregular service distributions in small instances.

Regarding max-min service time, $GRASP_{MCLP}$ tends to offer a more balanced allocation, with a narrower range between the maximum and minimum service durations in most cases. This reduces temporal disparity between nodes and supports more equitable coverage strategies.

In terms of computational efficiency, $GRASP_{MCLP}$ exhibits reasonable average CPU times, often well below the MILP model's timeout limit (3600s), while still ensuring feasibility. Notably, MCLP often encounters infeasibility or memory limitations in medium to large-scale instances.

Overall, $GRASP_{MCLP}$ provides a superior balance of high coverage, stable service distribution, and computational tractability, making it more suitable for large-scale or time-constrained applications compared to exact methods like MCLP.

The results of the second computational study are summarized in Table 5.3. In the irregular instance group (1-7), $GRASP_{CTP}$ demonstrates a consistent advantage over the exact CTP-based problem formulation in terms of solution quality and feasibility. For instance 30, $GRASP_{CTP}$ reaches 100% total coverage with a maximum–minimum service time range of 46.05–16.19, outperforming the CTP-based problem formulation which achieves 86% coverage with a wider range and slightly lower average time. In instance 45, $GRASP_{CTP}$ again surpasses the CTP-based problem formulation by improving coverage from 75% to up to 89% while maintaining a balanced standard deviation around 11–12. Furthermore, for instance 150, where the CTP-based problem formulation fails to return any solution, $GRASP_{CTP}$ provides feasible results with up to 68% coverage. These trends confirm that the heuristic algorithm remains computationally viable where the MILP-based approach either fails or exhausts available resources.

Looking at the structured instances (8-13), $GRASP_{CTP}$ continues to exhibit strong performance, particularly in larger configurations where CTP model feasibility diminishes. For instance 61, $GRASP_{CTP}$ improves total coverage from 65% to 88%, while significantly reducing the service-time variability (standard deviation drops from 15.62 to as low as 11.28). Even in the largest instance tested (169), where the CTP-based problem formulation fails to produce a feasible solution, $GRASP_{CTP}$ not only returns valid results but also achieves up to 90% coverage with standard deviation controlled below 9, and a manageable time span between minimum and maximum service durations.

Overall, across both irregular and regular structured instance groups, $GRASP_{CTP}$ proves to be a robust and scalable alternative to the exact CTP-based MILP model. It delivers consistently higher coverage, more equitable service time distributions (with lower standard deviations and tighter max–min ranges), and greater computational feasibility in large-scale settings. These findings emphasize the algorithm's practical advantage in real-world planning scenarios where time constraints and fairness requirements must be jointly optimized.

Table 5.3 Computational analysis for CTP-based problem formulation and $GRASP_{CTP}$

Instance no	CTP based Model					$GRASP_{CTP}$												Average CPU time *(s)*
						Best				Average				Worst				
	Objective *(min)*	Coverage (%)	Standard Deviation	Max-Min time	CPU time *(s)*	Objective *(min)*	Coverage (%)	Standard Deviation	Max-Min time	Objective *(min)*	Coverage (%)	Standard Deviation	Max-Min time	Objective *(min)*	Coverage (%)	Standard Deviation	Max-Min time	
1	675.59	90	14.07	64.34-32.17	15	668.58	100	12.41	46.92-16.76	570.17	90	12.72	46.53-17.90	483.45	79	12.76	46.53-18	17
2	789.609	86	10.19	54.46-27.23	1532	781.69	90	11.04	46.13-16.92	770.82	83	11.46	47.56-17.11	759.59	76	11.54	47.56-18.26	174
3	1043.28	75	9.87	54.74-26.62	3600	1260.52	89	12.15	47.98-16.54	1127.91	80	11.37	47.98-16.76	949.99	73	10.63	47.98-15.92	180
4	1066.77	76	9.35	40.71-19.61	3600	1306.02	61	11.00	47.98-16.74	1169.58	74	10.12	46.40-16.54	1048.00	61	10.71	47.98-17.27	225
5	2386.44	62	11.53	34.58-89.78	3600	2597.31	79	13.92	47.98-19.16	1893.33	69	11.46	47.56-15.27	1710.00	64	10.54	46.92-17.11	370
6	139.57	56	2.79	8.21-1	3600	2674.43	75	9.74	47.98-14.86	2482.58	76	9.35	47.40-15.62	2321.72	67	9.89	45.18-15.79	322
7	No feasible solutions found					2871.38	68	10.67	46.54-15.92	2519.28	60	9.84	47.03-14.14	2289.29	54	9.15	46.5-14.39	572
8	682.42	100	0.00	37.91	20	681.70	100	12.30	47.56-17.32	625.01	83	10.61	46.92-18.27	588.47	94	9.85	47.56-18.42	32
9	1487.92	75	19.78	85.02-42.51	3600	1514.95	92	12.66	47.60-18.02	1295.74	89	10.41	47.40-17.69	1064.04	92	11.14	46.92-17.27	120
10	1801.84	65	15.62	75.09-37.55	3600	1862.81	87	13.47	47.98-19.07	1637.68	88	11.28	46.47-16.85	1522.02	83	11.77	47.98-16.47	142
11	1843.26	60	20.10	110.91-19.09	3600	2439.65	81	11.34	47.40-16.76	2299.99	80	10.82	47.40-16.48	2137.12	77	10.57	45.60-16.20	275
12	357.13	63	16.64	45.80-1	3600	2887.85	75	11.42	46.92-15.96	2501.78	67	10.88	47.56-15.27	2273.97	67	8.84	47.40-16.39	260
13	No feasible solutions found					3478.83	73	10.22	47.56-14.06	3121.98	90	8.92	47.98-14.86	2837.86	87	7.48	47.56-14.41	412

The following figures (Figures 5.3 and 5.4) illustrate the solutions generated by $GRASP_{MCLP}$ and $GRASP_{CTP}$ on the irregular and regular structured problem instances, allowing for a visual comparison of their spatial coverage and service distribution as well highlighting differences in coverage patterns and route structures. Figure 5.3 illustrates the solutions generated by both algorithms on the 61-node regular structured instance. The left side presents the result obtained from $GRASP_{MCLP}$, including the service times provided to the covered nodes. The right side shows the output of $GRASP_{CTP}$, where in addition to service times, arrival and departure times are also displayed to provide further insight into the temporal dynamics of neighbouring visits.

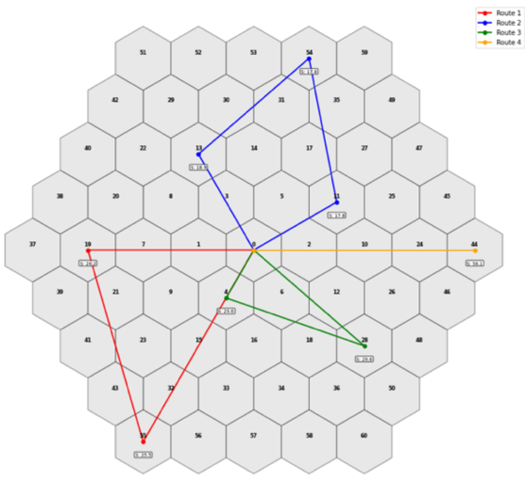

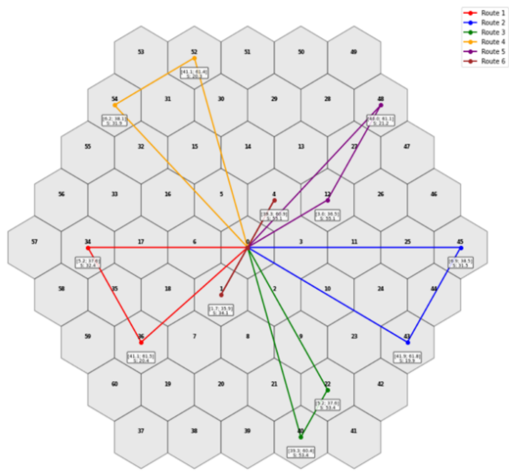

$\text{GRASP}_{\text{MCLP}}$

$\text{GRASP}_{\text{CTP}}$

Best Solution: [55, 19, 0, 13, 54, 11, 0, 28, 4, 0, 44]

Service Times: {55: 25.47, 19: 26.15, 13: 18.86, 54: 17.75, 11: 17.75, 28: 29.55, 4: 29.55, 44: 56.14, 43: 25.47, 32: 25.47, 56: 25.47, 38: 26.15, 20: 26.15, 7: 26.15, 21: 26.15, 39: 26.15, 37: 26.15, 29: 18.86, 30: 18.86, 14: 18.86, 3: 18.86, 8: 18.86, 22: 18.86, 53: 17.75, 31: 17.75, 35: 17.75, 59: 17.75, 17: 17.75, 27: 17.75, 25: 17.75, 10: 17.75, 2: 17.75, 5: 17.75, 12: 29.55, 26: 29.55, 48: 29.55, 50: 29.55, 36: 29.55, 18: 29.55, 1: 29.55, 6: 29.55, 16: 29.55, 15: 29.55, 9: 29.55, 45: 56.14, 24: 56.14, 46: 56.14 }

Best Solution: [34, 36, 0, 45, 43, 0, 22, 40, 0, 54, 52, 0, 0, 12, 48, 0, 1, 4]

Service Times: {34: 32.40, 36: 20.44, 45: 31.53, 43: 19.86, 22: 53.42, 40: 53.42, 54: 31.87, 52: 20.25, 12: 55.10, 48: 21.17, 1: 34.13, 4: 55.10, 17: 32.40, 33: 32.40, 35: 52.84, 56: 32.40, 57: 32.40, 58: 32.40, 7: 54.58, 18: 54.58, 19: 20.44, 59: 20.44, 60: 20.44, 25: 31.53, 44: 51.40, 46: 31.53, 23: 52.27, 24: 19.86, 42: 52.27, 9: 32.40, 21: 53.42, 41: 53.42, 39: 21.02, 31: 52.12, 32: 31.87, 53: 52.12, 55: 31.87, 30: 20.25, 51: 20.25, 3: 55.10, 11: 33.5, 13: 55.10, 26: 33.50, 27: 54.67, 28: 21.17, 47: 21.17, 49: 21.17, 2: 34.13, 6: 34.13, 8: 34.13, 5: 21.60, 14: 21.60}

Arrival Times: {34: 5.19, 36: 41.06, 45: 6.92, 43: 41.92, 22: 5.19, 40: 39.33, 54: 6.24, 52: 41.12, 12: 3.00, 48: 39.96, 1: 1.73, 4: 39.33}

Departure Times: {34: 37.59, 36: 61.50, 45: 38.46, 43: 61.79, 22: 37.59, 40: 60.35, 54: 38.12, 52: 61.37, 12: 36.50, 48: 61.14, 1: 35.86, 4: 60.93}

Figure 5.3 Illustration of the solution for regular-structured instance

Figure 5.4 presents the results for a 55-node irregular structured instance. As in the previous figure, the left side corresponds to the solution produced by $\text{GRASP}_{\text{MCLP}}$, highlighting the service times allocated to each covered node. The right side displays the $\text{GRASP}_{\text{CTP}}$ outcome, which includes not only service times but also arrival and departure times. This comparison allows for a clearer understanding of how the underlying spatial configuration influences route construction, temporal allocations, and neighbourhood-level scheduling in each algorithm.

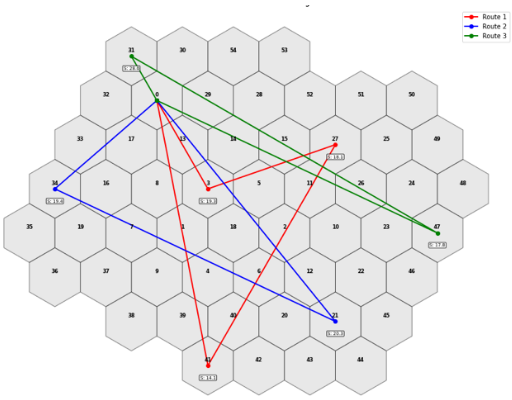

GRASP$_{MCLP}$

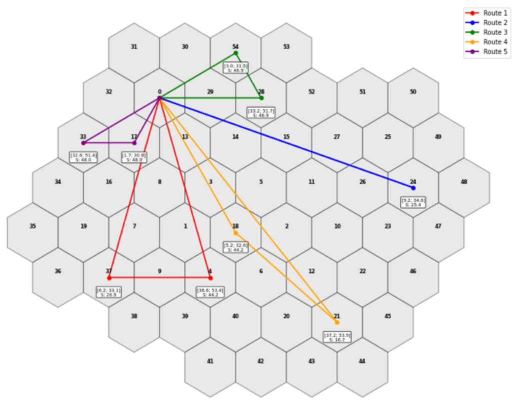

GRASP$_{CTP}$

Best Solution: [3, 27, 41, 0, 21, 34, 0, 31, 47]

Service Times: {3:19.25, 27:18.13, 41:14.05, 21:20.27, 34:19.38, 31:28.02, 47:17.75, 13: 19.25, 14: 19.25, 5: 19.25, 18: 19.25, 1: 19.25, 8: 19.25, 52: 18.13, 51: 18.13, 25: 18.13, 26: 18.13, 11: 18.13, 15: 18.13, 39: 14.05, 40: 14.05, 42: 14.05, 12: 20.27, 22: 20.27, 45: 20.27, 44: 20.27, 43: 20.27, 20: 20.27, 33: 19.38, 16: 19.38, 19: 19.38, 35: 19.38, 30: 28.02, 32: 28.02, 48: 17.75, 24: 17.75, 23: 17.75, 46: 17.75}

Best Solution: [37, 4, 0, 24, 0, 0, 54, 28, 0, 18, 21, 0, 17, 33]

Service Times: {37: 26.87, 4: 44.16, 24: 25.41, 54: 46.92, 28: 46.92, 18: 44.16, 21: 16.74, 17: 47.97, 33: 47.97, 7: 26.87, 9: 43.64, 19: 26.87, 36: 26.87, 38: 26.87, 1: 44.16, 6: 44.16, 39: 16.765, 40: 16.76, 23: 25.41, 25: 25.41, 26: 25.41, 47: 25.41, 48: 25.41, 49: 25.41, 29: 46.92, 30: 28.50, 53: 46.92, 14: 18.42, 15: 18.42, 52: 18.42, 2: 27.40, 3: 27.40, 5: 27.40, 12: 16.74, 20: 16.74, 22: 16.74, 43: 16.74, 44: 16.74, 45: 16.74, 8: 29.13, 13: 29.13, 16: 47.97, 32: 47.97, 34: 18.84}

Arrival Times: {37: 6.24, 4: 36.58, 24: 9.16, 54: 3.00, 28: 33.23, 18: 5.19, 21: 37.18, 17: 1.73, 33: 32.59}

Departure Times: {37: 33.12, 4: 53.35, 24: 34.58, 54: 31.50, 28: 51.65, 18: 32.59, 21: 53.92, 17: 30.86, 33: 51.44}

Figure 5.4 Illustration of the solution for irregular-structured instance

5.4 Chapter Conclusion

As demonstrated by the computational findings in this chapter, the exact optimization models were unable to produce optimal—or in many cases even feasible—solutions for many tested instances, particularly as instance size increased. To overcome this limitation, a constructive solution approach was adopted, since the size of the solution representation could not be predetermined, rendering traditional input-based formulations impractical. The incremental nature of the constructive method allowed for dynamic and efficient integration of neighbourhood structures during the search process, which proved essential for solution refinement. Accordingly, the GRASP metaheuristic was identified as a suitable foundation, and a metaheuristic algorithm was developed by combining GRASP with VNS and SA techniques. This proposed GRASP algorithm was shown to generate high-quality solutions within reasonable computational times. This chapter concluded with a detailed description of the proposed algorithm and a comprehensive performance evaluation across both regular and irregular structured instances.

CHAPTER SIX
RESULTS AND CONCLUSIONS

6.1 Summary of the Thesis

This thesis has investigated the design and optimization of DBS-based communication systems for emergency response, with an emphasis on achieving both spatial and temporal fairness in coverage. Motivated by the increasing need for resilient and adaptive communication infrastructures in disaster scenarios, the study focused on the optimal deployment and routing of multiple drone base stations (DBSs), integrating both exact mathematical formulations and metaheuristic methods. The proposed solution framework addressed the inherent challenges of limited energy resources, mobility constraints, and equitable service distribution across affected areas.

Chapter Two provided a comprehensive review of the relevant literature in the context of DBS-enabled communication systems, specifically through the perspective of operational research. The chapter offered a detailed classification of optimization problems encountered in the deployment of DBSs and critically assessed the modelling approaches used in existing studies. By identifying key limitations—particularly with respect to fairness, scalability, and adaptability—this review established the research gap and positioned the thesis within a novel and underexplored area of study.

In Chapter Three, the thesis introduced a novel mathematical formulation for a spatial-temporal coverage optimization problem, grounded in the structure of the classical Maximal Covering Location Problem (MCLP). The proposed MILP model aimed to determine both the hovering positions and routes of DBSs in disaster-areas, subject to battery and travel-time constraints. The formulation incorporated fairness via time-balancing constraints that enforce equitable service distribution. A second formulation was also introduced to explicitly maximize temporal coverage. Extensive computational experiments conducted on generated instances demonstrated the impact of fairness-enforcing constraints on coverage outcomes and energy efficiency. The results revealed the limitations of such exact formulations, particularly in their scalability beyond medium-sized instances.

To address these limitations, Chapter Four proposed an alternative approach in which fairness considerations were embedded directly into the objective function, rather than imposed through rigid constraints. Building on the classical Covering Tour Problem (CTP), a new family of MILP models was developed to incorporate three distinct fairness criteria: Total Pairwise Differences, Maximin (Rawlsian), and Distribution-based fairness. The models were evaluated using a unified performance framework that included normalized fairness metrics and coverage-based indicators. Among the three formulations, the Distribution-based model consistently achieved balanced and equitable service across underserved areas. Comparative results showed that, while the MCLP-based models offered tractability only in smaller cases, the CTP-based model provided more robust solutions across a broader range of instances, though its performance also degraded as instance size increased.

Recognizing the scalability issues of exact formulations, Chapter Five introduced a metaheuristic framework based on the Greedy Randomized Adaptive Search Procedure (GRASP). The algorithm was extended with Variable Neighbourhood Search (VNS) and Simulated Annealing (SA) components to enhance both diversification and intensification during the search. This constructive metaheuristic was particularly well-suited to the problem at hand, as the size of the solution representation could not be determined a priori and needed to be constructed incrementally. The proposed GRASP-based algorithms were evaluated on the previously generated instance sets. The results confirmed the ability of the proposed algorithm to generate high-quality solutions with reasonable computational effort, significantly outperforming the exact models in terms of feasibility, scalability, and coverage fairness, especially in large-scale problem settings.

In summary, this thesis proposed and systematically evaluated a set of exact and heuristic approaches for multi-DBS deployment under spatial-temporal fairness objectives. While exact formulations were shown to be effective for small to medium-scale instances, their computational limitations necessitated the development of more flexible heuristic strategies. The GRASP framework introduced in this study offers a promising direction for scalable and fair coverage planning in emergency communication systems, contributing both theoretically and practically to the field of operations research and humanitarian logistics.

6.2 Future Research Directions

This study lays the groundwork for several promising research directions that could enhance the applicability and robustness of DBS-based coverage models in real-world emergency response scenarios. One significant limitation of the current work is the assumption of a single-depot structure without explicit consideration of DBS recharging requirements. In practice, however, DBSs are energy-constrained and require periodic recharging to extend their operational range. Future studies could explore a multi-depot, multi-DBS CTP that integrates recharging logistics and energy routing decisions. Such extensions would offer a more realistic representation of DBS operations in complex and dynamic environments.

Another potential research direction involves the incorporation of system-level uncertainties into the model. While this study assumes deterministic parameters such as service times and travel durations, real-world scenarios often involve significant uncertainty due to factors like weather variability, wind conditions, or fluctuating demand at coverage locations. Embedding stochastic elements or adopting robust optimization frameworks would allow researchers to evaluate solution stability under uncertainty and generate more resilient deployment strategies. Furthermore, future models could accommodate heterogeneous DBS fleets with varying capabilities, payload capacities, or energy consumption profiles—further increasing the realism and practical applicability of the proposed framework.

Fairness in this thesis has been modelled through specific constructs in either the objective function or the constraints; however, alternative fairness metrics or multi-objective formulations may provide richer insights into trade-offs between equity, efficiency, and responsiveness. Future research could examine the impact of prioritizing different forms of equity (e.g., need-based or geographic parity) and how this influence system-wide performance.

Lastly, the modelling and algorithmic framework developed in this study could be extended to accommodate additional real-world constraints, such as no-fly zones, communication interference, or terrain-induced accessibility limitations. These considerations are particularly relevant for disaster-prone urban or mountainous areas. In parallel, the integration of DBS networks with ground-based infrastructure and human teams opens new avenues for hybrid coordination models, which could be explored in future interdisciplinary studies integrating operations research with decision support systems empowered by artificial intelligence.

REFERENCES

Ahmadian, N., Lim, G. J., Torabbeigi, M., & Kim, S. J. (2022). Smart border patrol using drones and wireless charging system under budget limitation. *Computers & Industrial Engineering, 164*, 107891, https://doi.org/10.1016/j.cie.2021.107891.

Aiex, R. M., Binato, S., & Resende, M. G. (2003). Parallel GRASP with path-relinking for job shop scheduling. *Parallel Computing, 29*(4), 393-430, https://doi.org/10.1016/S0167-8191(03)00014-0.

Akram, T., Awais, M., Naqvi, R., Ahmed, A., & Naeem, M. (2020). Multicriteria UAV Base Stations Placement for Disaster Management. *IEEE Systems Journal, 14*(3), 3475 - 3482, https://doi.org/10.1109/JSYST.2020.2970157.

Al-Hourani, A., Kandeepan, S., & Lardner, S. (2014). Optimal LAP Altitude for Maximum Coverage. *IEEE Wireless Communications Letters, 3*(6), 569-572, https://doi.org/10.1109/LWC.2014.2342736.

Alzenad, M., El-Keyi, A., Lagum, F., & Yanikomeroglu, H. (2017). 3-D Placement of an Unmanned Aerial Vehicle Base Station (UAV-BS) for Energy-Efficient Maximal Coverage. *IEEE Wireless Communications Letters, 6*(4), 434-437, https://doi.org/10.1109/LWC.2017.2700840.

Amrallah, A., Mohamed, E. M., Tran, G. K., & Sakaguchi, K. (2023). UAV Trajectory Optimization in a Post-Disaster Area Using Dual Energy-Aware Bandits. *Sensors, 23*(3), 1402, https://doi.org/10.3390/s23031402.

Arafat, M. Y., & Moh, S. (2019). Localization and Clustering Based on Swarm Intelligence in UAV Networks for Emergency Communications. *IEEE Internet of Things Journal, 6*(5), 8958 - 8976, https://doi.org/10.1109/JIOT.2019.2925567.

Asadi , A., & Pinkley, S. N. (2021). A stochastic scheduling, allocation, and inventory replenishment problem for battery swap stations. *Transportation Research Part E: Logistics and Transportation Review, 146*, 102212, https://doi.org/10.1016/j.tre.2020.102212.

Avellar, G. S., Pereira, G. A., Pimenta, L. C., & Iscold, P. (2015). Multi-UAV Routing for Area Coverage and Remote Sensing with Minimum Time. *Sensors, 15*(11), 27783-27803, https://doi.org/10.3390/s151127783.

Bah, M. D., Hafiane, A., & Canals, R. (2023). Hierarchical graph representation for unsupervised crop row detection in images. *Expert Systems with Applications, 216*, 119478, https://doi.org/10.1016/j.eswa.2022.119478.

Bai, G., Li, Y., Fang, Y., Zhang, Y. A., & Tao, J. (2020). Network approach for resilience evaluation of a UAV swarm by considering communication limits. *Reliability Engineering & System Safety, 193*, 106602, https://doi.org/10.1016/j.ress.2019.106602.

Banagar, M., Chetlur, V. V., & Dhillon, H. S. (2020). Handover Probability in Drone Cellular Networks. *IEEE Wireless Communications Letters, 9*(7), 933-937, https://doi.org/10.1109/LWC.2020.2974474.

Banik, D., Hossain, N. U., Govindan, K., Nur, F., & Babski-Reeves, K. (2023). A decision support model for selecting unmanned aerial vehicle for medical supplies: context of COVID-19 pandemic. *The International Journal of Logistics Management, 34*(2), 473-496, https://doi.org/10.1108/IJLM-06-2021-0334.

Barick, S., & Singhal, C. (2022). Multi-UAV Assisted IoT NOMA Uplink Communication System for Disaster Scenario. *IEEE Access, 10*, 34058–34068, https://doi.org/10.1109/ACCESS.2022.3159977.

Bibin Christopher, V., & Jasper, J. (2020). DHGRP: Dynamic Hexagonal Grid Routing Protocol with Mobile Sink for Congestion Control in Wireless Sensor Networks. *Wireless Personal Communications, 112*, 2213-2232, https://doi.org/10.1007/s11277-020-07146-z .

Boukoberine, M. N., Zhou, Z., & Benbouzid, M. (2019). A critical review on unmanned aerial vehicles power supply and energy management: Solutions, strategies, and prospects. *Applied Energy, 255*, 113823.

Bozkaya, E., Özçevik, Y., Akkoç, M., Erol, M. R., & Canberk, B. (2022). Energy-aware mobility for aerial networks: A reinforcement learning approach.

International Journal of Network Management, 32(1), 2185, https://doi.org/10.1002/nem.2185.

Campo, L. V., Ledezma, A., & Corrales, J. C. (2020). Optimization of coverage mission for lightweight unmanned aerial vehicles applied in crop data acquisition. *Expert Systems with Applications, 149*, 113227, https://doi.org/10.1016/j.eswa.2020.113227.

Chauhan, D., Unnikrishnan, A., & Figliozzi, M. (2019). Maximum coverage capacitated facility location problem with range constrained drones. *Transportation Research Part C: Emerging Technologies, 99*, 1-18, https://doi.org/10.1016/j.trc.2018.12.001.

Chen, Q. (2020). Joint Trajectory and Resource Optimization for UAV-Enabled Relaying Systems. *IEEE Access, 8*, 24108 - 24119, https://doi.org/10.1109/ACCESS.2020.2970439.

Cheng, C., Adulyasak, Y., & Rousseau, L. M. (2020). Drone routing with energy function: Formulation and exact algorithm. *Transportation Research Part B: Methodological, 139*, 364-387, https://doi.org/10.1016/j.trb.2020.06.011.

Cheon, H. R., Cho, J. W., & Kim, J. H. (2017). Dynamic resource allocation algorithm of UAS by network environment and data requirement. *2017 International Conference on Information and Communication Technology Convergence (ICTC)* (pp. 383-387). Jeju: IEEE.

Chittoor, P. K., Chokkalingam, B., & Mihet-Popa, L. (2021). A Review on UAV Wireless Charging: Fundamentals, Applications, Charging Techniques and Standards. *IEEE Access, 9*, 69235 - 69266, https://doi.org/10.1109/ACCESS.2021.3077041.

Chowdhury, S., Emeloglu, A., Marufuzzaman, M., Nurre, S. G., & Bian, L. (2017). Drones for disaster response and relief operations: A continuous approximation model. *International Journal of Production Economics, 188*, 167-184, https://doi.org/10.1016/j.ijpe.2017.03.024.

Chowdhury, S., Shahvari, O., Marufuzzaman, M., Li, X., & Bian, L. (2021). Drone routing and optimization for post-disaster inspection. *Computers & Industrial Engineering, 159*, 107495, https://doi.org/10.1016/j.cie.2021.107495.

Church, R. L., & Murray, A. T. (2008). *Business site selection, location analysis, and GIS.* Hoboken: John Wiley & Sons.

Cicek, C. T., Gultekin, H., & Tavli, B. (2019). The location-allocation problem of drone base stations. *Computers & Operations Research, 111*, 155-176, https://doi.org/10.1016/j.cor.2019.06.010.

Coutinho, W. P., Fliege, J., & Battarra, M. (2019). Glider Routing and Trajectory Optimisation in disaster assessment. *European Journal of Operational Research, 274*(3), 1138-1154, https://doi.org/10.1016/j.ejor.2018.10.057.

Cui, J., Hu, B., & Chen, S. (2021). A decision-making scheme for UAV maximizes coverage of emergency indoor and outdoor users. *Ad Hoc Networks, 112*, 102391.

Dalamagkidis, K. (2014). Classification of UAVs. K. P. Valavanis, & G. J. Vachtsevanos içinde, *Handbook of Unmanned Aerial Vehicles.* Netherlands: Springer Publishing Company, Incorporated.

Datta, A., Tallamraju, R., & Karlapalem, K. (n.d.). Multiple Drones driven Hexagonally Partitioned Area Exploration: Simulation and Evaluation. *arXiv:1906.00401*, https://doi.org/10.48550/arXiv.1906.00401.

Davoodi, S. M., & Goli, A. (2019). An integrated disaster relief model based on covering tour using hybrid Benders decomposition and variable neighborhood search: Application in the Iranian context. *Computers & Industrial Engineering, 130*, 370-380, https://doi.org/10.1016/j.cie.2019.02.040.

Deruyck, M., Wyckmans, J., Joseph, W., & Martens, L. (2018). Designing UAV-aided emergency networks for large-scale disaster scenarios. *EURASIP Journal on Wireless Communications and Networking, 2018*(1), 1-12, https://doi.org/10.1186/s13638-018-1091-8.

D'Andrea, R. (2014). Guest Editorial Can Drones Deliver? *IEEE Transactions on Automation Science and Engineering, 11*(3), 647–648.

Dorling, K., Heinrichs, J., Messier, G. G., & Magierowski, S. (2016). Vehicle Routing Problems for Drone Delivery. *IEEE Transactions on Systems, Man, and Cybernetics: Systems, 47*(1), 70-85, https://doi.org/10.1109/TSMC.2016.2582745.

Dukkanci, O., Kara, B. Y., & Bektaş, T. (2021). Minimizing energy and cost in range-limited drone deliveries with speed optimization. *Transportation Research Part C: Emerging Technologies, 125*, 102985, https://doi.org/10.1016/j.trc.2021.102985.

Dukkanci, O., Koberstein, A., & Kara, B. Y. (2023). Drones for relief logistics under uncertainty after an earthquake. *European Journal of Operational Research, 310*(1), 117-132.

Dukowitz, Z. (2019, November 1). *What Types of Drones Are There? A Guide to All the Different Drone Types on the Market*. Retrieved December 2021, from uavcoach.com: https://uavcoach.com/types-of-drones/

Ergezer, H., & Leblebicioğlu, K. (2014). 3D Path Planning for Multiple UAVs for Maximum Information Collection. *Journal of Intelligent & Robotic Systems , 73*, 737-762, https://doi.org/10.1007/s10846-013-9895-6.

Esubonteng, P. K., & Rojas-Cessa, R. (2022). RESTORE: Low-Energy Drone-Assisted NLoS-FSO Emergency Communications. *IEEE Access, 10*, 115282–115294, https://doi.org/10.1109/ACCESS.2022.3218014.

Farahani, R. Z., Asgari, N., Heidari, N., Hosseininia, M., & Goh, M. (2012). Covering problems in facility location: A review. *Computers & Industrial Engineering, 62*(1), 368-407, https://doi.org/10.1016/j.cie.2011.08.020.

Feo, T. A., & Resende , M. G. (1995). Greedy Randomized Adaptive Search Procedures. *Journal of Global Optimization, 6*, 109-133, https://doi.org/10.1007/BF01096763.

Fotouhi, A., Qiang, H., Ding, M., Hassan, M., Giordano, L. G., Garcia-Rodriguez, A., & Yuan, J. (2019). Survey on UAV Cellular Communications: Practical Aspects, Standardization Advancements, Regulation, and Security Challenges. *IEEE Communications Surveys & Tutorials , 21*(4), 3417-3442, https://doi.org/10.1109/COMST.2019.2906228.

Galán-Jiménez, J., Moguel, E., García-Alonso, J., & Berrocal, J. (2021). Energy-efficient and solar powered mission planning of UAV swarms to reduce the coverage gap in rural areas: The 3D case. *Ad Hoc Networks, 118*, 102517, https://doi.org/10.1016/j.adhoc.2021.102517.

Gendreau, M., Laporte, G., & Semet, F. (1997). The Covering Tour Problem. *Operations Research, 45*(4), 495-644, https://doi.org/10.1287/opre.45.4.568.

Gentili, M., Mirchandani, P. B., Agnetis, A., & Ghelichi, Z. (2022). Locating platforms and scheduling a fleet of drones for emergency delivery of perishable items. *Computers & Industrial Engineering, 168*, 108057, https://doi.org/10.1016/j.cie.2022.108057.

Ghelichi, Z., Gentili, M., & Mirchandani, P. B. (2022). Drone logistics for uncertain demand of disaster-impacted populations. *Transportation Research Part C: Emerging Technologies, 141*, 103735, https://doi.org/10.1016/j.trc.2022.103735.

Guerrero, J. A., & Bestaoui, Y. (2013). UAV Path Planning for Structure Inspection in Windy Environments. *Journal of Intelligent & Robotic Systems, 69*, 297-311, https://doi.org/10.1007/s10846-012-9778-2.

Guerriero, F., Surace, R., Loscri, V., & Natalizio, E. (2014). A multi-objective approach for unmanned aerial vehicle routing problem with soft time windows constraints. *Applied Mathematical Modelling, 38*(3), 839-852, https://doi.org/10.1016/j.apm.2013.07.002.

Guo, W., Devine, C., & Wang, S. (2014). Performance analysis of micro unmanned airborne communication relays for cellular networks. *9th International Symposium on Communication Systems, Networks & Digital Sign (CSNDSP)* (pp. 658-663). Manchester: IEEE.

Guo, Y., Yin, S., & Hao, J. (2019). Resource Allocation and 3-D Trajectory Design in Wireless Networks Assisted by Rechargeable UAV. *IEEE Wireless Communications Letters, 8*(3), 781-784, https://doi.org/10.1109/LWC.2019.2892721.

Gupta, L., Jain, R., & Vaszkun, G. (2016). Survey of Important Issues in UAV Communication Networks. *IEEE Communications Surveys & Tutorials, 18*(2), 1123-1152, https://doi.org/10.1109/COMST.2015.2495297.

Ha, Q. M., Deville, Y., Pham, Q. D., & Hà, M. H. (2018). On the min-cost Traveling Salesman Problem with Drone. *Transportation Research Part C: Emerging Technologies, 86*, 597-621, https://doi.org/10.1016/j.trc.2017.11.015.

Hassanalian, M., & Abdelkefi, A. (2017). Classifications, applications, and design challenges of drones: A review. *Progress in Aerospace Sciences, 91*, 99-131, https://doi.org/10.1016/j.paerosci.2017.04.003.

Hayajneh, K. F., Bani-Hani, K., Shakhatreh, H., Anan, M., & Sawalmeh, A. (2021). 3D Deployment of Unmanned Aerial Vehicle-Base Station Assisting Ground-Base Station. *Wireless Communications and Mobile Computing, 1*, 2937224, https://doi.org/10.1155/2021/2937224.

Hong, I., Kuby, M., & Murray, A. T. (2018). A range-restricted recharging station coverage model for drone delivery service planning. *Transportation Research Part C: Emerging Technologies, 90*, 198-212, https://doi.org/10.1016/j.trc.2018.02.017.

Hu, B., Yang, H., Wang, L., & Chen, S. (2019). A trajectory prediction based intelligent handover control method in UAV cellular networks. *China Communications, 16*(1), 1-14, https://doi.org/10.12676/j.cc.2019.01.001.

Huang, F., Chen, J., Wang, H., Ding, G., Gong, Y., & Yang, Y. (2019). Multiple-UAV-Assisted SWIPT in Internet of Things: User Association and Power Allocation. *IEEE Access, 7*, 124244 - 124255, https://doi.org/10.1109/ACCESS.2019.2938679.

Huang, H., Savkin, A. V., & Huang, C. (2021). Reliable Path Planning for Drone Delivery Using a Stochastic Time-Dependent Public Transportation Network. *IEEE Transactions on Intelligent Transportation Systems, 22*(8), 4941 - 4950, https://doi.org/10.1109/TITS.2020.2983491.

Javed, S., Hassan, A., Ahmad, R., Ahmed, W., Alam, M. M., & Rodrigues, J. J. (2023). UAV trajectory planning for disaster scenarios. *Vehicular Communications, 39*, 100568, https://doi.org/10.1016/j.vehcom.2022.100568.

Jeong, H. Y., Yu, D. J., Min, B. C., & Lee, S. (2020). The humanitarian flying warehouse. *Transportation Research Part E: Logistics and Transportation Review, 136*, 101901, https://doi.org/10.1016/j.tre.2020.101901.

Jin, X., Luo, Z., Shi, J., & Wang, L. (2024). Two-layer intelligent deployment of capsule airports and unmanned aerial vehicles for providing emergency communication services. *Expert Systems with Applications, 238*, 121795, https://doi.org/10.1016/j.eswa.2023.121795.

Kadioglu, E., Urtis, C., & Papanikolopoulos, N. (2019). UAV Coverage Using Hexagonal Tessellation. *27th Mediterranean Conference on Control and Automation (MED)* (pp. 37-42, https://doi.org/10.1109/MED.2019.8798564). Akko: IEEE.

Kalantari, E., Yanikomeroglu, H., & Yongacoglu, A. (2016). On the Number and 3D Placement of Drone Base Stations in Wireless Cellular Networks. *2016 IEEE 84th Vehicular Technology Conference (VTC-Fall)* (pp. 1-6). Montreal: IEEE.

Karsu, Ö., & Morton, A. (2015). Inequity averse optimization in operational research. *European Journal of Operational Research, 245*(2), 343-359, https://doi.org/10.1016/j.ejor.2015.02.035.

Keskin, B. B., Li, S. R., Steil, D., & Spiller, S. (2012). Analysis of an integrated maximum covering and patrol routing problem. *Transportation Research Part E: Logistics and Transportation Review, 48*(1), 215-232, https://doi.org/10.1016/j.tre.2011.07.005.

Khan, A., Gupta, S., & Gupta, S. K. (2022). Emerging UAV technology for disaster detection, mitigation, response, and preparedness. *Journal of Field Robotics*, 905-955, https://doi.org/10.1002/rob.22075.

Kim, S. J., Lim, G. J., & Cho, J. (2018). Drone flight scheduling under uncertainty on battery duration and air temperature. *Computers & Industrial Engineering, 117*, 291-302, https://doi.org/10.1016/j.cie.2018.02.005.

Košmerl, J., & Vilhar, A. (2014). Base stations placement optimization in wireless networks for emergency communications. *2014 IEEE International Conference on Communications Workshops (ICC)* (pp. 200-205). Sydney: IEEE.

Kyriakakis, N. A., Marinaki, M., Matsatsinis, N., & Marinakis, Y. (2022). A cumulative unmanned aerial vehicle routing problem approach for humanitarian coverage path planning. *European Journal of Operational Research, 300*(3), 992-1004, https://doi.org/10.1016/j.ejor.2021.09.008.

Lee, B., Park, P., Kim, K., & Kwon, S. (2014). The flight test and power simulations of an UAV powered by solar cells, a fuel cell and batteries. *Journal of Mechanical Science and Technology , 28*, 399-405, https://doi.org/10.1007/s12206-013-0936-7.

Li, D., Wang, X., & Sun, T. (2016). Energy-optimal coverage path planning on topographic map for environment survey with unmanned aerial vehicles. *Electronics Letters, 52*(9), 699-701, https://doi.org/10.1049/el.2015.4551.

Li, J., Lu, D., Zhang, G., Tian, J., & Pang, Y. (2019). Post-Disaster Unmanned Aerial Vehicle Base Station Deployment Method Based on Artificial Bee Colony Algorithm. *IEEE Access, 7*, 168327–168336, https://doi.org/10.1109/ACCESS.2019.2954332.

Line-of-sight propagation. (n.d.). Retrieved February 2025, from IEEE Technology Navigator: https://technav.ieee.org/topic/line-of-sight-propagation

Liu, Z., Sengupta, R., & Kurzhanskiy, A. (2017). A power consumption model for multi-rotor small unmanned aircraft systems. *2017 International Conference on Unmanned Aircraft Systems (ICUAS)* (pp. 310-315, https://doi.org/10.1109/ICUAS.2017.7991310). Miami: IEEE.

Lu, M., Bagheri, M., James, A. P., & Phung, T. (2018). Wireless Charging Techniques for UAVs: A Review, Reconceptualization, and Extension. *IEEE Access, 6*, 29865 - 29884, https://doi.org/10.1109/ACCESS.2018.2841376.

Macias, J. E., Angeloudis, P., & Ochieng, W. (2020). Optimal hub selection for rapid medical deliveries using unmanned aerial vehicles. *Transportation Research Part C: Emerging Technologies, 110*, 56-80, https://doi.org/10.1016/j.trc.2019.11.002.

Mack, E. (2018, February 13). *How delivery drones can help save the world.* Retrieved December 2020, from forbes.com:

https://www.forbes.com/sites/ericmack/2018/02/13/delivery-drones-amazon-energy-efficient-reduce-climate-change-pollution/

Malandrino, F., Chiasserini, C. F., Casetti, C., Chiaraviglio, L., & Senacheribbe, A. (2019). Planning UAV activities for efficient user coverage in disaster areas. *Ad Hoc Networks, 89*, 177-185.

Marsh, M. T., & Schilling, D. A. (1994). Equity measurement in facility location analysis: A review and framework. *European Journal of Operational Research, 74*(1), 1-17, https://doi.org/10.1016/0377-2217(94)90200-3.

Martinez-Alpiste, I., Golcarenarenji, G., Wang, Q., & Alcaraz-Calero, J. M. (2021). Search and rescue operation using UAVs: A case study. *Expert Systems with Applications, 178*, 114937, https://doi.org/10.1016/j.eswa.2021.114937.

Masroor, R., Naeem, M., & Ejaz, W. (2021). Efficient deployment of UAVs for disaster management: A multi-criterion optimization approach. *Computer Communications, 177*, 185-194, https://doi.org/10.1016/j.comcom.2021.07.006.

Meer, I. A., Ozger, M., & Cavdar, C. (2023). Cellular localizability of unmanned aerial vehicles. *Vehicular Communications, 44*, 100677.

Mladenović, N., & Hansen, P. (1997). Variable neighborhood search. *Computers & Operations Research, 24*(11), 1097-1100, https://doi.org/10.1016/S0305-0548(97)00031-2.

Mozaffari, M., Saad, W., Bennis, M., & Debbah, M. (2016). Efficient Deployment of Multiple Unmanned Aerial Vehicles for Optimal Wireless Coverage. *IEEE Communications Letters, 20*(8), 1647-1650, https://doi.org/10.1109/LCOMM.2016.2578312.

Mozaffari, M., Saad, W., Bennis, M., & Debbah, M. (2017). Wireless Communication Using Unmanned Aerial Vehicles (UAVs): Optimal Transport Theory for Hover Time Optimization. *IEEE Transactions on Wireless Communications, 16*(12), 8052-8066, https://doi.org/10.1109/TWC.2017.2756644.

Mozaffari, M., Saad, W., Bennis, M., Nam, Y. H., & Debbah, M. (2019). A Tutorial on UAVs for Wireless Networks: Applications, Challenges, and Open Problems.

IEEE Communications Surveys & Tutorials, 21(3), 2334-2360, https://doi.org/10.1109/COMST.2019.2902862.

Muntaha, S. T., Hassan, S. A., Jung, H., & Hossain, M. S. (2020). Energy Efficiency and Hover Time Optimization in UAV-Based HetNets. *IEEE Transactions on Intelligent Transportation Systems, 22*(8), 5103-5111, https://doi.org/10.1109/TITS.2020.3015256.

Naji-Azimi, Z., Renaud, J., Ruiz, A., & Salari, M. (2012). A covering tour approach to the location of satellite distribution centers to supply humanitarian aid. *European Journal of Operational Research, 222*(3), 596-605, https://doi.org/10.1016/j.ejor.2012.05.001.

Nejdati, A., Izbirak, G., Vizvari, B., & Arkat, J. (2016). Complete Coverage Path Planning for a Multi-UAV Response System in Post-Earthquake Assessment. *Robotics, 5*(4), 26, https://doi.org/10.3390/robotics5040026.

Nemer, I. A., Sheltami, T. R., & Mahmoud, A. S. (2020). A game theoretic approach of deployment a multiple UAVs for optimal coverage. *Transportation Research Part A: Policy and Practice, 140*, 215-230, https://doi.org/10.1016/j.tra.2020.08.004.

Non-line-of-sight propagation. (n.d.). Retrieved February 2025, from wikipedia.org: https://en.wikipedia.org/wiki/Non-line-of-sight_propagation

Oktari, R. S., Munadi, K., Idroes, R., & Sofyan, H. (2020). Knowledge management practices in disaster management: Systematic review. *International Journal of Disaster Risk Reduction, 51*, 101881, https://doi.org/10.1016/j.ijdrr.2020.101881.

Oruc, B. E., & Kara, B. Y. (2018). Post-disaster assessment routing problem. *Transportation Research Part B: Methodological, 116*, 76-102, https://doi.org/10.1016/j.trb.2018.08.002.

Otto, A., Agatz, N., Campbell, J., Golden, B., & Pesch, E. (2018). Optimization approaches for civil applications of unmanned aerial vehicles (UAVs) or aerial drones: A survey. *Networks, 72*(4), 411-458, https://doi.org/10.1002/net.21818.

Outay, F., Mengash, H. A., & Adnan, M. (2020). Applications of unmanned aerial vehicle (UAV) in road safety, traffic and highway infrastructure management:

Recent advances and challenges. *Transportation Research Part A: Policy and Practice, 141*, 116-129, https://doi.org/10.1016/j.tra.2020.09.018.

Pan, C., Yi, J., Yin, C., Yu, J., & Li, X. (2019). Joint 3D UAV Placement and Resource Allocation in Software-Defined Cellular Networks With Wireless Backhaul. *IEEE Access, 7*, 104279 - 104293, https://doi.org/10.1109/ACCESS.2019.2927521.

Park, J., Lee, H., Eom, S., & Lee, I. (2019). UAV-Aided Wireless Powered Communication Networks: Trajectory Optimization and Resource Allocation for Minimum Throughput Maximization. *IEEE Access, 7*, 134978-134991, https://doi.org/10.1109/ACCESS.2019.2941278.

Park, Y., Nielsen , P., & Moon, I. (2020). Unmanned aerial vehicle set covering problem considering fixed-radius coverage constraint. *Computers & Operations Research, 119*, 104936.

Parvaresh, N., Kulhandjian, M., Kulhandjian, H., D'Amours, C., & Kantarci, B. (2022). A tutorial on AI-powered 3D deployment of drone base stations: State of the art, applications and challenges. *Vehicular Communications, 36*, 100474, https://doi.org/10.1016/j.vehcom.2022.100474.

Prins, C. (2009). A GRASP × Evolutionary Local Search Hybrid for the Vehicle Routing Problem. In F. B. Pereira, & J. Tavares, *Bio-inspired Algorithms for the Vehicle Routing Problem.* Heidelberg: Springer.

Qadir, Z., Ullah, F., Munawar, H. S., & Al-Turjman, F. (2021). Addressing disasters in smart cities through UAVs path planning and 5G communications: A systematic review. *Computer Communications, 168*, 114-135, https://doi.org/10.1016/j.comcom.2021.01.003.

Ramos-Ramos, D., González-Vegas, A., Berrocal, J., & Galán-Jiménez , J. (2024). Energy-Aware Microservice-Based Application Deployment in UAV-Based Networks for Rural Scenarios. *Journal of Network and Systems Management, 32*(3), 53, https://doi.org/10.1007/s10922-024-09825-9.

Rawls, J. (2017). A Theory of Justice. In L. May, *Applied Ethics.* New York: Routledge.

Resende, M. G., & Ribeiro , C. C. (2003). A GRASP with path-relinking for private virtual circuit routing. *Networks, 41*(2), 104-114, https://doi.org/10.1002/net.10065.

Ruiz Estrada, M. A., & Ndoma, İ. (2017, September 27). *The Role of Unmanned Aerial Vehicles (UAVVs) in the Case of Natural Disasters Response.* Retrieved October 2021, from SSRN: https://papers.ssrn.com/sol3/papers.cfm?abstract_id=3043008

Russon, M. A. (2018, May 1). *Drones to the rescue*. Retrieved September 2020, from bbc.com: https://www.bbc.com/news/business-43906846

Sacramento, D., Pisinger, D., & Ropke, S. (2019). An adaptive large neighborhood search metaheuristic for the vehicle routing problem with drones. *Transportation Research Part C: Emerging Technologies, 102*, 289-315, https://doi.org/10.1016/j.trc.2019.02.018.

Savuran, H., & Karakaya , M. (2016). Efficient route planning for an unmanned air vehicle deployed on a moving carrier. *Soft Computing , 20*, 2905-2920, https://doi.org/10.1007/s00500-015-1970-4.

Shaheed, M. H., Abidali, A., Ahmed, J., Ahmed, S., Burba, I., Fani, P. J., . . . Munjiza, A. (2015). Flying by the Sun only: The Solarcopter prototype. *Aerospace Science and Technology, 45*, 209-214, https://doi.org/10.1016/j.ast.2015.05.016.

Shahzadi, R., Ali, M., Khan, H. Z., & Naeem, M. (2021). UAV assisted 5G and beyond wireless networks: A survey. *Journal of Network and Computer Applications, 189*, 103114, https://doi.org/10.1016/j.jnca.2021.103114.

Shakhatreh, H., Sawalmeh, A., Al-Fuqaha, A., Dou, Z., Almaita, E., Khalil, I., . . . Guizani, M. (2019). Unmanned aerial vehicles (UAVs): A survey on civil applications and key research challenges. *IEEE Access, 7*, 48572-48634, https://doi.org/10.1109/ACCESS.2019.2909530.

Sharafeddine, S., & Islambouli, R. (2019). On-demand deployment of multiple aerial base stations for traffic offloading and network recovery. *Computer Networks, 156*, 52-61, https://doi.org/10.1016/j.comnet.2019.03.016.

Simic, M., Bil, C., & Vojisavljevic, V. (2015). Investigation in Wireless Power Transmission for UAV Charging. *Procedia Computer Science, 60*, 1846-1855, https://doi.org/10.1016/j.procs.2015.08.295.

Sinnl, M. (2021). Mixed-integer programming approaches for the time-constrained maximal covering routing problem. *OR Spectrum, 43*, 497-542, https://doi.org/10.1007/s00291-021-00635-y.

Song, B. D., Park, H., & Park, K. (2022). Toward flexible and persistent UAV service: Multi-period and multi-objective system design with task assignment for disaster management. *Expert Systems with Applications, 206*, 117855, https://doi.org/10.1016/j.eswa.2022.117855.

Tahir, A., Böling, J., Haghbayan, M. H., Toivonen, H. T., & Plosila, J. (2019). Swarms of Unmanned Aerial Vehicles — A Survey. *Journal of Industrial Information Integration, 16*, 100106, https://doi.org/10.1016/j.jii.2019.100106.

Tiotsop, L. F., Servetti, A., & Masala, E. (2020). An integer linear programming model for efficient scheduling of UGV tasks in precision agriculture under human supervision. *Computers & Operations Research, 114*, 104826, https://doi.org/10.1016/j.cor.2019.104826.

Tokekar, P., Vander Hook, J., Mulla, D., & Isler, V. (2016). Sensor Planning for a Symbiotic UAV and UGV System for Precision Agriculture. *IEEE Transactions on Robotics, 32*(6), 1498-1511, https://doi.org/10.1109/TRO.2016.2603528.

Torres, M., Pelta, D. A., Verdegay, J. L., & Torres, J. C. (2016). Coverage path planning with unmanned aerial vehicles for 3D terrain reconstruction. *Expert Systems with Applications, 55*, 441-451, https://doi.org/10.1016/j.eswa.2016.02.007.

Tuna, G., Nefzi, B., & Conte, G. (2014). Unmanned aerial vehicle-aided communications system for disaster recovery. *Journal of Network and Computer Applications, 41*, 27-36, https://doi.org/10.1016/j.jnca.2013.10.002.

Valavanis, K. P., & Vachtsevanos, G. J. (2014). *Handbook of Unmanned Aerial Vehicles.* Netherlands: Springer Publishing Company, Incorporated.

Vazquez-Carmona, E. V., Vasquez-Gomez, J. I., Herrera-Lozada, J. C., & Antonio-Cruz, M. (2022). Coverage path planning for spraying drones. *Computers & Industrial Engineering, 168*, 108125, https://doi.org/10.1016/j.cie.2022.108125.

Wang, H., Ding, G., Gao, F., Chen, J., Wang, J., & Wang, L. (2018). Power Control in UAV-Supported Ultra Dense Networks: Communications, Caching, and Energy Transfer. *IEEE Communications Magazine, 56*(6), 28-34, https://doi.org/10.1109/MCOM.2018.1700431.

Wang, J., & Wu, Y. (2019). A Continuous Approximation Approach Based on Regular Hexagon Partition for the Facility Location Problem under Disruptions Risk. *Complexity, 2019*(1), 5280161, https://doi.org/10.1155/2019/5280161.

Worden, M. R., Murray, C. C., Karwan, M. H., & Ortiz-Peña, H. J. (2020). Sensor tasking for unmanned aerial vehicles in disaster management missions with limited communications bandwidth. *Computers & Industrial Engineering, 149*, 106754, https://doi.org/10.1016/j.cie.2020.106754.

Wu, J., Wang, H., Li, N., Yao, P., Huang, Y., & Yang, H. (2018). Path planning for solar-powered UAV in urban environment. *Neurocomputing, 275*, 2055-2065, https://doi.org/10.1016/j.neucom.2017.10.037.

Xu, J., Murray, A. T., Church, R. L., & Wei, R. (2023). Service allocation equity in location coverage analytics. *European Journal of Operational Research, 305*(1), 21-37, https://doi.org/10.1016/j.ejor.2022.05.032.

Yan, H., Chen, Y., & Yang, S. H. (2020). UAV-Enabled Wireless Power Transfer With Base Station Charging and UAV Power Consumption. *IEEE Transactions on Vehicular Technology, 69*(11), 12883 - 12896, https://doi.org/10.1109/TVT.2020.3015246.

Yan, S., Peng, M., & Cao, X. (2019). A Game Theory Approach for Joint Access Selection and Resource Allocation in UAV Assisted IoT Communication Networks. *IEEE Internet of Things Journal, 6*(2), 1663 - 1674, https://doi.org/10.1109/JIOT.2018.2873308.

Yanmaz, E. (2023). Joint or decoupled optimization: Multi-UAV path planning for search and rescue. *Ad Hoc Networks, 138*, 103018, https://doi.org/10.1016/j.adhoc.2022.103018.

Ye, H. T., Kang, X., Joung, J., & Liang, Y. C. (2019). Optimal Time Allocation for Full-Duplex Wireless-Powered IoT Networks with Unmanned Aerial Vehicle. *ICC 2019 - 2019 IEEE International Conference on Communications (ICC)* (pp. 1-6). Shanghai: IEEE.

Yin, S., Li, L., & Yu, F. R. (2019). Resource Allocation and Basestation Placement in Downlink Cellular Networks Assisted by Multiple Wireless Powered UAVs. *IEEE Transactions on Vehicular Technology, 69*(2), 2171 - 2184, https://doi.org/10.1109/TVT.2019.2960765.

Zakora, B., & Molodchick, A. (2014). *Classification of UAV (Unmanned Aerial Vehicle).* Retrieved November 2021, from read.meil.pw.pl: http://read.meil.pw.pl/abstracts/StudentAbstract_Zakora_Molodchik. pdf

Zeng, Y., & Zhang, R. (2017). Energy-Efficient UAV Communication With Trajectory Optimization. *IEEE Transactions on Wireless Communications, 16*(6), 3747-3760, https://doi.org/10.1109/TWC.2017.2688328.

Zeng, Y., Xu, J., & Zhang, R. (2019). Energy Minimization for Wireless Communication With Rotary-Wing UAV. *IEEE Transactions on Wireless Communications, 18*(4), 2329-2345, https://doi.org/10.1109/TWC.2019.2902559.

Zeng, Y., Zhang, R., & Lim, T. J. (2016). Wireless communications with unmanned aerial vehicles: opportunities and challenges. *IEEE Communications Magazine, 54*(5), 36-42, https://doi.org/10.1109/MCOM.2016.7470933.

Zhan, C., Zeng, Y., & Zhang, R. (2018). Energy-Efficient Data Collection in UAV Enabled Wireless Sensor Network. *IEEE Wireless Communications Letters, 7*(3), 328-331, https://doi.org/10.1109/LWC.2017.2776922.

Zhang, G., Jia, N., Zhu, N., Adulyasak, Y., & Ma, S. (2023). Robust drone selective routing in humanitarian transportation network assessment. *European Journal of Operational Research, 305*(1), 400-428, https://doi.org/10.1016/j.ejor.2022.05.046.

Zhang, J., Campbell, J. F., Sweeney II, D. C., & Hupman, A. C. (2021). Energy consumption models for delivery drones: A comparison and assessment. *Transportation Research Part D: Transport and Environment, 90*, 102668, https://doi.org/10.1016/j.trd.2020.102668.

Zhang, M., Li, W., Wang, M., Li, S., & Li, B. (2022). Helicopter–UAVs search and rescue task allocation considering UAVs operating environment and performance. *Computers & Industrial Engineering, 167*, 107994, https://doi.org/10.1016/j.cie.2022.107994.

Zhao, N., Lu, W., Sheng, M., Chen, Y., Tang, J., Yu, R. F., & Wong, K. K. (2019). UAV-Assisted Emergency Networks in Disasters. *IEEE Wireless Communications, 26*(1), 45-51.

Zhao, Z., Cumino, P., Esposito, C., Xiao , M., Rosário, D., Braun, T., . . . Sargento, S. (2022). Smart Unmanned Aerial Vehicles as base stations placement to improve the mobile network operations. *Computer Communications, 181*, 45-57, https://doi.org/10.1016/j.comcom.2021.09.016.

Zhou, X., Chen, Y., Li, Y., Liu, B., & Yu, Z. (2023). Spatiotemporal Data-Driven Multiperiod Relocation Optimization of Emergency Medical Services: Maximum Equality Objective. *ISPRS International Journal of Geo-Information,, 12*(7), 269; https://doi.org/10.3390/ijgi12070269.

Zorbas, D., Pugliese, L. D., Razafindralambo, T., & Guerriero, F. (2016). Optimal drone placement and cost-efficient target coverage. *Journal of Network and Computer Applications, 75*, 16-31, https://doi.org/10.1016/j.jnca.2016.08.009.